2

MCR-72-108

Development of an
X-RAY SURFACE ANALYZER FOR PLANETARY EXPLORATION

FINAL REPORT

April 1972

(NASA-CR-127526) DEVELOPMENT OF AN X-RAY SURFACE ANALYZER FOR PLANETARY EXPLORATION Final Report B.C. Clark (Martin Marietta Corp.) Apr. 1972 113 p CSCL 03B

N72-27846

Unclas

G3/30 15581

Approved by:

Benton C. Clark

Benton C. Clark, PhD
Program Manager

MARTIN MARIETTA CORPORATION
Denver, Colorado 80201

TABLE OF CONTENTS

APPENDICES

ABSTRACT

Determination of the surface composition of the planet Mars could provide information which is essential to a better understanding of the past and present history of the planet, and of the physio-chemical properties of the planetary surface and its compatibility with known life forms. For this reason, NASA/Hqs. has sponsored the development of an ultra-miniature X-ray fluorescence spectrometer which can obtain data on element composition not provided by present spacecraft instrumentation. The apparatus employs two radioisotope sources (^{55}Fe and ^{109}Cd) which irradiate adjacent areas on a soil sample. Fluorescent X-rays emitted by the sample are detected by four thin-window proportional counters. Using pulse-height discrimination, the energy spectra are determined. Virtually all elements above sodium in the periodic table are detected if present at sufficient levels. Minimum detection limits range from 30 ppm to several per cent, depending upon the element and the matrix. For most elements, they are below 0.5%. Accuracies likewise depend upon the matrix, but are generally better than ± 0.5% for all elements of atomic number greater than 14. Elements below sodium are also detected, but as a single group.

The instrument has been designed so that it can be fabricated in flight configuration for very low weight and still satisfy stringent spacecraft compatability requirements. Development is in a highly advanced state. Performance data were taken with flight-configured radioisotope sources and proportional counters, built by manufacturers with excellent experience in providing similar devices for space missions. Critical electronic circuits have been built and tested using Viking-approved parts. Systems analyses have been performed to determine thermal, power, and data-handling requirements. A computer model of the instrument has been developed and tested with good results. This model was used to optimize instrument parameters during the design phase, and has now been expanded to perform automatic analysis of the output data.

SUMMARY CHART

Experiment:	Geochemical Investigation of the Composition of Planetary Surfaces.
Instrument:	X-ray Fluorescence Spectrometer.
Measurement:	Quantitative analysis for major, minor, and some trace elements, including Mg, Al, Si, P, S, Cl, K, Ca, Ti, Fe, Ni, Zn, Sr, Zr, and others. C, O, and Na are determined as a group.
Sensitivity:	30 parts per million to several per cent, depending upon the element.
Flight History:	Sources and detectors have extensive flight history. X-ray fluorescence employed by Russians on Lunokhod I moon rover and by U. S. on Apollo 15.
Sample Req:	Analysis does not require contact and is non-destructive. Samples may be those used in other experiments or instrument may be deployed to the surface.
Min. Sample Size:	1.5 inch diameter, 0.06 inch thick (less than 3 c.c.).
Desired Distance Between Spectrometer and Sample:	0.5 to 1.0 inch.
Description:	Two sealed radioisotope sources (Fe-55 and Cd-109) bombard the sample with soft X-rays, producing fluorescent X-rays characteristic of each element in the sample. Fluorescent emissions are detected by four thin-window proportional counters. Electronic system counts and stores pulses which pass a programmable single-channel analyzer.
Lifetime:	Only limit is radioisotopes. Half-lifes are 2.60 yrs. for Fe-55 and 1.24 yrs. for Cd-109.
Mechanical:	No moving parts. One to two pounds total weight. Volume less than 100 cubic inches.
Electrical:	Fully compatible with flight requirements. Less than 2.0 watt from unregulated 30 VDC. 4.0 hour analysis period/soil sample. 5,000 bits/soil sample.
Environmental:	All components heat sterilizable, very rugged, withstand ultrahigh vacuum, extremes in temperature.
Radiation Safety:	Low hazard. Radioisotopes are electroplated onto foils which are then hermetically sealed into aluminum capsules.

ULTRAMINIATURE X-RAY FLUORESCENCE SPECTROMETER

1. INTRODUCTION

In 1969, in response to NASA's announcement of opportunity for participation on the 1973 Viking mission to Mars, we proposed an ultraminiature X-ray fluorescence spectrometer for geochemical analysis of the Martian surface. Although rated high on scientific merit, the proposed investigation was not accepted because the spectrometer was not considered sufficiently developed. Subsequently, the Viking mission was slipped to a 1975 launch. Meanwhile, development of the X-ray spectrometer has gone forward under contract NAS-w 2248 from the Planetary Programs Division, OSSA, NASA/Headquarters. This report discusses the work accomplished under this effort.

Until recently, only the alpha particle method of chemical analysis (Tu-68*) had been applied to remote analysis of a planetary surface. However, the X-ray fluorescence technique has now been successfully applied in two different investigations. First, Soviet scientists included an instrument very similar to our originally proposed design on their Moon rover, Lunokhod I. Dubbed "RIFMA", this device employed radioisotope excitation, proportional counter detection, and thin filters to make hundreds of elemental analyses of the lunar surface as Lunokhod I conducted its traverses (Ko-71). Second, American scientists (Go-70) have flown on the Apollo 15 Command Service Module an array of proportional counters to detect fluorescent X-rays from the lunar surface as the spacecraft orbited the Moon. Stimulation of the fluorescent X-rays was provided by the normal solar X-ray flux. This experiment was quite successful in detecting chemical differences between lunar highlands and mare, and will be flown again on Apollo 16.

2. DESCRIPTION

Elemental analysis by this instrument is based upon the phenomena that when a sample is bombarded by X-rays to produce photoelectric interactions, each element in the sample emits (fluoresces) X-rays with energy characteristic of that particular element. Elements of higher atomic number emit X-rays of higher energy. It was by this technique that Moseley, in 1913, was able to finally assign atomic numbers to the rare earth and higher elements in Mendeleev's periodic table.

The ultraminiature X-ray fluorescence spectrometer employs radioisotope sources rather than an X-ray tube to produce X-rays with which to bomard the sample. These sources decay via electron capture, thereby producing monochromatic X-rays characteristic of their daughter products. Fluorescent X-ray emissions are detected and their energies determined by thin-window proportional counters. As presently designed (see Figure 1) the instrument is a

---

*References are listed in Appendix A.

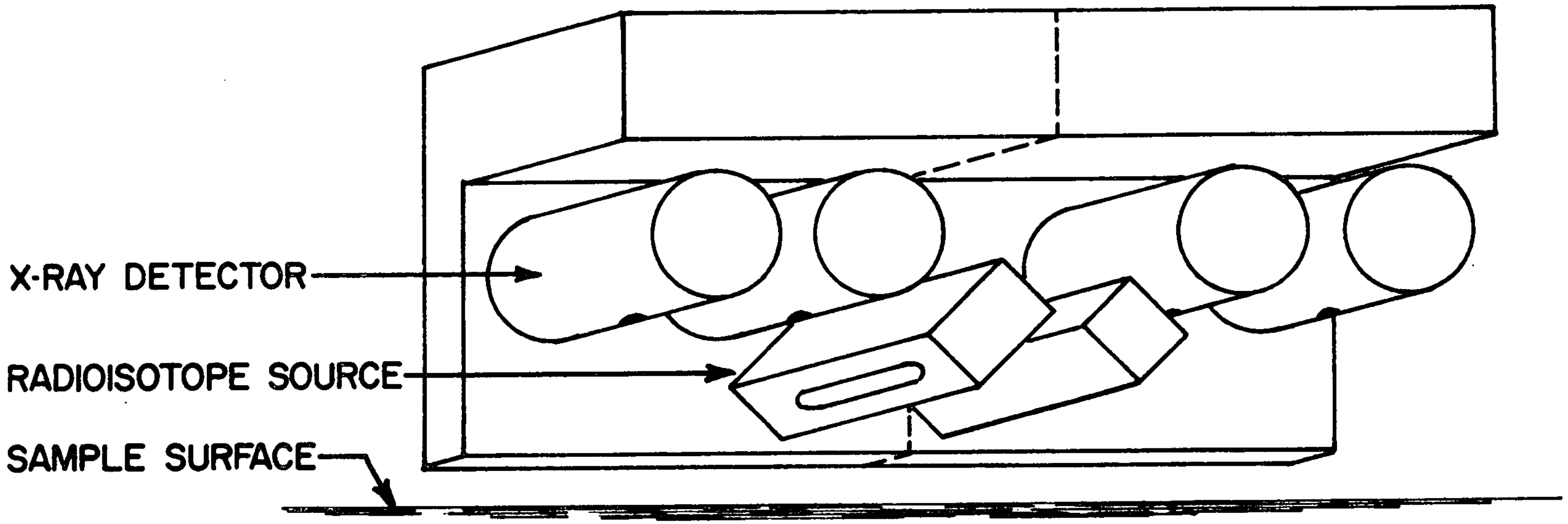

Fig. 1 Ultraminiature X-Ray Fluorescence Spectrometer for Remote Geochemical Analysis

dual unit with one source-detector set for lighter elements (Mg through Ti) and a second set for heavier elements (K through U). The former uses an Fe-55 radioisotope source (5.9 keV X-ray, approx. 150 mCi activity) and neon-carbon dioxide filled proportional counters with beryllium and aluminum entrance windows. The latter uses a Cd-109 radioisotope source (22.2 keV X-ray, approx. 50 mCi activity) and xenon-neon-carbon dioxide filled proportional counters with two mil thick beryllium entrance windows. With the sample situated a nominal one inch from the detectors, the light and heavy element subsystems view adjacent areas approximately one inch in diameter on the same sample (alternatively, a single sample may be placed sequentially under each subsystem).

The entire instrument, including all electronics (amplifiers, power supplied, digital data memory, and spacecraft interface circuits) weighs one to two pounds and occupies a volume of less than 100 cubic inches. The proportional counter detectors are very rugged and heat sterilizable (see Appendix G). Radiation safety has been a key design ingredient. Radioisotope sources are electroplated, heat bonded, then hermetically sealed into aluminum capsules (for further description, see Appendix F).

3. MATHEMATICAL MODEL OF INSTRUMENT RESPONSE

In conjunction with the experimental program to develop the ultraminiature approach to X-ray fluorescence analysis, a theoretical model of the instrument has been derived (described more fully in Appendix B). This model includes all pertinent instrumental parameters as well as matrix absorption and enhancement effects. It is based upon the fundamental physics of X-ray absorption excitation, and scattering, and employs the most modern available values of the applicable physical constants; the mass absorption coefficients of Frazer (Fr-68), Henke (He-69), and UCRL-50400, and the fluorescent yields as summarized by Fink, et. al. (Fi-67). Verification of the practicality of this "fundamental parameters method" in reducing X-ray fluorescence data for chemical analyses was first made by Criss and Birks (Cr-68). Since then, the use and development of this approach has been pursued by many workers in the field (Bi-69, Cu-68, Fr-70, and Be-70).

Quite satisfactory results have been obtained using this model as can be seen in Figure 2 by the comparison of experimental data with the theoretical predictions. The model gives such good agreement, that it has been confidently used to investigate the effects of varying experimental parameters. Through such studies, we have optimized the design of the spectrometer for geochemical analyses. Not only has the entire model been programmed for a digital computer but data on the major and minor element compositions of a large variety of earthbound and extraterrestrial rocks (Appendix M) has been punched onto computer cards. Thus, very comprehensive studies of instrument response in different situations is possible. Computer simulation is of great value not only because it aids in interpretation of experimental results and in design optimization, but also because it could provide the quick look capability in analyzing data as

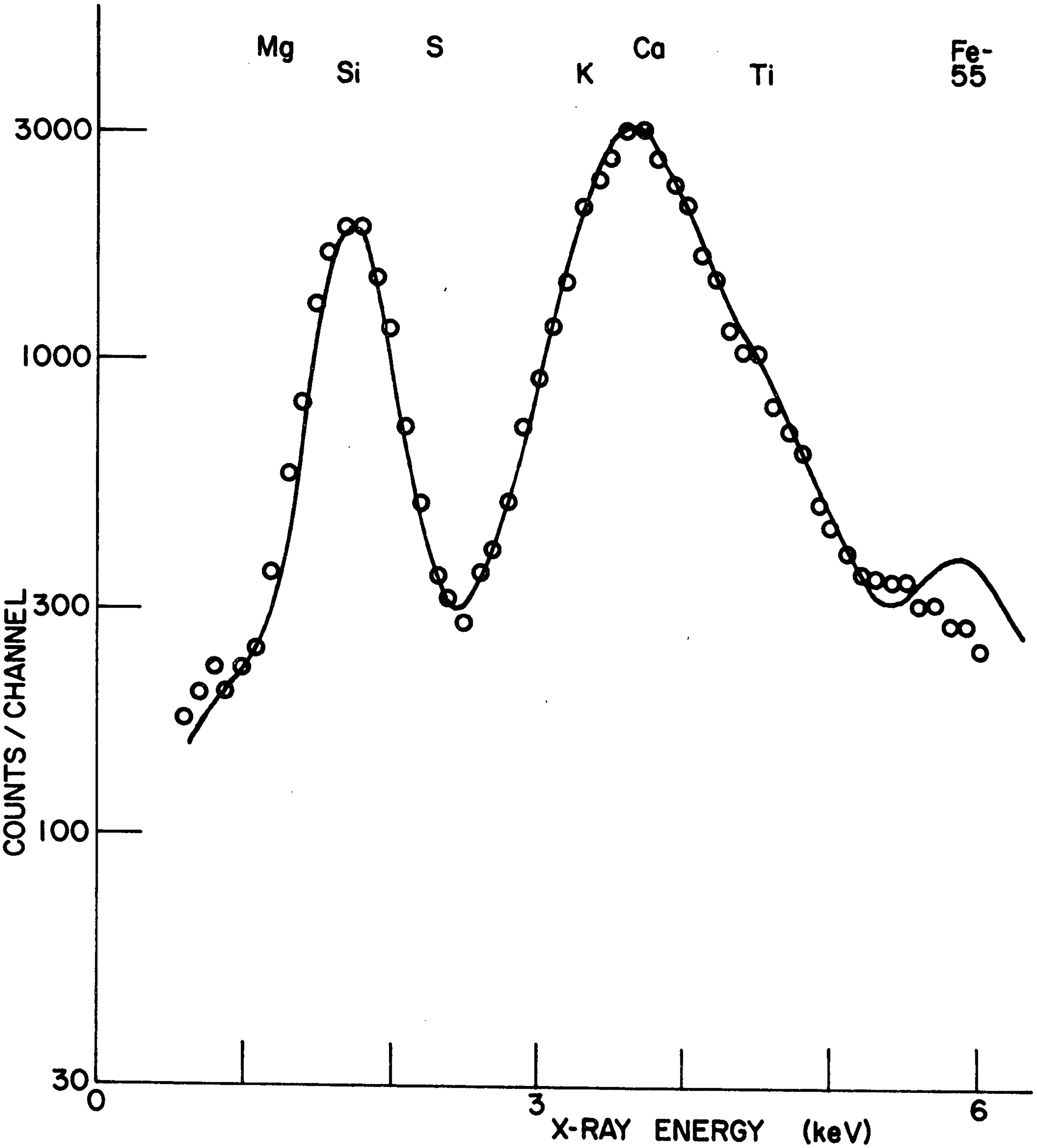

FIGURE 2
MEASURED vs THEORETICAL SPECTRUM FOR BASALT (BCR-1)

it comes back from Mars, which would be required to take advantage of the remote-programming capability of the spectrometer. In no case, however, would it be planned that the computerized interpretation of the data would be used alone. Laboratory simulation of results obtained on Mars is required for final analysis.

4. PERFORMANCE

What performance should be required of a geochemical experiment for the first in-situ measurements on Mars? Although one might ideally desire to determine the abundance of all elements in the surface material, such an experiment is technically difficult and not sufficiently developed for landing on Mars in the near future. Less ambitious experiments must therefore be considered. The lowest order objective is the capability of discriminating between major rock types. For example, the alpha backscatter experiment (Tu-68) on the Surveyor flights was highly successful in showing the lunar mare are basaltic, even though only eight elements were detected, K could not be distinguished from Ca, and the Mg and Fe analyses were apparently low by the order of 30%. Thus, the first question we ask of the X-ray fluorescence spectrometer is whether it has sufficient resolving power to identify major rock types. Figure 3 shows the clear separation of nine types of igneous rocks (calc-alkali rhyolite through dunite, including one lunar sample). Easily seen is the change in silicon content due to the progression of acidic to basic, as well as shifts in K/Ca ratio, and changes in Ti content.

Perhaps an even more valuable test is the discrimination capability of the instrument between proposed models of the Martian surface. Visible and infrared spectrometric observations of Mars have led to three widely discussed interpretations of the composition of the surface material:

Theory	Proponents
(1) Abundant limonite	Dollfus (Do-51); Sagan and Pollack (Sa-65, Sa-66, Po-69, Po-70, Co-69, Eg-69)
(2) Oxidized basalt	Adams and McCord (Ad-68, Ad-69a, Mc-71, Mc-71a)
(3) Minerals coated with ferric oxides	Binder and Cruikshank (Bi-64, Bi-66); Van Tassel and Salisbury (Va-64, Sa-68, Sa-69)

That the X-ray techniques of analysis can readily test these theories is shown in Figures 4 and 5. Limonite is very high in iron, basalt is intermediate, while the iron oxide coated test specimen (Simpson desert sand), even though blood-red in color, contains less than one per cent iron (but clearly detected at 6.4 keV using Cd-109 excitation, Figure 4). Likewise, different Si, K, Ca, and Ti contents easily separate these Martian analogs (Figure 5).

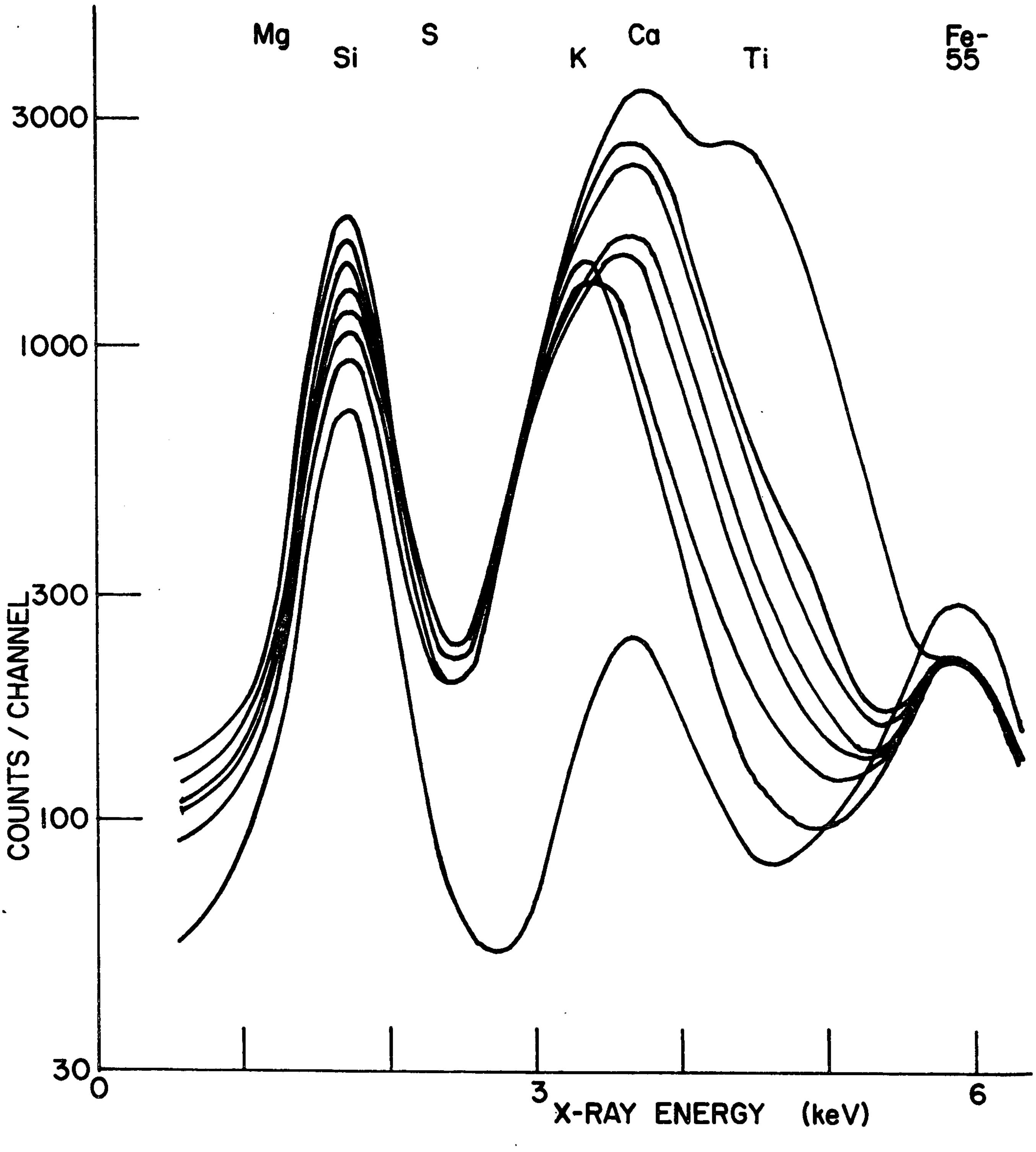

FIGURE 3
SPECTRAL SIGNATURES OF IGNEOUS ROCKS

FIGURE 4

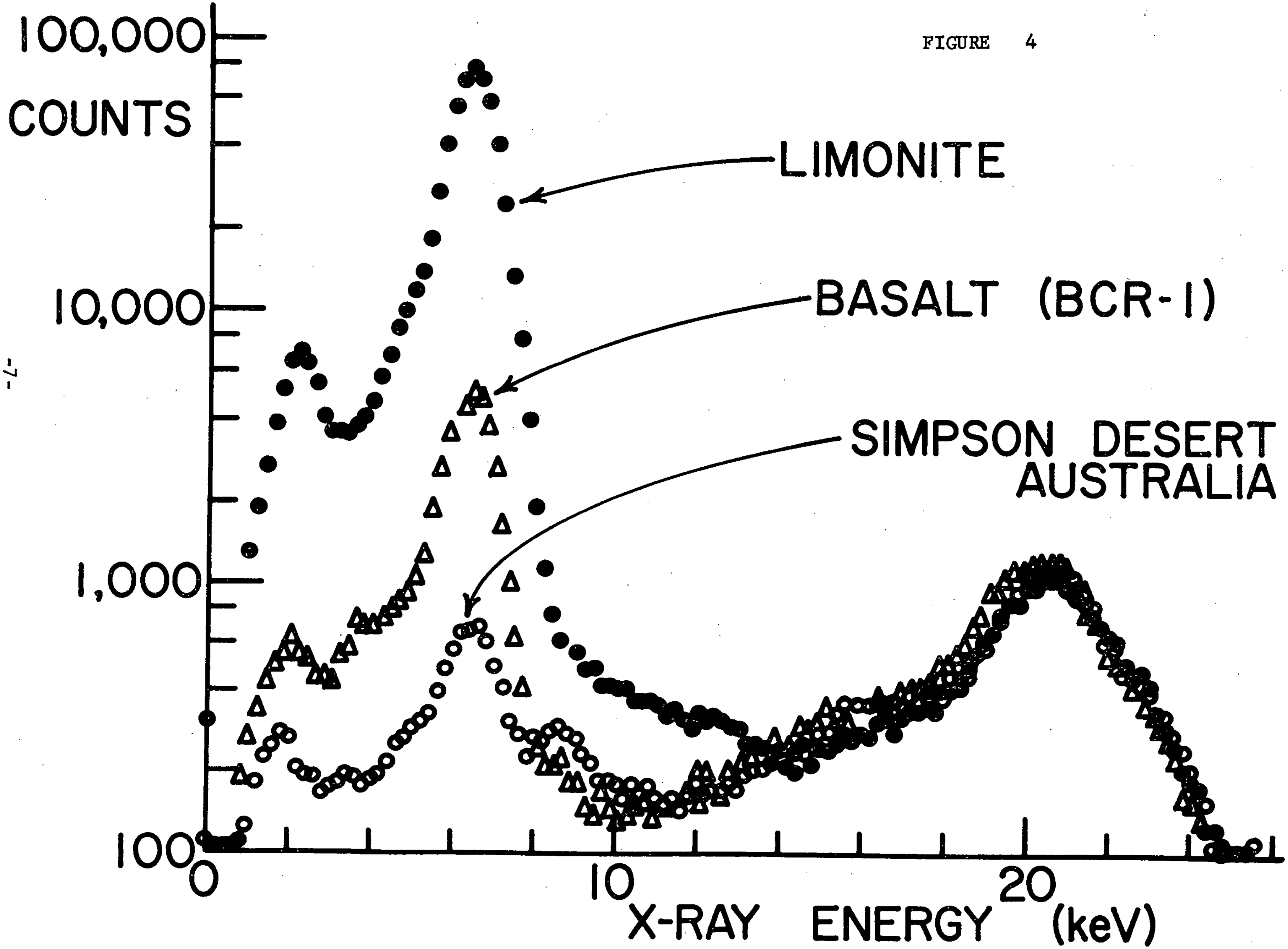
100,000
COUNTS
10,000
1,000
100
0
10
20
X-RAY ENERGY (keV)
LIMONITE
BASALT (BCR-1)
SIMPSON DESERT
AUSTRALIA

FIGURE 5

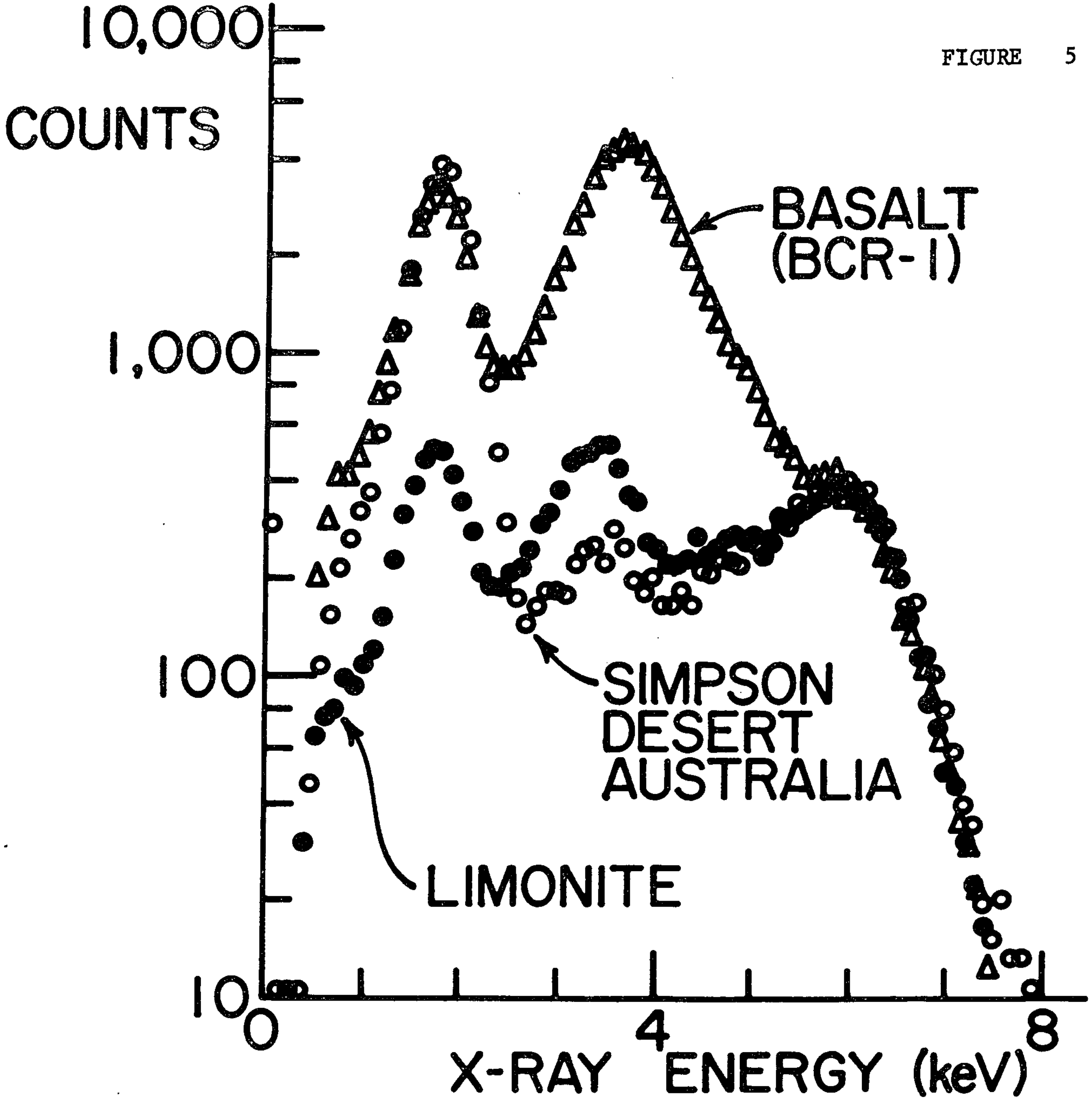
10,000
COUNTS
1,000
100
10
BASALT
(BCR-1)
SIMPSON
DESERT
AUSTRALIA
LIMONITE
0
4
8
X-RAY ENERGY (keV)

In addition to providing the capability of determining gross rock type, the X-ray fluorescence spectrometer has outstanding sensitivity (for its small size) for many elements. All elements in the periodic table above Mg emit fluorescent X-rays within the energy range of this instrument and are thus susceptible to detection provided they are present at sufficient levels. We have conducted extensive laboratory tests to determine achievable detection limits for a number of elements. Detectability depends, of course, upon the relative abundance of other constituent elements, i.e., upon the matrix. In Table I, the minimum detection limits are given for 22 elements in matrices in which they are likely to be present at low concentrations. Some examples of test data are given in Appendix C. Typical spectral data from which such limits are obtained is shown in Figure 6. These two spectra of CAAS standard syenite and the USGS standard andesite (AGV-1) have had the backscatter peak subtracted. Clearly seen are low concentrations (few hundred ppm) of Pb, Sr, and Zr.

Accuracy of the analysis is also an important criterion for evaluation of the performance of the instrument. As discussed above, a computer program has been developed for data analysis. Element concentrations are estimated by inspection of the experimental spectra, with the computer converting the input data to a calculated spectrum. This theoretical spectrum is then compared with the measured spectrum and the deviations determined. From these results, a new set of input data is generated. In application, the convergence is found to be sufficiently rapid to justify this approach to data analysis. Each iteration requires only one second of computer time. Birks (Cr-68) and many workers since have demonstrated the utility of this method of data analysis for X-ray fluorescence spectrometry. With this method, we have successfully demonstrated the ability to detect differences of ± 0.5% by weight for elements above Si. For many elements such as Ti, Ca, and Fe, the absolute accuracies are usually better than this.

5. RATIONALE OF DESIGN APPROACH

The X-ray fluorescence spectrometer in the version shown in Figure 1 is believed to be the optimum approach to providing the simplest possible method of geochemical analysis for a first mission to Mars. A whole spectrum of more sophisticated and advanced versions of the instrument exists. But each increase in sophistication is accompanied by increases in weight, complexity, and cost.

Methods of upgrading the experiment would include: (1) adding more radioisotope sources, (2) adding an X-ray tube, (3) using organic thin film windows on the proportional counters, and/or (4) employing cryogenically-cooled solid state detectors. Though desirable from the scientific standpoint, these methods invoke considerable engineering problems. A discussion of such trade-offs is given in Appendix I.

TABLE I

MINIMUM DETECTION LIMITS FOR THE X-RAY FLUORESCENCE SPECTROMETER

ELEMENT	MINIMUM DETECTION LIMIT (%)	MATRIX/COMMENTS
Al	2.0	Basalt
Ca	0.02	Silica, Dunite
Cl	0.3	Igneous (any)
Cr	0.5	Estimate
Cu	0.5	Granite
Fe	0.03	Silica
K	0.02	Silica
K	0.8	Basalt
Mg	2.0	Ultra-basic rocks
Ni	0.8	Iron-silicate
P	1.5	Basalt (Estimate)
Pb	0.05	Syenite (CAAS)
Rb	0.05	Estimate
S	0.8	Basalt
Si	0.2	Estimate
Sr	0.03	Syenite (CAAS)
Th	0.08	Syenite (CAAS)
Ti	0.1	Silica
Ti	0.25	Basalt
U	0.08	Syenite (CAAS)
Y	0.02	Estimate
Zn	0.1	Granite
Zr	0.02	Andesite (AGV-1)

FIGURE 6

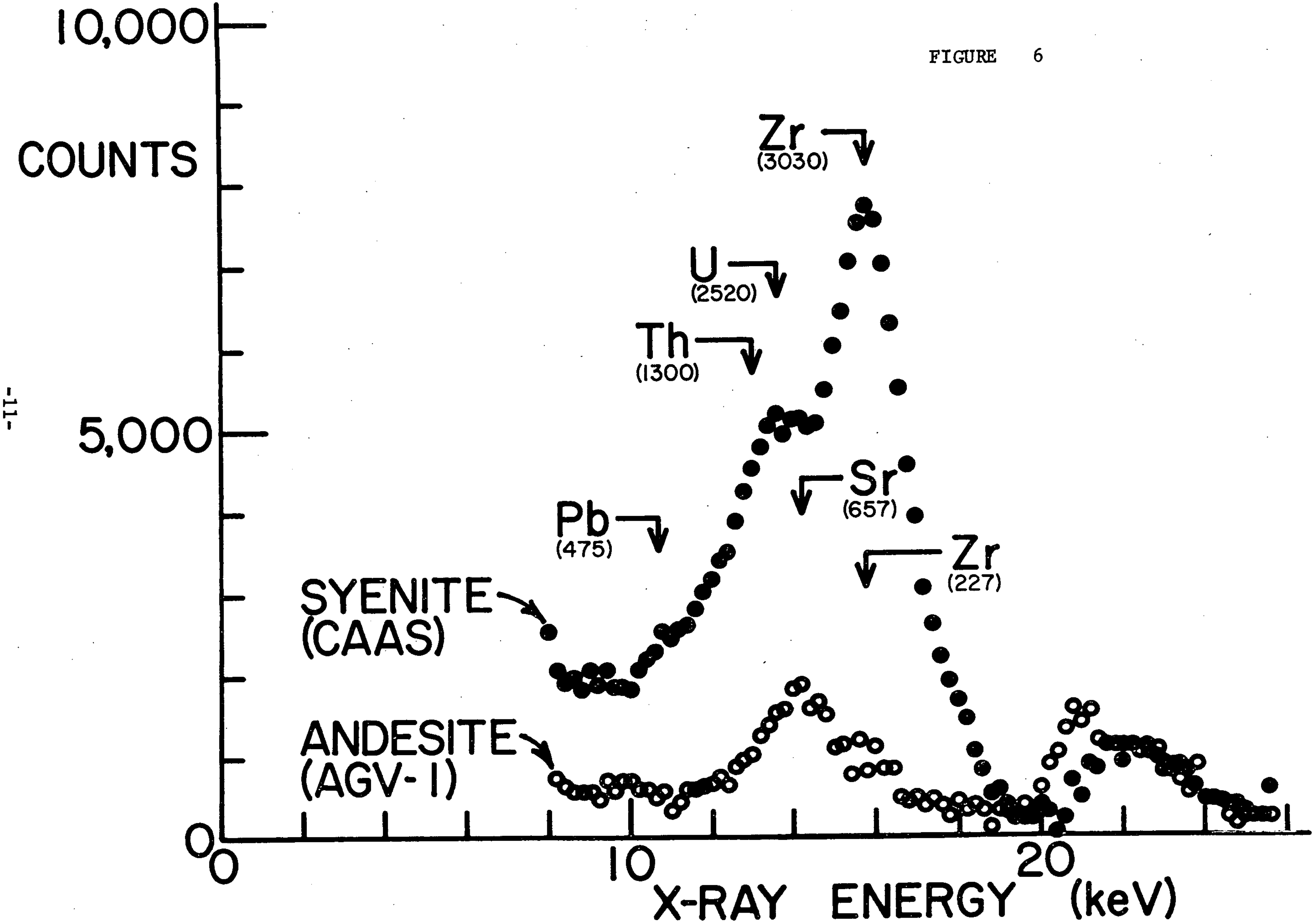
10,000
COUNTS
5,000
0
Zr (3030)
U (2520)
Th (1300)
Pb (475)
Sr (657)
Zr (227)
SYENITE (CAAS)
ANDESITE (AGV-1)
0
10
20
X-RAY ENERGY (keV)

It has been often suggested that an alpha source be used for stimulation of X-ray emission because of high yields for elements of low atomic number. However, a very difficult problem in radiation safety arises because the highly radiotoxic alpha source cannot be placed in a hermetically sealed capsule without completely absorbing the short-ranged alpha particles. Extremely thin window covers must be used and even though the probability of rupture may be low, it is well-known that because of aggregate recoil, a leak of radioactive material from sources of this type is virtually impossible to control.

6. COMPATIBILITY WITH VIKING MISSION CONSTRAINTS

Every effort has been made to achieve a design which satisfies not only the scientific objectives of the investigation, but also the constraints imposed by the mission of the spacecraft. Thus,

a. Weight is minimal.

b. Power and data requirements are minimal (see Appendix E).

c. Inherently rugged components with previous flight history have been selected so that no difficulty in surviving the environments of shock, vibration, hard vacuum, humidified atmosphere, and Martian atmosphere are foreseen.

d. Sample requirements are minimal.

e. Radiation safety problems are minimal because of high integrity, hermetically-sealed sources (Appendix F).

f. High reliability is inherent in the design because the two subsystems have overlapping response for intermediate elements (Si, S, K, Ca, Ti) so that each may serve as a backup for the other.

g. Command and control requirements are minimal.

7. STATUS OF DEVELOPMENT

This instrument now exists in a highly advanced stage of development. All performance data quoted above have been taken with radiation sources and detectors which are of flight weight and configuration, are rugged, and heat sterilizable (for details see Appendices F and G). Both the counters and detectors have extensive flight history and are available from manufacturers with proven experience in supplying similar devices for space missions. Electronic design has also begun (Appendix E).

8. PERFORMANCE VERIFICATION

To provide an objective evaluation of the scientific performance capabilities of this instrument, an analysis was performed on December 8, 1971, of four powdered rock speimens ("unknowns") supplied by NASA. Eleven elements were detected in each unknown: Mg, Al, Si, K, Ca, Ti, Fe, Rb, Sr, Zr, and "O." In addition to establishing the concentration of each of these eleven elements, upper limits were found for the majority of elements in the periodic table, including P, S, Cl, Ni, Zn, and Pb. Upper limits were also derived for CO_2. Accuracies rivalled and sometimes exceeded those obtained using wet chemistry techniques (interlab comparisons). The results were quite adequate for determining (a) enrichment and depletion factors relative to presumed primordial abundances, (b) normative mineralogy and the rock density that can be inferred therefrom, and (c) rock type (assuming magmatic origin) and degree of differentiation. The radioactive element K was assayed accurately even at low concentrations and the important geochemical ratio, K/Ca, was quantitatively determined for each unknown. All data were taken with the X-ray spectrometer in flight-configured form and using miniature, heat-sterilizable radiation sources and detectors. A full discussion of the results and their interpretations is given in Appendix N.

9. CONCLUSION AND RECOMMENDATIONS

An ultraminiature X-ray fluorescence spectrometer has been built and tested to demonstrate the feasibility of performing in situ elemental analysis on planetary surfaces. The stage of development of this instrument is quite advanced and has reached the point that it should be given every consideration for inclusion on missions to the surfaces of the planets and planetary satellites.

APPENDIX A

REFERENCES

Ad-68	J. B. Adams, "Lunar and Martian Surfaces: Petrologic Significance of Absorption Bands in the Near-Infrared", Science 159 (1968) 1453.
Ad-69	J. B. Adams, J. E. Conel, J. A. Dunne, F. Fanale, G. B. Holstrom, and A. A. Loomis, "Strategy for Scientific Exploration of the Terrestrial Planets", Rev. Geophysics 7 (1969) 623.
Ad-69a	J. B. Adams and T. B. McCord, "Mars: Interpretation of Spectral Reflectivity", J. Geophys. Res. 74 (1969) 48, 51.
Ah-65	L. H. Ahrens, Distribution of the Elements in Our Planet, McGraw-Hill, New York (1965).
Al-61	L. H. Aller, The Abundance of the Elements, Interscience Publishers, New York (1961).
An-70	A. T. Anderson, Jr., A. V. Crewe, E. J. Olsen, J. V. Smith, and P. J. Wyllie, "Petrologic History of Moon Suggested by Petrography Mineralogy, and Crystallography", Science 167 (1970) 587.
Be-70	D. R. Beaman and J. A. Isasi, "A Critical Examination of Computer Programs Used in Quantitative Microprobe Analysis", Anal. Chem. 42 (1970) 1540.
Bi-64	A. B. Binder and D. P. Cruikshank, "Comparison of the IR Spectrum of Mars with the Spectra of Selected Terrestrial Rocks and Minerals", Commun. Lunar Planetol. Lab. 2 (1964) 193.
Bi-66	A. B. Binder and D. P. Cruikshank, "Lithological and Mineralogical Investigation of the Surface of Mars", Icarus 5 (1966) 521.
Bi-69	L. S. Birks, "Current Trends in X-ray Fluorescence Spectrometry", Appl. Spectroscopy 23 (1969) 303.
Ca-67	A. G. W. Cameron, "A New Table of Abundances of the Elements in the Solar System", in Origin and Distribution of the Elements, ed. by L. H. Ahrens, Pergamon Press, New York (1968).
Cl-24	F. W. Clarke, "The Data of Geochemistry", U. S. Geol. Survey Bull. 770 (1924) 841.
Cl-69	B. C. Clark, "An Investigation into the Radiobiological Consequences of K-Shell Ionizations of Phosphorus Atoms Using Soft X-rays", Ph.D. Thesis, Columbia University (1969).

Cl-69a B. C. Clark, A. K. Baird, Proposal to NASA (OSSA), "Geochemical Investigation of the Surface Composition of Mars", (October 1969).

Co-69 K. L. Coulson, "Polarimetry of Mars", Appl. Optics 8 (1969) 1287.

Cr-68 J. W. Criss and L. S. Birks, "Calculation Methods for Fluorescent X-ray Spectrometry", Anal. Chem. 40 (1968) 1080.

Cu-66 J. L. Culhane, J. Herring, P. W. Sanford, G. O'Shea, R. D. Phillips, "Advances in the Design and Performance of X-ray Proportional Counters", J. Sci. Instrum. 43 (1966) 908.

Cu-68 F. Cuttitta and H. J. Rose, Jr., Appl. Spectrosc. 22 (1968) 321.

Da-33 R. A. Daly, Igneous Rocks and the Depths of the Earth, McGraw-Hill, N. Y. (1933).

Do-51 A. Dollfus, "La Polarisation de la Lumiere Renvoyee par les Differentes Regiones de la Surface de la Planete Mars et son Interpretation", Acad. Sci. Paris, Compte Rendus, 233 (1951).

Eg-69 W. G. Egan, "Polarimetric and Photometric Simulation of the Martian Surface", Icarus 10 (1969) 223.

En-70 A. E. J. Engel and C. G. Engel, "Lunar Rock Compositions and Some Interpretations", Science 167 (1970) 527.

Er-69 W. G. Ernst, Earth Materials, Prentice-Hall, Inc., New Jersey (1969).

Fi-67 R. W. Fink, R. C. Jopson, Hans Mark, and C. D. Swift, "Atomic Fluorescence Yields", Rev. Mod. Phys. 38 (1966) 513.

Fr-68 J. Z. Frazer, "A Computer Fit to Mass Absorption Coefficient Data", Univ. of Calif. S.I.O. 67-29 (1968).

Fr-70 R. S. Frankel and D. W. Aitken, "Energy Dispersive X-ray Emission Spectroscopy", Appl. Spectrosc. 24 (1970) 557.

Fu-70 L. H. Fuchs, "Infrared Emission Spectra: Enhancement of Diagnostic Features by the Lunar Environment", Science 169 (1970) 865.

Go-70 P. Gorenstein, H. Gursky, I. Adler, and J. Trombka, "System for Non-Dispersive Analysis of Lunar X-rays from Apollo", Adv. X-ray Anal. 13 (1970) 330.

Gr-70 J. Green and L. Larmore, "The Exploration of the Planets from Space", McDonnell Douglas Corp. Research Communication 134, MDC Q0036 (1970).

HCP-59 Handbook of Chemistry and Physics, 40th Ed., Chemical Rubber Pub. Co., Cleveland (1959).

He-64 B. L. Henke, "X-ray Fluorescence Analysis for Na, F, O, N, C, and B", Adv. in X-ray Anal. 7 (1964) 21.

He-65 B. L. Henke, "Application of Multilayer Analyzers to 15-150 Angstrom Fluorescence Spectroscopy for Chemical and Valence Bond Analysis", Adv. in X-ray Anal. 9 (1965) 432.

He-69 B. L. Henke, "Low Energy X-ray and Electron Physics", presented at the 18th Annual Denver X-ray Conference, Aug., 1969.

Jo-68 P. A. Johnston, G. C. Huth, R. J. Locker, "A Solid-State X-ray Fluorescence Analyzer for Use in Hostile Environments", Trans. IEEE on Nuclear Sci. (1968) 432.

Ko-71 Kocharov, G. E., Victorov, S. V., Voropaev, O. M., Dzevanovskaya, A. Yu., Kirian, G. V., Petrov, V. V. and Sakulsky, V. A., Investigation of the Chemical Composition of the Lunar Surface Along the Route of "Lunokhod-1", COSPAR, Seattle, Washington, 1971.

Le-69 R. B. Leighton, et al, "Mariner 6 and 7 Television Pictures", Science 165 (1969) 684, 788.

LSPET-69 Lunar Sample Preliminary Examination Team, "Preliminary Examination of Lunar Samples from Apollo 11", Science 165 (1969) 1211.

LSPET-70 Lunar Sample Preliminary Evaluation Team, "Preliminary Examination of Lunar Samples from Apollo 12", Science 167 (1970) 1325.

Ma-62 B. Mason, Meteorites, John Wiley and Sons, N. Y. (1962).

Ma-65 K. W. Madlem, "Matrix and Particle Size Effects in Analyses of Light Elements by Soft X-ray Spectrometry", Adv. in X-ray Anal. 9 (1965) 441.

Ma-66 B. Mason, Principles of Geochemistry, J. Wiley and Sons, N. Y. (1966).

Ma-70 J. A. Maxwell, S. Abbey, W. H. Champ, "Chemical Composition of Lunar Material", Science 167 (1970) 530.

Mc-69 T. B. McCord and J. B. Adams, Science 163 (1969) 1058.

Mc-70 T. B. McCord and T. V. Johnson, "Lunar Spectral Reflectivity and Implications for Remote Mineralogical Analysis", Science 169 (1970) 855.

Mc-70a T. B. McCord, J. B. Adams, and T. V. Johnson, "Asteroid Vesta: Spectral Reflectivity and Compositional Implications", Science 168 (1970) 1445.

Mc-71 T. B. McCord, J. H. Elias, and J. A. Westphal, "Mars: The Spectral Albedo of Small Bright and Dark Regions", Icarus 14 (1971) 245.

Mc-71a T. B. McCord and J. A. Westphal, "Mars: Narrow Band Photometry during the 1969 Apparition", Astrophys. J. 168 (1971) 141.

Me-66 A. E. Metzger, R. E. Parker, J. I. Trombka, "A Non-Dispersive X-ray Spectrometer for Lunar and Planetary Geochemical Analysis", Trans. IEEE on Nuclear Science, (1966) 554.

Mu-58 T. Mulvey, A. J. Campbell, Brit. J. Appl. Phys. 9 (1958) 406.

Mu-71 B. C. Murray, L. A. Soderblom, R. P. Sharp, and J. A. Cutts, "The Surface of Mars - 1. Cratered Terrains", to be published in J. Geo. Res. (1971).

No-54 S. R. Nockolds, "Average Chemical Composition of Some Igneous Rocks", Geol. Soc. American Bull. 65 (1954) 1007.

Oc-70 J. T. O'Conner, "Martian Geochemistry and Surface Features", presented at the International Association of Planetoloty (IUGS) Special Meeting on The Surface Features of Mars, Huntington Beach, California (1970).

Ok-70 J. A. O'Keefe, "Apollo 11: Implications for the Early History of the Solar System", EOS 51 (1970) 633.

Ok-70a J. A. O'Keefe, "Tektite Glass in Apollo 12 Sample", Science 168 (1970) 1209.

Pa-70 J. H. Patterson, A. L. Turkevich, E. J. Franzgrote, T. E. Economou, and K. P. Sowinski, "Chemical Composition of the Lunar Surface in a Terra Region near the Crater Tycho", Science 168 (1970) 825.

Pl-69 W. T. Plummer, R. K. Carson, "Mars: Is the Surface Colored by Carbon Suboxide?", Science 166 (1969) 1142.

Po-55 A. Poldervaart, "Chemistry of the Earth's Crust", in "Crust of the Earth", Geol. Soc. American, Spec. Paper 62 (1955) 119.

Po-69 J. B. Pollack and C. Sagan, "An Analysis of Martian Photometry and Polarimetry", Space Sci. Rev. 9 (1969) 243.

Po-70 J. B. Pollack, R. N. Wilson, and G. G. Goles, "A Reexamination of the Stability of Goethite on Mars", J. Geophys. Res. 75 (1970) 7491.

Po-70a J. B. Pollack, D. Pitman, B. N. Khare, and C. Sagan, "Geothite on Mars: A Laboratory Study", Spec. Rept. 314, Smithsonian Astrophysical Observatory, Cambridge, Mass. (1970).

Ra-61 K. Rankama and T. G. Sahama, Geochemistry, University of Chicago Press (1961)

Rh-66 J. R. Rhodes, "Radioisotope X-ray Spectrometry", The Analyst 91 (1966) 683.

Ri-70 A. E. Ringwood and E. Essene, "Petrogenesis of Lunar Basalts and the Internal Constitution and Origin of the Moon", Science 167 (1970) 607.

Ro-70 H. J. Rose, F. Cuttitta, E. J. Dwornick, M. K. Carron, R. P. Christian, J. R. Lindsay, D. T. Ligon, R. R. Larson, "Semimicro Chemical and X-ray Fluorescence Analysis of Lunar Samples", Science 167 (1970) 520.

Sa-65 C. Sagan, J. P. Phaneuf, M. Ihnat, "Total Reflection Spectrophotometry and Thermogravimetry Analysis of Simulated Martian Surface Materials", Icarus 4 (1965) 43.

Sa-66 C. Sagan, "Mariner IV Observations and the Possibility of Iron Oxides on the Martian Surface", Icarus 5 (1966) 102.

Sa-68 J. W. Salisbury and G. R. Hunt, "Martian Surface Materials", Science 161 (1968) 365.

Sa-69 J. W. Salisbury and G. R. Hunt, "Compositional Implications of the Spectral Behavior of the Martian Surface", Nature 222 (1969) 132.

Sc-63 C. C. Schnetzler and W. H. Pinson, Jr., "The Chemical Composition of Tektites", in Tektites, ed. by J. A. O'Keefe, Chicago Press (1963).

Se-68 B. Seller, H. Wilson, and F. A. Hanser, "Generation and Practical Use of Monoenergetic X-rays from Alpha-Emitting Isotopes", NYO-3491-3 (1968).

Su-56 H. E. Suess and H. C. Urey, "Abundances of the Elements", Rev. Mod. Phys. 28 (1956) 53.

Tr-66 J. I. Trombka, I. Adler, R. Schmadebek, R. Lamouthe, "Non-Dispersive X-ray Emission Analysis for Lunar Surface Geochemical Exploration", NASA Rpt. X-641-66-344(1966).

Tu-68 Turkevich, A. L., Franzgrote, E. J., and Patterson, J. H., "Chemical Analysis of the Moon at the Surveyor 7 Landing Site: Preliminary Results", Science 162 (1968) 117.

UCRL-50400 E. F. Plechaty and J. R. Terrall, "Integrated Systems for Production of Neutronics and Photonics Calculational Constants", Vol. 6, UCRL-50400 (1969).

Va-64 R. A. Van Tassel and J. W. Salisbury, "The Composition of the Martian Surface", Icarus 3 (1964) 264.

Wa-56 F. G. Watson, Between the Planets, Harvard Univ. Press, Cambridge (1956).

Wa-67 J. S. Watt, "The Use of Gamma-Ray Excited X-Ray Sources in X-Ray Fluorescence Analysis", J. Appl. Rad. Isotopes 18 (1967) 383.

We-70 G. W. Wetherill, "Position Paper on the Need for Measurement of the Major Element Composition of the Martian Surface", presented to the Planetary Exploration Group of the National Academy of Sciences at the Woods Hole Conference, 1970.

Wi-70 H. B. Wiik and P. Ojanpera, "Chemical Analysis of Lunar Samples 10017, 10072, and 10084", Science 167 (1970) 531.

Wo-63 J. A. Wood, "Physics and Chemistry of Meteorites", in *The Moon, Meteorites, and Comets*, ed. by B. M. Middlehurst and G. P. Kuiper, Univ. of Chicago Press (1963).

Wo-70 J. S. Wood, J. S. Dickey, Jr., U. B. Marvin, B. N. Powell, "Lunar Anorthsites", Science 167 (1970) 602.

APPENDIX B

MATHEMATICAL MODEL OF INSTRUMENT RESPONSE

The following is a derivation of an expression for the number of counts per second in a proportional counter sensing characteristic electromagnetic radiation given off by a multi-component specimen and attenuated by divers media between the irradiating source and the specimen and between the specimen surface and the proportional counter.

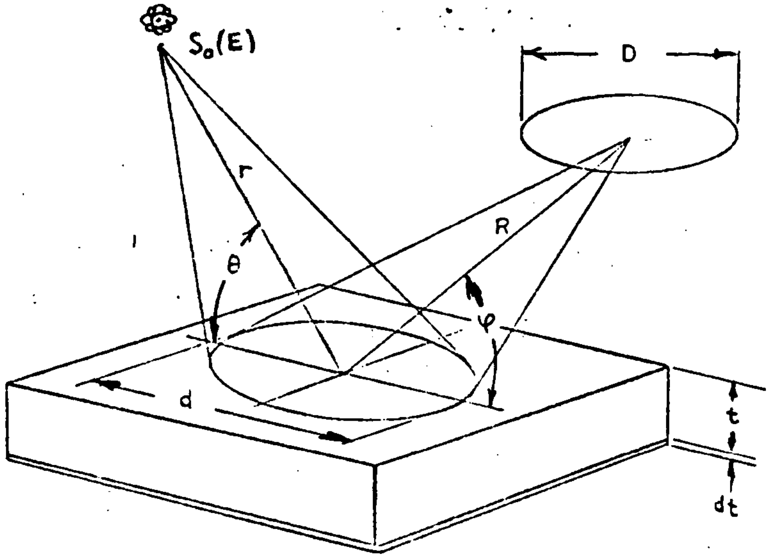

Let $S_o(E)$ = Source strength at energy E in $\frac{\text{photons}}{\text{sec}}$

$\Psi(E_j)$ = Counts per second due to photons of energy E_j (i.e., characteristic radiation from the j^{th} element of the compound)

d = Effective specimen diameter (cm)

D = Diameter of end-window of proportional counter (cm)

r = Source-to-specimen distance (average, cm)

R = Specimen-to-counter window distance (average, cm)

$\mu(E)$ = Mass absorption coefficient of sample for photon energy, E.

$\mu_j(E)$ = Mass absorption coefficient of the j^{th} element in the sample for photon energy, E.

w_j = Weight percent of the j^{th} element in the sample

$\delta\alpha_j$ = K-edge absorption coefficient jump ratio for the j^{th} element

Y_j = K-shell fluorescent yield for the j^{th} element

E_l = Lower energy limit setting of the single channel analyzer

E_u = Upper energy limit setting of the single channel analyzer

$\sigma(E)$ = Standard deviation of the pulse-height distribution produced in the proportional counter by absorption of photon of energy, E.

The irradiating source intensity is provided by any of the following mechanisms:

1. Bremsstrahlung from an x-ray tube, or
2. Characteristic radiation given off by a foil bombarded by α-particles from a radioisotopic source, or
3. Soft x-rays given off by the daughter products of electron-capture radioisotopes.

The amount of excitation radiation (photons/sec) reaching a masked-off area (diameter, d) of the specimen and a distance t below the surface of the specimen is given by

$$S_o(E) \left(\frac{d}{4r}\right)^2 \sin\theta \, e^{-\mu(E)(\csc\theta)t}.$$

At the incremental layer t to t + dt the fraction

$$w_j \left(\frac{\delta\alpha_j - 1}{\delta\alpha_j}\right) \mu_j(E)\, dt$$

is absorbed by the K shell of the j^{th} component of the specimen. The probability of emission of K-shell fluorescent radiation by the j^{th} component after excitation is Y_i, so that the amount of j^{th} component radiation emitted in the incremental layer is

$$w_j \mu_j (E) \left(\frac{\delta\alpha_j - 1}{\delta\alpha_j}\right) Y_j S_o (E) \left(\frac{d}{4r}\right)^2 \sin\theta$$

$$\otimes e^{-\mu(E)(\csc\theta)t} \, dt$$

The fluorescent radiation emitted by the j^{th} component is attenuated by the specimen and only the fraction

$$e^{-\mu(E_j)(\csc\varphi)t}$$

reaches the specimen surface. This radiation is given off in 4π steradians so that only the fraction (approximately)

$$\left(\frac{D}{4R}\right)^2$$

is in the solid angle subtended by the proportional counter.

The contribution of the incremental layer to the total characteristic radiation intensity from the j^{th} component is thus

$$dI(E_j) = S_o(E) w_j Y_j \mu_j(E) \left[\frac{\delta\alpha_j - 1}{\delta\alpha_j}\right] \left(\frac{d}{4r}\right)^2 \left(\frac{D}{4R}\right)^2$$

$$\otimes \sin\theta \, e^{-(\mu(E)\csc\theta + \mu(E_j)\csc\varphi)t} \, dt$$

whereby the total amount of characteristic radiation of energy E_j reaching the surface of the specimen is obtained by evaluating the integral

$$I(E_j) = \int_0^\infty dI(E_j)$$

where it is assumed that the sample is infinitely thick (a good approximation for samples greater than 100 mg/cm^2 thick, i.e., about 0.01 inch for geological samples, irradiated by photons of energy below 25 KeV).

Performing this integral yields the result

$$I(E_j) = S_0(E) w_j \left[\left(\frac{\delta\alpha_j - 1}{\delta\alpha_j} \right) Y_j \left(\frac{dD}{16rR} \right)^2 \mathcal{E}(E_j|E) \right] \tag{1}$$

where we have defined the matrix absorption factor as

$$\mathcal{E}(E_j|E) = \frac{w_j \mu_j(E) \sin\theta}{\mu(E)\csc\theta + \mu(E_j)\csc\varphi} \tag{2}$$

but

$$\frac{\csc\varphi}{\csc\theta} \simeq 1$$

so that

$$\mathcal{E}(E_j|E) \simeq \frac{w_j \mu_j(E) \sin^2\theta}{\mu(E) + \mu(E_j)}$$

Defining a geometric factor, G,

$$G = \left(\frac{dD}{16rR} \right)^2$$

and designating $\epsilon(E_j, \sigma, E_l, E_u)$ as the probability that an absorption of a photon of energy E_j, in the counter, produces a pulse in the window of the single channel analyzer (described by upper (E_u), and lower (E_l) energy limits), then

$$\Psi(E_j) = \epsilon(E_j, \sigma, E_l, E_u) I(E_j)$$

represents the counts per second of radiation of energy E_j before attenuation by various filters.

The computation of $\epsilon(E_j, \sigma, E_\ell, E_u)$ is accomplished by a computer program that normalizes the variable E by the Gaussian transformation

$$Z = \frac{E - E_j}{\sigma} \qquad Z_\ell = \frac{E_\ell - E_j}{\sigma} \qquad Z_u = \frac{E_u - E_j}{\sigma}$$

The distribution is then given by

$$\frac{1}{\sqrt{2\pi}} e^{-\frac{Z^2}{2}}$$

The functional ϵ is given by

$$\epsilon(E_j, \sigma, Z_\ell, Z_u) = \frac{1}{\sqrt{2\pi}} \int_{Z_\ell}^{Z_u} e^{-\frac{v^2}{2}} dv$$

and this integral is evaluated by quadrature.

Now, if $\tau_s(E)$ is the transmission of the filter for the source radiation, $\tau_c(E_j)$ is the transmission of the counter filter, $\tau_w(E_j)$ the transmission of the counter window, and $\alpha(E_j)$ is the probability of absorption in the counter gas, then the net number of counts per second due to radiation of energy E_j in the counter is

$$\Psi(E_j) = \alpha(E_j)\tau_s(E)\tau_w(E_j)\tau_c(E_j)\,\epsilon(E_j, \sigma, E_\ell, E_u)\,I(E_j) \qquad (3)$$

where $I(E_j)$ is given by Equation (1) above.

The above derived relationship does not account for excitation of elements of the multi-component specimen by fluorescent radiation from other elements (matrix enhancement). However, the necessary equations have been developed by Criss and Birks (Cr-68), and we have incorporated the necessary additions to account for secondary fluorescence into our computer program of the mathematical model of instrument response.

In addition to the sample effects discussed above, the results can be seriously affected by various types of inhomogeneities in the sample. The figure in the following page portrays these possibilities. For the first type, inhomogeneity with depth, we have modified the equations above to account for finite sample thickness and layering phenomena. This is an important consideration because of the possibility that weathered coatings may cover the soil grains found on Mars. Lateral inhomogeneities are relatively unlikely to occur because of the small sample size (less than on inch in diameter). Particle effects are relatively unimportant provided the sample is a natural soil. Experimentally, the only cases of this type where differences have been noted between ground and unground samples are for whole rock specimens wherein the crystals are large and of distinctly different composition.

From the mathematical model outlined above, we have constructed a computer program to allow systematic variation of all parameters which could affect the scientific performance of the instrument. This computer program includes the following factors: energy and source strength of two independent radioisotope excitation sources, source to sample distance, sample to detector distance, sample size, detector window diameter, detector window composition and thickness, detector gas filling composition and pressure, angle of incidence of excitation radiation, exit angle of fluorescent radiation, measurement time, thickness and composition of two independent filters, filter absorption, fluorescent radiation produced in each filter, amount of radiation coherently scattered by sample from sources, detector resolution, detector gain, drift in system gain, low and high energy discriminator settings, the sample matrix effects of (1) internal absorption of fluorescent emissions and (2) secondary fluorescent excitation of one element by another element in the sample, background gamma radiation spectrum from the radioisotope thermo-electric generators, fluorescent yields of the elements, mass absorption coefficients of the elements, and sample composition. The program is capable of two distinct output modes. The first of these plots and prints out the pulse height spectrum predicted for a given set of conditions. The second is used to calculate the standard deviation and minimum detection limit for each element under the prescribed instrument setup conditions.

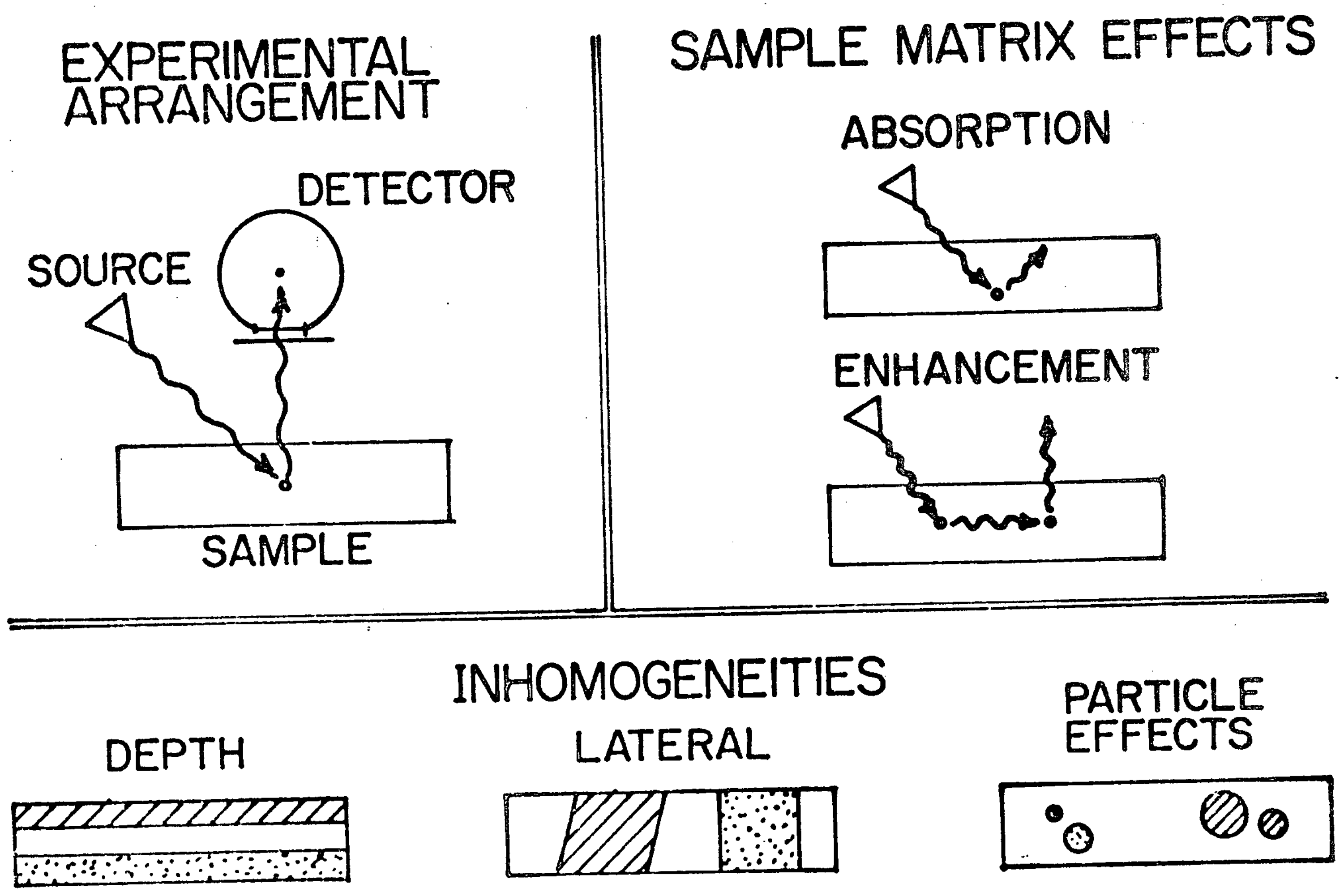
EXPERIMENTAL ARRANGEMENT
DETECTOR
SOURCE
SAMPLE
SAMPLE MATRIX EFFECTS
ABSORPTION
ENHANCEMENT
INHOMOGENEITIES
DEPTH
LATERAL
PARTICLE EFFECTS

APPENDIX C

MINIMUM DETECTION LIMITS

On the following pages are a few illustrative examples of some of the methods used to establish the minimum detection limits given in Table I of the text.

Iron and Nickel , Importance of and Detection of

Iron is a key element in the geochemical evolution of planetary matter. It is extremely abundant from the cosmic standpoint, being even more abundant than silicon according to Cameron, and only slightly behind silicon, sulfur, and magnesium according to Aller. As a whole, the earth probably contains more iron than any other element, even oxygen (e.g., see Mason). On the earth's surface, iron is ubiquitous, except in certain sedimentary differentiates such as desert sands and carbonate deposits. The redish color of Mars is almost certainly due to ferric oxide, but this does not necessarily imply a high iron content. For example, we have found that certain of the blood-red sands of Australia contain less than 1% iron. The detection of iron with the Advanced Breadboard is shown in Fig. 1. In an SiO_2 matrix, 0.03% iron is detected. In a $CaCO_3$ matrix, the sensitivity is less, but still at least 0.25%.

Nickel is also a key element. It is an important constituent of meteorites (up to 20%) and is considered to have a high cosmic abundance since its concentration in the sun is likewise high. An important constraint upon theories of planetary evolution is to explain the strong depletion in nickel in the earth and lunar surfaces. Nickel is strongly siderophilic and therefore probably concentrated in the earth's iron core. But the moon and Mars do not appear to have large cores. Thus, the concentration of nickel in the surface of Mars is potentially of great diagnostic significance.

Nickel is difficult to resolve by the alpha backscatter technique and would only be detected if at least as abundant as iron (highly improbable). It is also somewhat difficult to resolve with X-ray fluorescence because of interference from iron. Nonetheless, we have detected nickel as low as 0.3% in an iron matrix (see Fig. 2) and as low as 1% in an iron-silicate matrix.

Good Sensitivity for Detecting Titanium

As a diagnostic indicator, titanium is often a key element. Nearly all meteorites are low in this element ($< 0.1\%$), whereas in the earth's crust, the average abundance is much higher ($> 0.5\%$). The finding that titanium is high (up to 7.5%) in samples from the lunar maria places an important experimental constraint on theories of the origin and history of the moon.

Sands on earth are sometimes relatively rich in this element as compared to other elements since the titanium bearing minerals rutile, titanium-magnetite, and ilmenite are resistant to chemical and mechanical breakdown. On Mars, eolian action may also produce segregation of titanium minerals.

Measurement of this element is therefore important. The XRFS is well suited for titanium determinations because the Fe-55 source can be used to excite titanium without exciting iron, its most common accompanying element. The only potentially interfering element is calcium. To establish the minimum detection limit, we selected a silica-rich sand matrix.

With the energy discriminators set for titanium and taking a four minute count, a level of 0.1% titanium was detected as an increase by 600 counts over the background count of 1800 (chiefly due to backscatter of Fe-55 photons) in the blank. Even with a five-fold excess of calcium, titanium at the 0.3% level was easily detected. All this was without the use of filters. With selective filtration, we think we can lower the minimum detection limit significantly.

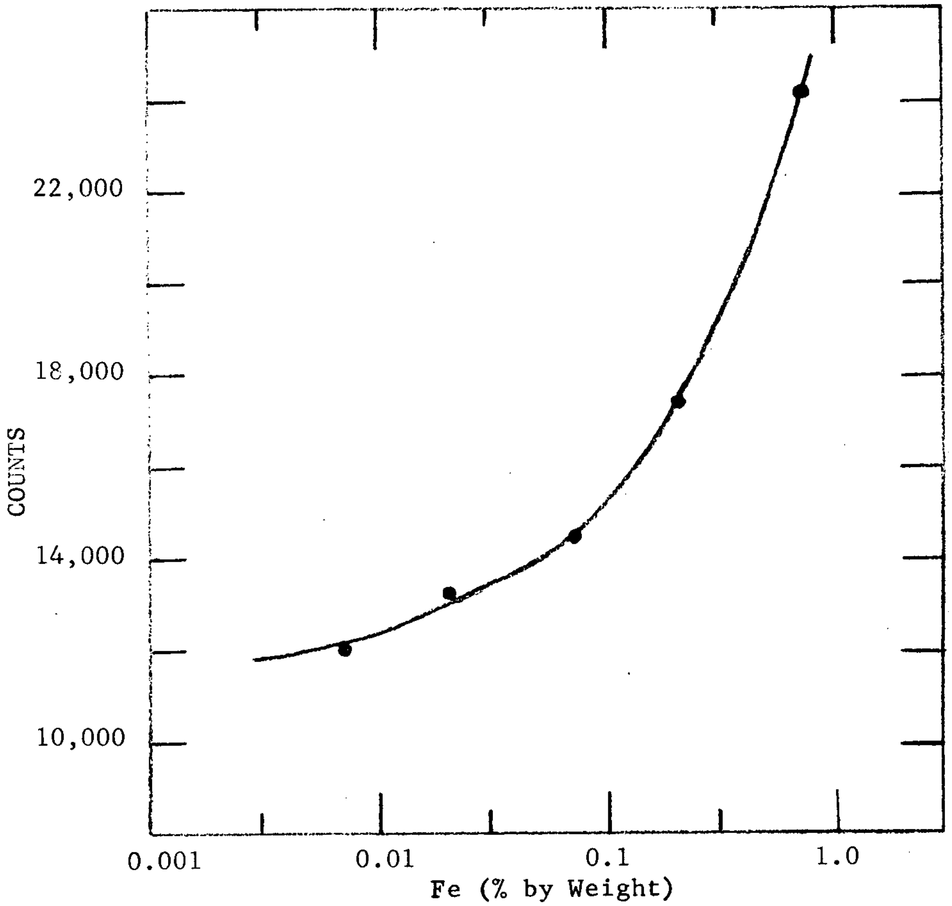

Fig. 1. Counts recorded in the Fe channel versus Fe concentration in a silicate matrix.

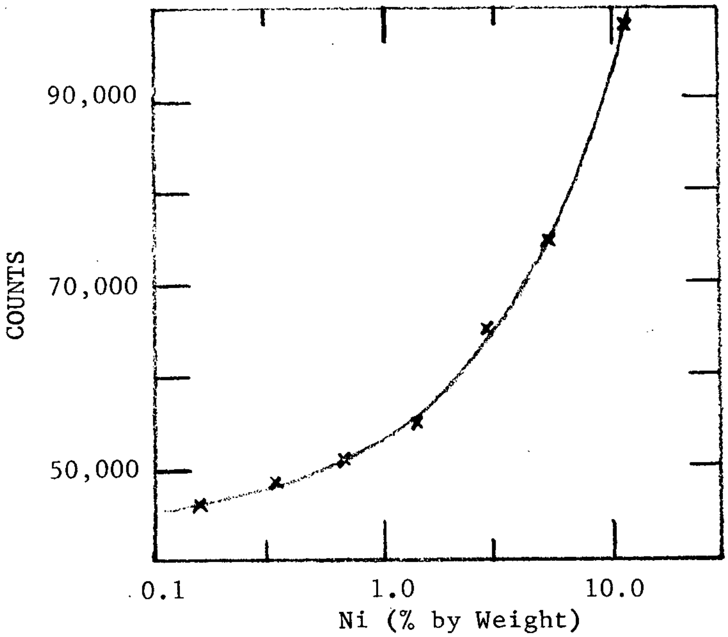

Fig. 2. Counts recorded in the Ni channel versus Ni concentration in an Fe matrix.

APPENDIX D

EFFECT OF THE MARTIAN ATMOSPHERE

XRFS Performance Unaffected by Martian Atmosphere

Some time ago we calculated the effect of the Martian atmosphere on the XRFS. Fluorescent x-rays emitted from the sample could be attenuated as they travel the 2 cm path to the detector. However, the calculations showed this to be very minor. For a pure CO_2 atmosphere at 6 millibars and 0°C, x-rays from all elements above Si are transmitted at greater than 99%, and for Mg, Al, and Si, the transmission factors are all quite high, being 95%, 96%, and 98%, respectively. Even for hypothetical worst-case Martian atmospheres, containing up to 5% N_2 and 5% Ar, the transmission factors remain at the levels given above. We concluded that although the Martian atmosphere should be allowed for in the analysis of the data, there is no significant degradation in the quality of the data obtained and hence no degradation of instrument performance. In the graph below, we offer experimental evidence recently obtained showing the near-equivalence of spectra taken in vacuum versus spectra taken under 6 millibars of CO_2 for two different specimens.

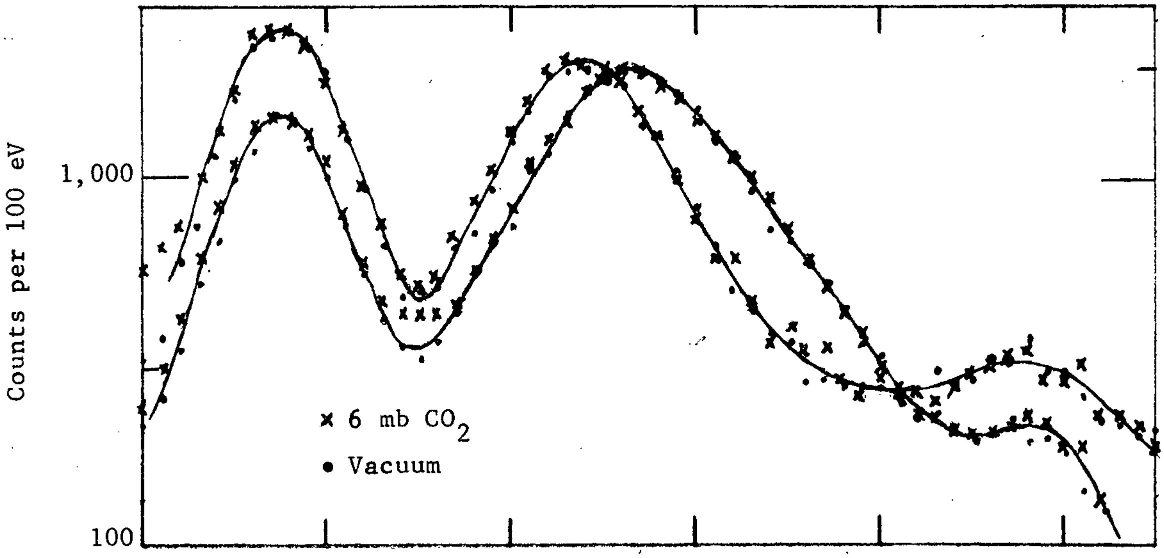

Counting time: 1 minute, each spectrum.
The two examples shown are G-2 and BCR-1.

APPENDIX E

ELECTRONICS

Description

The X-ray fluorescence spectrometer consists of two radioisotope sources (no electrical requirements), four proportional counter detectors, and the necessary support electronics, including power converter and regulator, detector bias voltage supply, preamplifier-amplifier train, window discriminator, data accumulator, memory, and all command and control logic necessary to interface with the Viking Lander. Fig. 1 shows the block diagram of the instrument while Fig. 2 presents the circuit in greater detail. (Note: only two counters are shown in Fig. 1 for simplicity.)

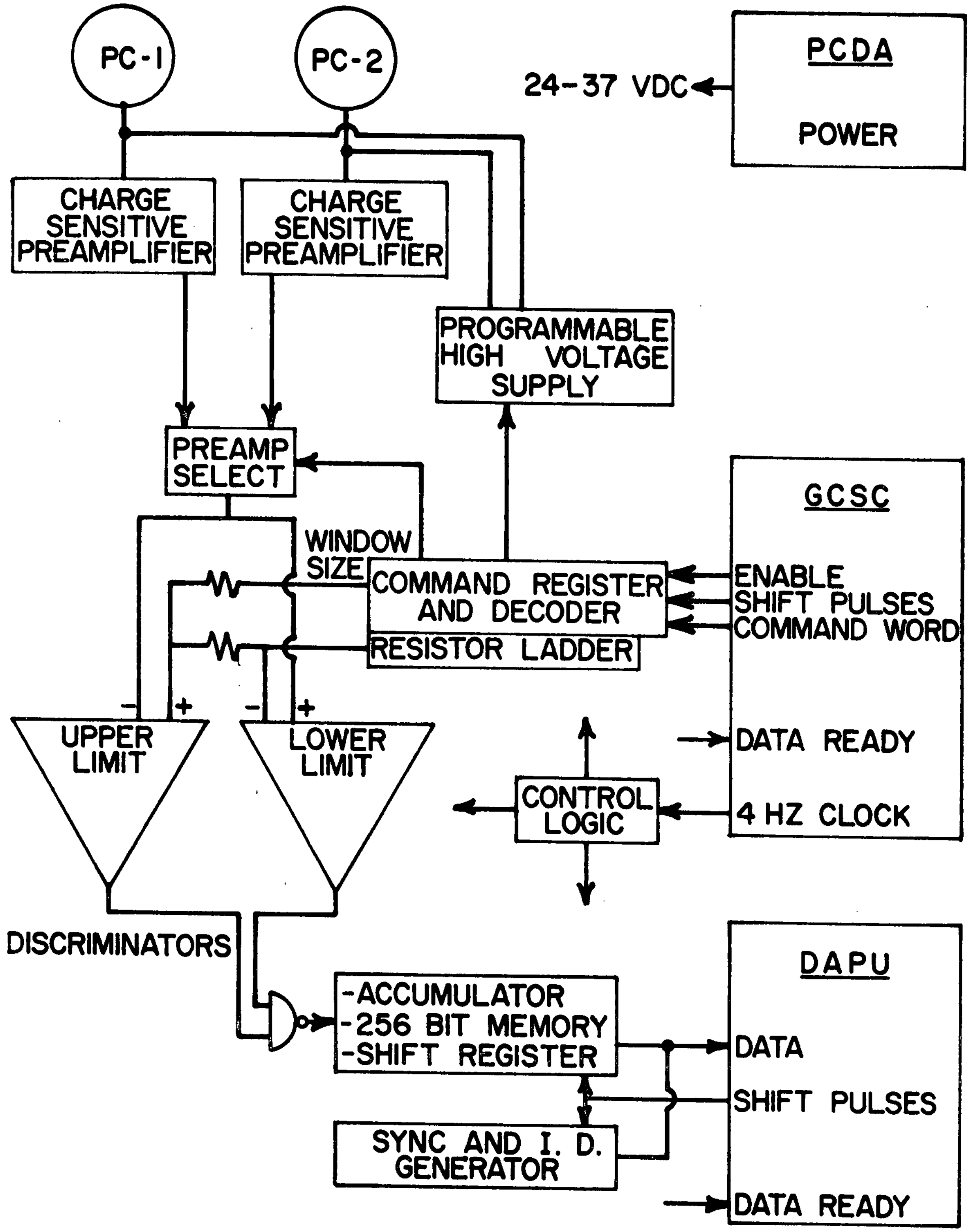

X-RAY INSTRUMENT WITH 16 MINUTE MEMORY (256 Bits)

Charge Sensitive Preamplifier/Amplifier

The proportional counters convert the X-rays into impulses of charge. Each impulse contains a quantity of charge proportional to the energy of the X-ray. The quantity of charge in each impulse ranges from 6×10^{-15} Coulomb to 1.2×10^{-13} Coulomb, corresponding to X-rays with energies from 1 KeV to 20 KeV, respectively. The charge sensitive amplifier does three things with these charge impulses: (1) the output of the charge sensitive amplifier is a voltage pulse whose peak value is proportional to the quantity of charge contained in each impulse, (2) the output pulse shape is adjustable by the circuit configuration so that it resembles a Gaussian curve (this shape is optimum for an accurate analog to digital conversion, i.e., as performed by the window discriminator) and (3) the pulse duration rise time and fall time is chosen such that no interaction between pulses occur at pulse rates up to 10,000 per second. The tail of any given pulse must be down to less than 1/256 of its peak amplitude before the start of the next pulse. A preamplifier/amplifier circuit specifically developed for this application is shown in Fig. 4. This circuit has been designed, fabricated, and tested in printed circuit form using Viking approved parts and design techniques.

Preamplifier Select Switch

Either preamplifier can be switched into the system by use of an electronic switch. This device uses field effect transistors which can route pulses without injection of noise or distortion of waveshapes. The switches are operated by one bit in the command register.

Window Discriminator

The pulses from the preamplifier select switch are sorted out into 256 channels which correspond to 256 different voltage levels (and likewise correspond to 256 different X-ray energy levels). Each channel has a width which corresponds to either 0.1 KeV or 0.2 KeV X-ray energy. Only one channel is monitored at any given time. The lower limit of each channel is determined by comparing the incoming pulses with a voltage established in a resistor ladder. The ladder voltage is controlled by 8 bits of the command register. The width of each window is controlled by one bit in the command register.

The window discriminator is composed of the resistor ladder, 2 operational amplifiers used as comparators, and a 4-input NAND gate. Each operational amplifier compares the incoming pulse with a reference voltage. The reference voltage (V_R) for the lower limit discriminator (LLD) is established by the resistor ladder and command word. If the pulse exceeds the reference voltage then a positive logic level appears momentarily at the output of the LLD. The reference voltage ($V_R + \Delta V$) for the upper limit discriminator (ULD) is established by the same reference used by the LLD plus a small incremental voltage. The small incremental voltage (ΔV) comes from another resistor tied to one bit of the command register. This small increment determines the energy window width. If the incoming pulse is less than this composite reference voltage ($V_R + \Delta V$) on the ULD then a positive logic level appears on the ULD output. If the pulse voltage is higher than this composite reference then no output appears.

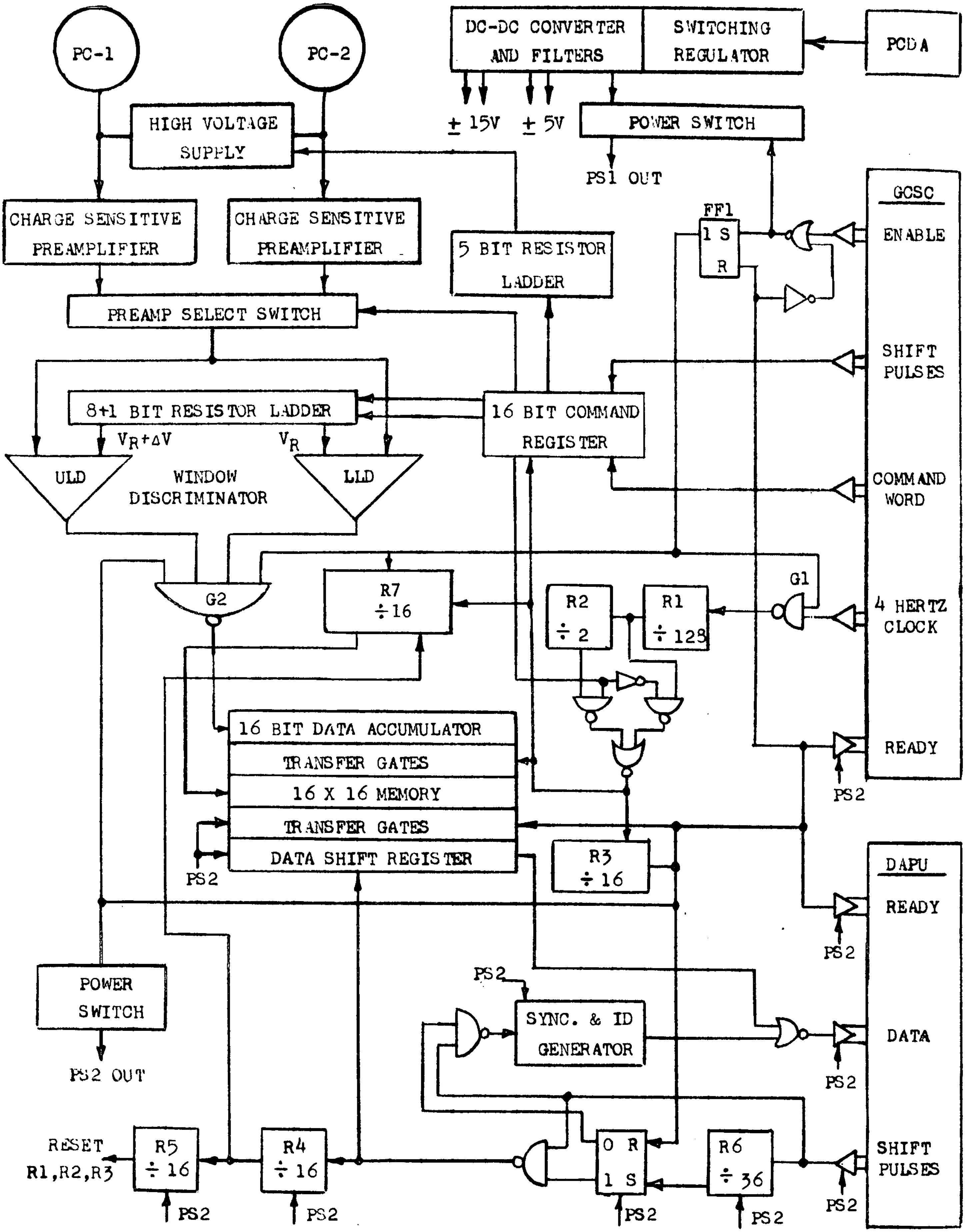

FIGURE 2. X-RAY INSTRUMENT DATA AND LOGIC DIAGRAM

The NAND gate will respond only if both discriminators put out a positive logic level. (The third and fourth lines into the NAND, coming from the system inhibit logic to be discussed later, must also be positive for the NAND to respond.) Thus, if an output from the NAND occurs, this means that the original pulse must have been greater than V_R and less than $V_R + \Delta V$. The output pulses from the NAND are negative in direction and have a duration of less than 0.1 microsecond. The width of this pulse is much shorter than the preamp output pulse and also depends on the shape of that pulse.

16 Bit Data Accumulator

The pulses from the window discriminator are counted in a 16 bit binary ripple counter. This counter is capable of holding $2^{16}-1 = 65,535$ pulses. Each accumulation of pulses in this register represents events in one channel of the 256 available channels. The duration of this counting period is either 32 or 64 seconds as commanded by one bit of the command register. The precise timing of this counting period is implemented by the R1 (divide by 128) and R2 (divide by 2) counters. These counters use the 4Hz clock from the Lander Computer (GCSC) for input. If only a 32 second counting period is utilized the command bit labelled data transfer frequency locks out the divide by 2 counter. This makes all data control functions occur at twice the normal rate. This mode will be utilized if a particular geological specimin provides higher X-ray count rates than nominal. If a counting period of 64N seconds is desired for each channel then the entire 256 channel spectrum is exercised N times. This will only be necessary for low X-ray yield.

16 x 16 Memory

The 16 x 16 memory is mostly contained in one microcircuit. A small amount of supporting logic is also required. Once each counting period the contents of the 16 bit accumulator is transferred to 16 bits of the 256 bit memory. This transfer occurs each time the R1 (or R1 and R2) counters become full. The memory address register is a 4 bit register R7. After the transfer is complete, a trigger pulse increments these 4 bits by one binary count. This trigger also moves the window discriminator up to the next window.

The pulses going to the accumulator are not inhibited during this transfer to the memory since the transfer can be made in less than 16 microseconds. Even at the highest anticipated counting rate (10,000 counts/sec), the average time between pulses going into the window discriminator is 100 microseconds. After the discriminator the minimum time between pulses is in milliseconds. The inhibitor therefore would not improve accuracy during data transfer to the memory.

After 16 words of 16 bits each have been stored, the memory contents must be transferred to the Data Acquisition and Processing Unit (DAPU). This normally occurs every 17.1 minutes. The divide by 16 counter (R3) raises the data-ready flag to the DAPU and GCSC. The instrument must now wait for the Lander to transfer data to the DAPU. In the meantime, the output of the window discriminator is inhibited from sending more data to the accumulator. This is necessary because the time from data ready to shifting data out to the DAPU is variable. It may be less than one second or more than 15 seconds.

Data Transfer Logic

Data transfer to the DAPU is accomplished in the following sequence:

1. The first 36 shift pulses from the DAPU are used to clock out a 31 bit psuedorandom synchronization word and a 5 bit instrument identification word. A divide by 36 counter and several other logic elements route the shift pulses to the sync and I.D. generator during this period.

2. Beginning with shift pulse number 37, the shift pulses are routed to the data shift register where the last 16 bits of the memory are contained. These bits are shifted to the DAPU after which the next 16 bits are transferred from the memory to the shift register. This requires the 4 bit memory address register to count backwards by one binary number for each 16 shift pulses.

3. After 16 words have been shifted out of the memory the data ready flag must be lowered. This is accomplished with the R5 counter. After the memory address register has received 16 count backward pulses, the R5 counter resets the R1, R2, and R3 counters tied to the 4 Hz clock. The reset of the R3 counter lowers the data ready flag which terminates the DAPU shift pulses.

4. Note that the R3 counter operates power switch number 2. Those portions of the data logic with the PS2 arrow are powered down over 99% of the time with this switch. These devices are only on for the duration of data ready and data transfer to the DAPU.

Command Logic

After application of power from the Power Conditioning and Distribution Assembly (PCDA) the enable line from the GCSC rises. This applies power to those devices having a PS1 arrow attached. Sixteen shift pulses and a 16 bit command word are then clocked into the command register. The command world contains the following information:

1. Eight bits to set the LLD of the window discriminator to its starting position.

2. Five bits to set the high voltage supply to a voltage between 400 and 1220 volts.

3. One bit to set the window size (0.1 or 0.2 KeV) on the window discriminator.

4. One bit to determine either 32 or 64 second counting periods per channel.

5. One bit to select one of the preamplifiers.

When the enable line falls at the end of the command word transfer, flip-flop 1 is set. This turns on gate G1 and allows the 4 Hertz clock to enter the instrument. The logic then begins counting for the 32 or 64 second intervals. At the same time G2 is turned on and the pulses from the window discriminator are allowed to pass to the accumulator. After 16 of the 32 or 64 second counting periods have occurred the ready flat is raised which turns flip-flop 1 off. After data transfer to the DAPU FF1 is set and the next 16 counting periods commence.

Power Converter

The power consumption of the X-ray instrument is under one watt. This is accomplished by first utilizing a switching regulator to convert the Lander 24-37 VDC to a 20 volt regulated source. This 20 volts then operates a DC-DC converter which provides ± 15 volts and ± 5 volts to the instrument. The blocking oscillator and the operational amplifiers utilize the ± 15 volts. The interface transmitter-receivers and logic microcircuits utilize the ± 5 volts.

Detector Bias Voltage Supply (Fig. 3)

This supply must furnish 400 to 1220 VDC with 0.1% regulation over a 4 hour operating period. The range of voltages available to proportional counter 1 is 400 to 1020 volts in 31 increments of 20 volts each. Proportional counter 2 is provided 600 to 1220 volts, also in 31 increments of 20 volts each. The 31 increments are provided by inserting a resistor ladder in the feedback loop of a stabilized voltage reference, A2. The resistance of the resistor ladder depends on the state of 5 low V_{sat} transistors (2N2432). These transistors are driven by 5 stages of the command register.

The output of the stabilized voltage reference is compared at A1 to a sample of the high voltage. The output of comparator A1 provides the DC voltage which runs a blocking oscillator. A blocking oscillator was chosen because of its extreme reliability and small size. A high voltage winding on the blocking oscillator transformer provides up to 300 volts peak-to-peak. This pulsed voltage is rectified and filtered in a voltage quadrupler. By using only a 10:1 turns ratio transformer and a voltage quadrupler, very few parts experience the full 1220 volts. No two points in the transformer experience more than 150 + 15 = 165 volts difference. Each capacitor and diode in the multiplier never sees more than 300 volts between its terminals. The two final filter capacitors C1 and C2, however, must be capable of withstanding 1020 and 1220 volts, respectively.

The largest load on this high voltage supply is caused by the 10^{-9} amp. leakage in the quadrupler diodes. This is at least 3 orders of magnitude above the load provided by the proportional counters. This will allow fairly small parts to be utilized in this supply since only $P = 1220$ volts x 10^{-9} amp. = 1.22 microwatts is required. The high voltages are the only constraint to very dense packaging.

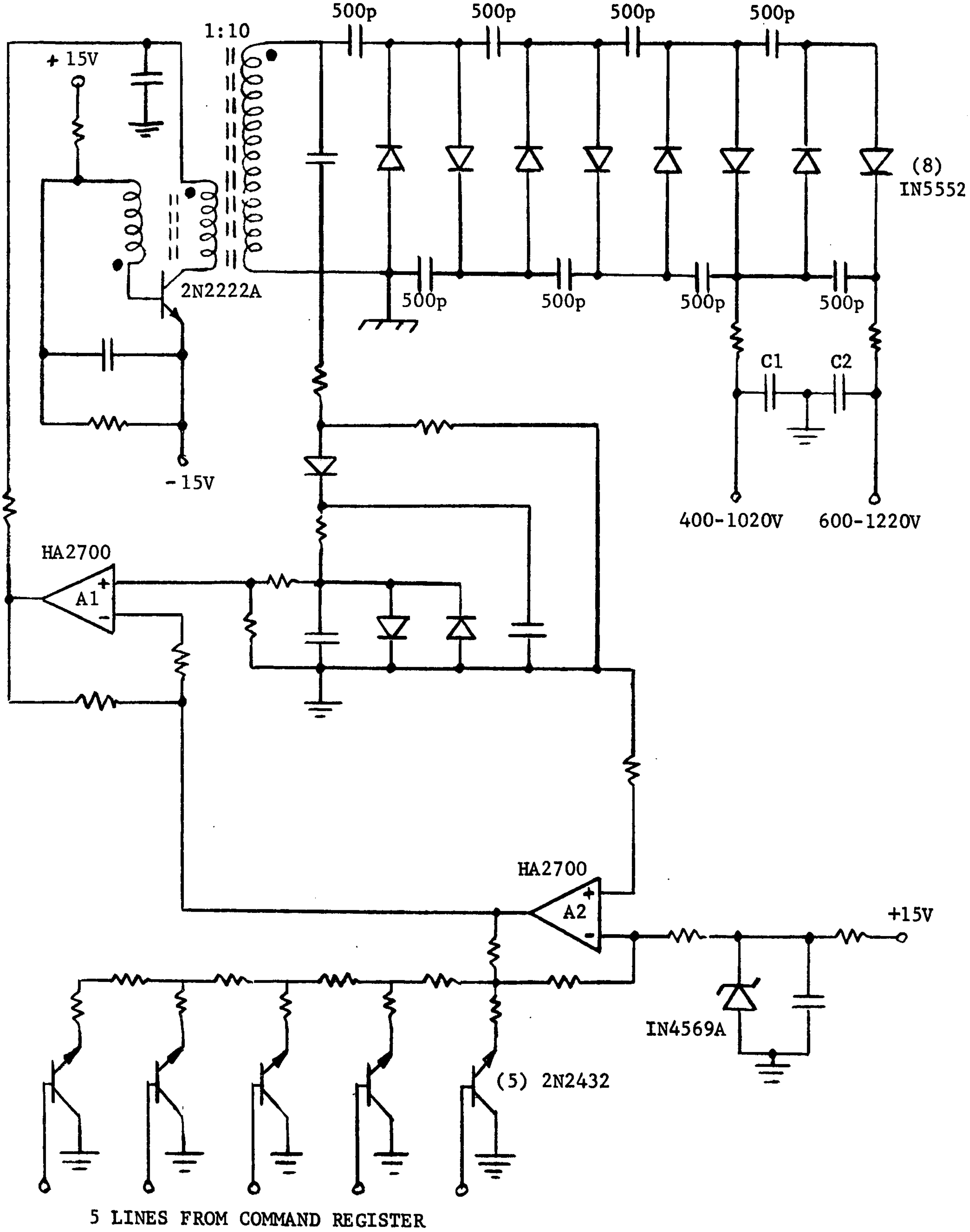

FIGURE 3. HIGH VOLTAGE POWER SUPPLY

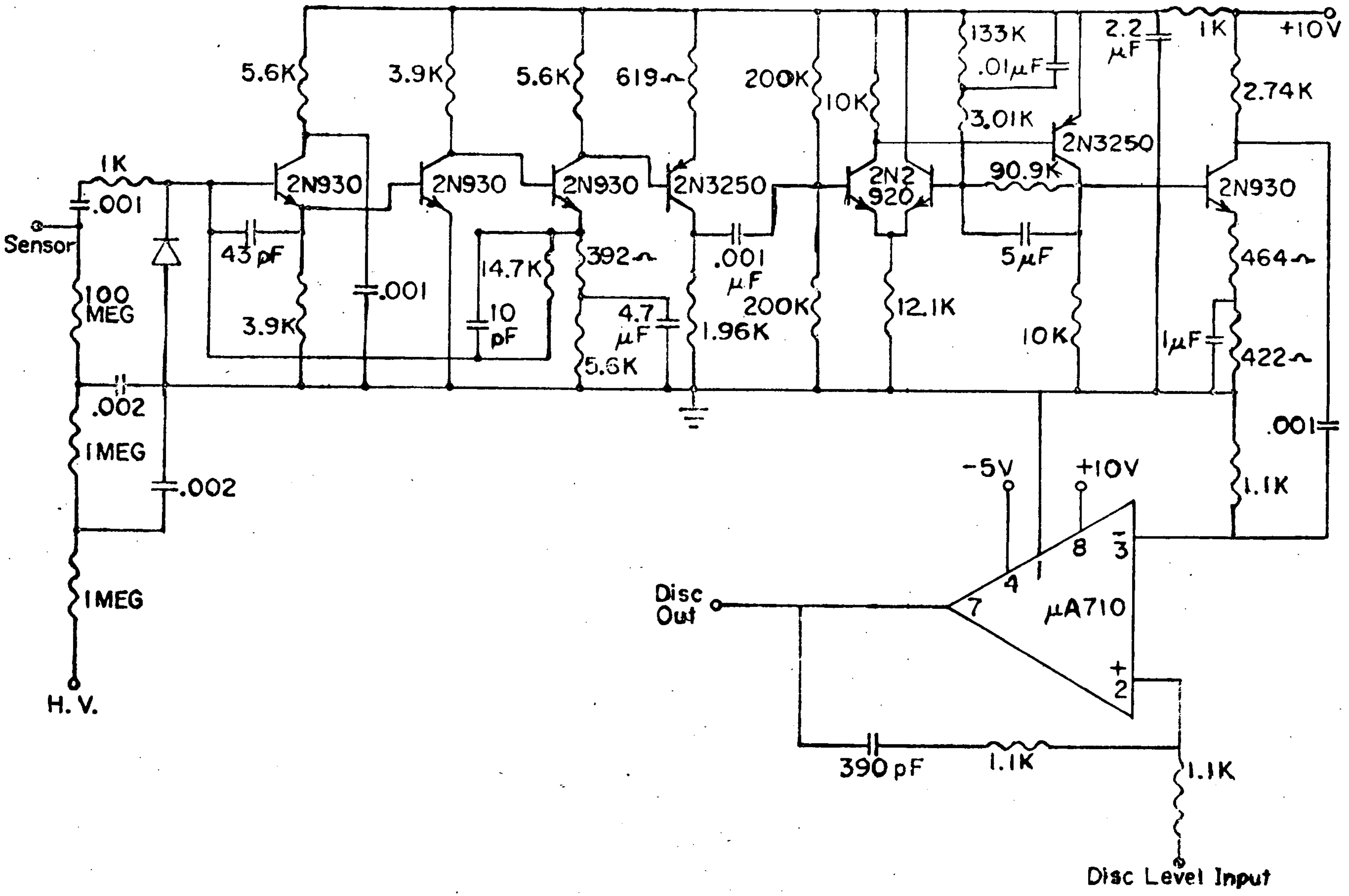

Fig. 4. Preamplifier, Amplifier, and Discriminator Electronics

MANDATORY PARTS LIST (ONE INSTRUMENT)

MPL Number	Description	Chip or Packaged	Quantity
SV99D54-100	Quad 2-Input Gate	C	10
SV99D54-104	Hex Inverter	C	2
SV99D54-110	Triple 3-Input Gate	C	1
SV99D54-173	Dual J-K Flip-Flop	C	24
SV99D54-195	SR/SL Register	C	10
SV99D245-1	Triple Line Transmitter	C	1
SV99D245-2	Triple Line Receiver	C	2
SV2N2222A	General Purpose NPN	C	6
SV2N2432A	Low V(SAT) Chopper	C	7
SV2N2484	Low Noise NPN	C	8
SV2N2920	Dual NPN	C	1
SV2N3251A	General Purpose PNP	C	4
SV2N5196	Dual FET	C	1
SV1N3595	Low Leakage Diode	C	14
SV1N4565A	Voltage Reference	P	5
SV1N5552	600 Volt Diode	P	8
SV79D1	Zener Diode	P	2
SV90DM39003	Tantalum Capacitor	P	15
SV90DM39014	Ceramic Capacitor	P	12
	Ferrite Toroid	P	1

CONDITIONAL PARTS LIST (ONE INSTRUMENT)

Number	Description	Chip or Packaged	Quantity
HA2700	Low Power Operational Amp.	C	4
1101	256 Bit Memory	P	1
	Disk Capacitors (600 V)	P	9
	Disk Capacitors (2000 V)	P	4

XRFS POWER SUMMARY

Electronics Group	Power (Watts)
High Voltage Supply	.060
Preamplifiers	.040
Command Logic	.210
Interfaces	.020
Memory-Accumulator	.120
Data Logic	.020
Discriminator	.020
	.490
Assume 70% efficient converter	.210
Total average input power	0.70 watts

APPENDIX F

RADIOISOTOPE SOURCES

A careful survey of available radioisotope sources led to the decision (see Appendix N) to use independent Fe-55 and Cd-109 soft X-ray sources to stimulate the fluorescent radiation from the samples. These radioisotopes are excellent choices from the standpoint of radiation safety for the following reasons:

1. Neither emit penetrating radiation, their emanations being confined to soft X-rays and very low energy gamma rays.

2. Both are available with very high radiochemical purity, thereby avoiding hazardous radiation from contaminating radioisotopes.

3. Being metals, they may be electroplated onto a supporting structure, providing for excellent containment.

Source design and fabrication procedures have been carefully tailored to this particular application to guarantee compatibility with the Viking Lander system and provide the greatest possible safeguards with respect to radiation safety. The fabrication technique devised is shown in the figure on page J-2. After the radioactive material is electroplated onto a suitable foil (Fe-55 onto nickel foil, Cd-109 onto silver foil), the foil is heat treated. In the case of Fe-55, the treatment is at 800°C, producing a diffusion bond between plating and substrate. In the case of Cd-109, the treatment is at a lower temperature (160°C) because of the high vapor pressure of cadmium. At this point the sources are of very high integrity. Even if the foils were not encapsulated, the sources would not leak radioactive material. However, to provide an extra degree of protection, each foil is placed in an aluminum tube and the ends cold-welded shut to provide a hermetically sealed unit.

Procurement specifications for these sources are given on pages J-3 through J-5. Test procedures followed on prototype sources already delivered are given on pages J-6 and J-7. In the past five months, these prototype sources have been exposed to many harsh environments, including repeated cycling to vacuum. No losses in radioactivity have occurred.

The vendor selected for prototype units is Isotope Products Laboratories, Burbank, California 91502. This company has a long record of supplying radiation sources for use on space missions and is well acquainted with the stringent quality control, testing, and documentation requirements of space programs. Page J-10 summarizes the relevant experience of this company.

SPACE-RATED RADIOISOTOPE SOURCE

MARTIN MARIETTA
DENVER DIVISION

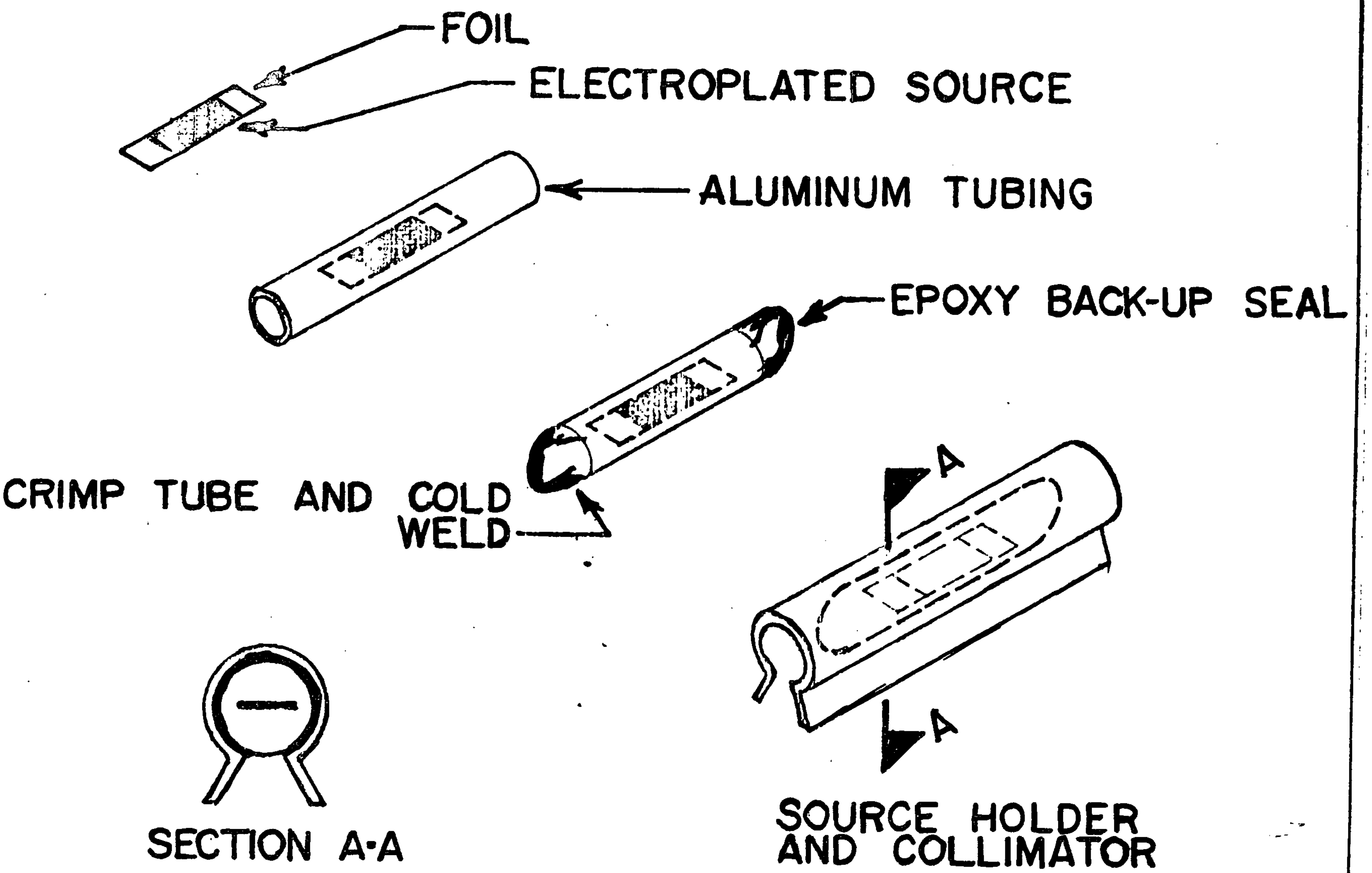

PROCUREMENT SPECIFICATION FOR IRON-55 SOURCE

Physical Description: The source shall be fabricated to the dimensions given in Figure 1. The radioactivity shall occupy the area indicated by cross-hatching and shall be uniformly distributed over this area.

Source Material: Iron-55 radioisotope with less than 0.1% contamination by other radionuclides shall be employed. The specific activity shall be determined, and shall not be less than 20 Ci/g.

Materials of Fabrication: The radioactivity shall be electroplated on one side of a nickel foil (minimum purity, 99.9%). The plating shall consist of not less than 99.9% iron. The plated foil shall be placed inside aluminum tubing of 0.0005 inch or less wall thickness and cold welded at each end.

Source Strength: The quantity of Fe-55 radionuclide after annealing and post-annealing testing shall be not less than (TBD) mCi.

Fabrication Procedures: Upon completion of plating, the radioactive source shall be examined visually for plating uniformity and then annealed at 800°C in a hydrogen atmosphere for not less than 60.0 minutes.

Testing:

1. Post-annealing. The source shall be placed in distilled water and subjected to ultrasonic vibration (equipment specification, TBD) at a power setting of (TBD) for not less than 5 seconds. The source shall then be removed and the water checked for radioactivity. This test may be repeated using fresh water should first results indicate significant losses of radioactive material. All results, however, shall be reported.

2. Post tube seal. The completed source shall be immersed in a suitable fluid under temperature and pressure conditions optimized to detect leaks via bubble formation. The source shall also be exposed to vacuum (less than 0.1 Torr) for not less than one hour and then inspected for integrity of the aluminum tube seal.

PROCUREMENT SPECIFICATION FOR CADMIUM-109 SOURCE

Physical Description. The source shall be fabricated to the dimensions given in Figure 1. The radioactivity shall occupy the area indicated by cross-hatching and shall be uniformly distributed over this area.

Source Material. Cadmium radioisotope with less than 1% contamination by other radionuclides shall be employed. The specific activity shall be determined, and shall not be less than 2.5 Ci/g.

Materials of Fabrication. The radioactivity shall be electroplated on a silver foil (minimum purity, 99.0%). The plating shall consist of not less than 99.0% cadmium. The plated foil shall be placed inside aluminum tubing of 0.005 inch wall thickness and cold welded at each end.

Source Strength. The quantity of Cd-109 radionuclide after annealing and post-annealing testing shall be not less than (TBD) mCi.

Fabrication Procedures. Upon completion of plating, the radioactive source shall be examined visually for plating uniformity and then annealed at 160°C in a suitable atmosphere for not less than 60.0 minutes.

Testing

1. Post-annealing. The source shall be placed in distilled water and subjected to ultrasonic vibration (equipment specification TBD) at a power setting of (TBD) for not less than 5 seconds. The source shall then be removed and the water checked for radioactivity. This test may be repeated using fresh water should first results indicate significant losses of radioactive material. All results, however, shall be reported.
2. Post tube seal. The completed source shall be immersed in a suitable fluid under temperature and pressure conditions optimized to detect leaks via bubble formation. The source shall also be exposed to vacuum (less than 0.1 Torr) for not less than one hour and then inspected for integrity of the aluminum tube seal.

TESTING PROCEDURE IN ACCORDANCE WITH
ATTACHMENT A PR 367666
RADIOISOTOPE SOURCE, CADMIUM-109

Quality assurance tests were performed at the following three stages of fabrication process:

1. Fabrication of the dummy capsule.
2. Fabrication of a tracer active element.
3. Fabrication of active element and capsule. Except for the radioactive content the tracer active element corresponds identically to the active element in all respect including total mass of electro-deposited cadmium. The activity level is approximately 0.001 that of the active element.

TEST PROCEDURE

1. Dummy Capsule
   - A. A sealed dummy capsule was subjected to a vacuum of 0.1 torr for one minute and visually observed for deformation. No dimensional change could be seen.
   - B. The dummy cold welded capsule was submerged under 1" of toluene and subjected to a vacuum of 10 cm. Hg. No bubbling could be observed from the body or welded ends.
2. Tracer Active Element
   - A. The tracer element was observed at 20X and no evidence of peeling or roughness could be seen. 70 - 80% of the active deposit appeared to be on one side.
   - B. The tracer element was vibrated ultra-sonically in distilled water for one minute. No change in the surface condition could be observed.

C. The tracer element was heated in an oven at 160° in air for one hour. No visible change was evident nor was there any decrease in activity.

3. Active Element and Capsule

A. The active element was examined at 20X. No peeling of the electro deposited surface could be seen. 70 - 80% of the deposit was on one side of the silver ribbon.

B. The encapsulated source was placed under 1" of toluene and subjected to a vacuum of 10 cm Hg. No bubbling could be observed from the body or from the welded ends.

C. The encapsulated source was wipe tested and no sign of removable activity detected.

Karl Amlauer
Technical Director

KA:gh

May 28, 1971

RELATED EXPERIENCE

ISOTOPE PRODUCTS LABORATORIES

ORGANIZATION	EXPERIMENT
Aerospace Corporation	OV-117
American Science and Engineering	Apollo 14-19
Analog Technology Corporation	OSO-H, Apollo 16
AVCO Missiles	Re-entry studies
University of California-Space Science Laboratory	
University of Calif. San Diego	OSO, Pioneer
Cornell University	
John Hopkins University	IMP H & J
University of Minnesota	ATS F
Jet Propulsion Laboratory	
Lockheed Missile and Space Co.	ATS
Mass. Institute of Technology	OSO H
Goddard Space Flight Center	OSO H and others
Naval Research Laboratory	
TRW	Solrad*

APPENDIX G

X-RAY DETECTORS (PROPORTIONAL COUNTERS)

The X-ray detectors employed are proportional counters which were specifically designed and manufactured for this application. These types of detectors have an outstanding record of flight history (see pages K-11 through K-13 of this appendix), and have been used extensively by workers in the fields of cosmic rays, Van Allen belt exploration, and X-ray astronomy. Numerous trade-off studies were performed and eventually led to the selection of proportional counters over other types of detectors (see discussion in Appendix N).

Specifications and performance characteristics of the counters are given in pages K-2 through K-9. The vendor selected to provide prototype devices was Reuter-Stokes, Cleveland, Ohio 44128. This company has excellent experience in fabricating proportional counters to rigid space-program requirements, as evidenced by the data provided on page K-10. In the four months of testing of the prototype counters, no degradation of resolution or other performance parameters has been observed, despite repeated cycling to vacuum and exposure to rather severe transportation and handling environments. Drifts in gas gain have been less than ±3% total over the four month test period.

PROPORTIONAL COUNTER SPECIFICATION

Type SK-666

Window: 0.002 inch beryllium

Gas fill: 20% xenon, 76% neon, 1% helium, 3% carbon dioxide

Liner: Aluminum

Other specifications: Per following pages

Type SK-667

Window: 0.001 inch beryllium

Gas fill: 96% neon, 1% helium, 3% carbon dioxide

Liner: None

Other specifications: See following pages

PROCUREMENT SPECIFICATION FOR PROPORTIONAL COUNTER

1. Physical Description - The proportional counter (PC) shall be fabricated to the dimensions given in Figure 1. The PC shall be as lightweight as possible within the design objectives given below, but in any case shall not exceed 30.0 grams. The anode wire shall be one mil nominal diameter. The counter body shall be stainless steel. When a liner is specified, it shall be of aluminum, not less than 0.040 inch thick. The filling gas shall be sealed into the PC at a pressure of 860 ± 10 Torr.

2. Design Objectives - The application of this PC is to measure the spectra of soft X-rays entering the thin window. The design must consider the following deleterious environments to which the non-operating PC may be exposed:

(1) Heat sterilization, consisting of heating to 135°C in a dry nitrogen atmosphere for 120 hours.

(2) Ultrahigh vacuum (10^{-14} Torr) for nine months.

(3) Handling shock.

3. Fabrication Procedures - During vacuum-furnace processing, a temperature of not less than 150°C shall be employed. Prior to filling the PC with its working gas, a leak check shall be performed by filling the counter with helium to a pressure of not less than 760 Torr and measuring a leak rate using a helium leak detector. A leak in excess of 10^{-10} Std cc/sec shall be grounds for rejection of the PC.

4. Testing - Ability to meet the design objectives given in paragraph 2 shall be verified by testing the PC in the following sequence:

(a) The PC shall be dropped on a wooden workbench surface, twice from a horizontal position and once from a vertical position. Each time, the lowest point on the PC shall be not less than three inches above the workbench surface.

(b) The PC shall be heated slowly to a temperature of not less than 135°C and maintained at this temperature for not less than two hours.

(c) The PC shall be placed in an evacuated chamber. A helium leak detector shall be employed to detect leakage of the helium in the fill gas through the PC structure. A detected rate of more than 10^{-10} std cc/sec shall be grounds for rejection of the PC.

(d) The PC shall be tested for performance using an Fe-55 radioisotope source. Resolution of the 5.9 keV X-ray shall be less than 20%, or the PC shall be rejected.

5. Reporting - Test results shall be provided upon delivery. Material certifications shall be provided on all materials of construction with the exception of the anode wire and spring.

6. Shipping Container - The PC shall be packaged in a container sufficient to prevent mechanical damage during transportation and to maintain the relative humidity around the PC below 60% at all times.

RELATED EXPERIENCE

REUTER-STOKES

Experience with counter performance, shock and vibration, etc, testing, particularly on NASA Contracts.

The following are contracts which are being or have been fulfilled and on which administrative procedures, quality control, detailed written procedures, certified shock and vibration, etc., equal or exceed those of your requirement.

American Science and Engineering
P. O. #47630-4
Prime Contract NAS5-11092

NASA Goddard Space Flight Center
Contract NAS5-17917

TRW Systems Group
P. O. #AS-866R

Keithley Instruments, Inc.
P. O. #69735
Prime Contract NAS5-21575

We have also fulfilled numerous contracts for low energy x-ray detectors to be used on balloons or rockets, but with less stringent administrative and quality control requirements. These include NASA Goddard Space Flight Center contracts NAS5-11373, NAS5-16856, and NAS5-16513.

Hanscom Field, AFCRL/L.C.
Contract F-19650-70-M-2778

Naval Research Laboratories
Contract N00173-69C-0219

University of Calgary
Contract 51001

Los Alamos Scientific Laboratory
Contract KB1-51143-1

Columbia University
Contract 183104

Flight History of Gas Filled Counters

Gas filled counters* have appeared prominently in space research since the very beginning of space flight. They were included on Sputniks II and III and on the early Explorers, and were the experiments responsible for discovery of the Van Allen radiation belts.

Advancing beyond the early models flown, space scientists have developed a wide variety of sophisticated gas filled counter systems. These have been used for spaceborne measurements of galactic cosmic ray radiation, trapped proton and electron radiation, solar x-rays, the earth's neutron albedo flux, solar flare proton and alpha radiation, and the emissions of galactic x-ray sources. Very intensive research utilizing proportional counters on space platforms is now planned for the areas of systematic x-ray astronomy, and analysis of lunar x-rays for geochemical investigations of the lunar surface composition.

The widespread use of Geiger and proportional counters in space research can be attributed to (1) highly reliable operation, (2) wealth of design experience, (3) inherent versatility and adaptability to different measurement objectives, and (4) an outstanding ability to measure low energy radiation (especially below 100 keV).

In Table I some of the space experiments performed using gas filled counters are listed to indicate the wide variety of applications where these devices have been utilized to date. This table is only indicative, since it references only a few of the scores (perhaps hundreds) of such instruments which have been flown on Soviet satellites, particularly the Cosmos, Elektron, and Proton series. Also, no reference is made to the large number of probes which have carried proportional counters for studying solar and galactic x-rays (e.g., the programs sponsored by the Air Force Cambridge Research Laboratory and the Naval Research Laboratory for the past ten years). Further, the table is only a sampling of past programs and does not include future programs such as the array of proportional counters now being fabricated as part of one of the experiments on the Apollo Applications Program; nor the large area arrays planned for Apollo flights in 1970-71 for analysis of lunar x-rays.

In summary, it appears probable a thorough study would show that more than 175 proportional counters and 250 Geiger counters have been flown on satellites and probes by Western scientists alone during the past ten years. This outstanding history of successful applications makes the gas filled counter the most effective and extensively employed type of detector used in space radiation studies.

---

*The term "gas filled counters" covers both Geiger-Mueller counters and proportional counters, since these devices are identical in construction, differing only in operating voltage, and sometimes in gas filling.

TABLE I

FLIGHT HISTORY OF GAS-FILLED COUNTERS

Spacecraft	Experimenter/Institution	Instrumentation*/Purpose
Alouette 2, C	McDiarmid/NRC of Canada	Four GM tubes/trapped radiation
Ariel 1	Boyd/Univ. College London	Two P.C./soft x-rays
ESRO 1	Rybner/U. of Denmark	Four GM tubes/trapped radiation
ESRO 2	Elliot/Imperial College	Two P.C./cosmic rays
ESRO 2	Stewardson/U. Leicester	Five P.C./soft x-rays
Explorer I, III, IV, VII, XXV	Van Allen/U. Iowa	Two to four GM tubes/trapped radiation
Explorer VI	Simpson/U. Chicago	14 P.C./cosmic rays
Explorer XII, XIV	McDonald/GSFC	Two GM tubes/cosmic rays
Hitchhiker I	Amer. Sci. Engr. Corp.	GM tube/trapped radiation
Injun 1, 3	Van Allen/U. Iowa	Five GM tubes/trapped radiation
IMP-F	Harris/U. Adelaide	P.C./solar x-rays
Mariners 2, 4	Anderson/Rice Univ.	GM tube/cosmic rays
OAO A1	Fisher/Lockheed Corp.	Array of P.C./observational astronomy
OAO C	Boyd/Univ. College	Three P.C./stellar x-rays
OGO E	Kreplin/NRL	Three P.C./solar radiation
OGO E	Anderson/U. Calif.	P.C. telescope/x-rays
OSO I	Hess/Lawrence Rad. Lab.	$^{10}BF_3$ P.C./albedo neutrons
OSO D	Boyd/Univ. College	Seven P.C./soft x-rays

C.2

TABLE I (Continued)

OV-1	Smart/AFCRL	Two GM tubes/electrons
OV-1	Friedman/Aerospace Corp.	P.C./solar x-rays
OV-5	Vette/Aerospace Corp.	Three GM tubes/trapped radiation
OV-5	DeGiacomo/AFCRL	P.C./galactic soft x-rays
Pioneer II, III	Hubbard/U. Chicago	Seven P.C./cosmic ray telescope
Ranger I, II	Simpson/U. Chicago	Seven P.C./trapped and cosmic
Sputnik II	Mandelstam /Acad. Sci. USSR	Six P.C./cosmic rays
Sputnik III	Mandelstam /Acad. Sci. USSR	Two P.C./cosmic rays
Traac	NASA	Two GM tubes/trapped radiation
UK-1	Pounds/U. Leicester	Two P.C./soft x-rays
Vanguard I	Naval Research Lab.	GM tube/cosmic rays
Vela 2A-3B	Hones/Los Alamos Sci. Lab.	Two GM tubes/nuclear detonations
Zond 3	Vernov/USSR	GM tube/cosmic rays

*Abbreviations used are:

GM tube: Geiger-Mueller counter tube
P.C.: Proportional Counter

APPENDIX H

MOUNTING LOCATION AND SAMPLE PRESENTATION

There are conceptually a large variety of methods by which the X-ray fluorescence spectrometer could be made to come into contact with Martian surface material. However, all cases simplify to two categories.

1. Instrument views undisturbed surface, or
2. Soil sample is collected and brought to the instrument.

In the first case, the instrument is either deployed to the surface by some suitable mechanism or combination of mechanisms. In the second case, the soil sample acquisition unit (furlable boom type) scoops a sample, then releases it to the instrument in some suitable manner. The advantages and disadvantages of these possibilities depend upon the details of implementation. What follows is a preliminary evaluation of several suggested approaches:

1. Instrument mounted on top of thermal compartment.

   Advantages: Considerable space available.
   Sampler can bring multiple samples.

   Disadvantages: Cold exposure requires heater power.
   If sampler fails, experiment fails.

2. Instrument mounted on bottom of thermal compartment.

   Advantages: Experiment independent of sampler success.

   Disadvantages: Sampled area not viewed by imagery.
   Uncontrolled sample-to-instrument distance.
   Cold exposure requires heater power.
   Higher level radiation sources required.
   Potential site alteration study required.

3. Instrument in footpad.

   Advantages: Space available.
   Sample guaranteed.

   Disadvantages: Cold exposure.
   High impact shock.
   If leg sinks, soil fills instrument.
   Only one sample.
   In-flight calibration not feasible.

4. Instrument mounted at end of surface sampler boom.

   Advantages: Can survey compositional variations.

   Disadvantages: If sampler fails, experiment fails.
   Cold exposure.
   Impacts sampler system (cost, etc.).

5. Deployed to surface.

   Advantages: Space available.

   Disadvantages: If deployment mechanism fails, experiment fails.
   Cold exposure.
   Only one sample available.
   Weight and cost penalty for deployment mechanism.

6. Mounted in excess space in Lander thermal compartment.

   Advantages: Multiple samples possible.
   Controlled thermal environment.
   In-flight calibration possible.

   Disadvantages: New inlet tube adds thermal leak.
   Valve required to protect inlet.
   If sampler fails, experiment fails.

7. Mounted on dump compartment for biology experiment.

   Advantages: Multiple samples possible.
   Controlled thermal environment.
   Soil inlet already exists.
   In-flight calibration possible.

   Disadvantages: If sampler fails, experiment fails.
   Radioactive emissions must be controlled to prevent impact on carbon-14 detection.

In terms of engineering impact to the Viking Lander, the last possibility, i.e., mounting the instrument onto the biology instrument dump, is thought to be the simplest and least expensive approach. However, a more detailed trade study is being conducted and will determine whether the present assessment is correct.

APPENDIX I

INSTRUMENT DESIGN TRADE-OFF STUDIES

Design of any instrument for a space mission requires careful consideration of the constraints associated with such flights: harsh environments, limited weight and power, etc. One must also continually face the reality that every increase in scientific sophistication of the instrument produces a penalty in terms of engineering complexity. This penalty expresses itself as decreased reliability and increased cost. The Viking mission to Mars is no different in these respects, except that the constraints are more stringent, in general, than for most previous space missions. This is because of the highly ambitious nature of the undertaking. The search for life, coupled with the goal of detecting trace quantities of organic compounds, and the desire to achieve a soft landing are new tasks never before attained by an unmanned scientific mission. Table N-I lists some of the constraints that have been considered in the design trade-offs for the X-ray fluorescence spectrometer. In addition, all trade-offs have been made in the framework of a general philosophy of: keep it simple, keep it lightweight, keep it cheap!

Radiation Source Trade-Offs

Excitation of the sample with radioisotope X-ray sources has the disadvantage that only certain energy sources are available and also the problem that radiation safety problems in handling the spacecraft arise when isotopes are placed on-board. In general, it would re preferable to use a miniature X-ray tube (e.g., Me-66) operated under variable conditions of tube potential and tube current to excite an unknown sample. However, an X-ray tube and its power supply would add at least two pounds to the instrument weight. An alternative approach is to directly excite the sample with alpha particles (Tr-66, Se-68). This is a very efficient way of exciting elements below silicon. However, as the X-ray yields vary inversely as about the 12th power of the atomic number (Se-68), this technique is virtually useless for elements above calcium. In addition, a very difficult problem of radiation safety arises because the highly radiotoxic alpha source must be sealed in an extremely thin-windowed device. Even though the probability of self-rupture or even accidental rupture of this window may be small, the actual occurrence of such a failure after the spectrometer were mounted on the Lander spacecraft could cause severe contamination of the spacecraft to the point where it could not be used for the required ground tests. It is well known that because of the high recoil energy of alpha particles, once a leak occurs with a source of this type, the radioactive material moves around very fast and is virtually impossible to control. Decontamination of a spacecraft could be prohibitively expensive.

TABLE N-I

SCIENTIFIC PERFORMANCE

versus

Weight and Volume Available
Type and Amount of Power Available
Sterilization Heat Soak
Radiation Safety
Reliability
Failure Detection
Interchangeability
Attachment Points
Electrical Connectors
Operating Safety
Dissimilar Metals
Stress Corrosion
Electromagnetic Compatibility
Thermal Dissipation
Age-Sensitive Elastomeric Compounds
Malfunction Isolation and Test Points
Quality Assurance Factors
Cleanliness Control
RTG Radiation Environment
Operating and Useful Life
Emissions, Outgassing, and Vapor Pressure
Workmanship Implementation
Mandatory Parts, Materials, and Processes
Identification, Standardization, and Traceability
Experiments Radioisotope Environment
Electrical Ground System
Packaging Against Amplification

In Table N-II, we list some of the possible radioisotope sources that could be used in this application. The final decision has been to select Fe-55 and Cd-109. Other sources were rejected on the following grounds:

(1) Po-210 is an alpha emitter. As discussed above, the alpha contamination problem is best avoided.

(2) V-49 is expensive, and provides very little advantage over Fe-55.

(3) As-73 has a half-life which is too short for a Mars mission.

(4) Am-241 is also an alpha emitter, and provides little advantage over Cd-109.

Table N-II

CHARACTERISTICS OF CANDIDATE RADIOISOTOPES FOR AN X-RAY FLUORESCENCE SPECTROMETER

Isotope	Half-Life (Years)	Emissions of Interest
^{210}Po	0.38	5.30 MeV alpha*
^{49}V	0.90	TiK X-rays (4.5 keV)
^{55}Fe	2.60	MnK X-rays (5.9 keV)
^{73}As	0.22	GeK X-rays (9.9 keV)
^{109}Cd	1.24	AgK X-rays (22 keV)
^{241}Am	458	NpL X-rays (11 to 22 keV) 60 keV gamma-ray

*Alpha sources could be sealed in magnesium or aluminum foils to produce alpha-excited X-rays at 1.25 and 1.49 keV, respectively.

X-Ray Detector Trade-Offs

For detection and analysis of the fluorescent radiation emitted by the sample, several alternatives were considered and rejected, including wavelength dispersion by crystal diffraction (large weight penalty) and detectors which do not provide energy dispersion (thin window Geiger counters and solid state detectors operated in the avalanche mode) coupled with the Ross balanced filter technique (for recent review, see Rhodes, Rh-66). Although this approach is an effective one for limited investigations (Jo-68) it would be difficult to use for more than about a half dozen elements unless the instrument were considerably heavier and larger than that presently envisioned. Scintillation detectors were also considered, but their large size and weight, inferior resolution (see Fig. N-1) and much higher susceptibility to the interfering radiation from the RTG's renders them much less satisfactory than proportional counters.

To some extent an increase in sensitivity and accuracy is possible by using fine grained multi-channel pulse height analysis of an energy dispersion detector output. This is the technique now commonly used in X-ray analysis systems employing cryogenically cooled solid state detectors and FET pre-amplifiers. Such systems are impractical for this application because heat sterilization could cause irreversible damage and the attainment of cryogenic temperatures on the lander would be a major engineering challenge. Multi-channel pulse height analysis of the proportional counter iutputs is also possible, but the electronic circuitry required for performing this analysis and storing the data would be prohibitive in size and weight. In the present design the programmable single channel analyzer can actually be operated so as to produce data from which an entire spectrum can be determined with the only sacrifice being an increase in the required data acquisition time. Considerable savings in weight power and reliability are realized, however, with the single channel analyzer feature.

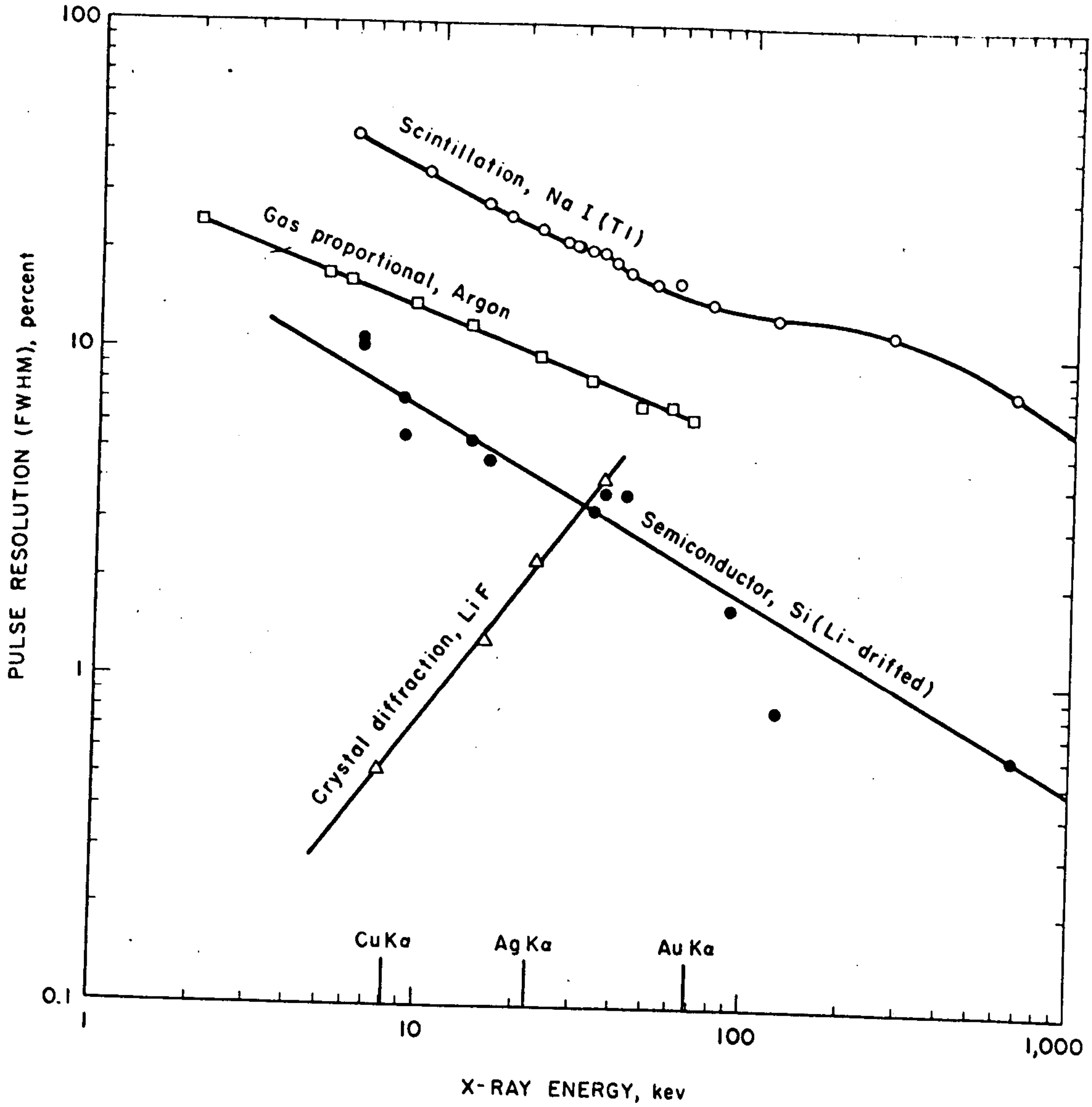

Figure N-1 Experimental values of pulse resolution (FWHM) for X-ray detectors.

□ Bisi and Zappa[16] ○ Narayan[17]
● values reported for TMC 80 mm^2 Si detectors
△ flat LiF crystal, 5-mil fine collimator

APPENDIX J

BACKGROUND RADIATION INTERFERENCE

One limitation on the performance capabilities of the X-ray fluorescence spectrometer is due to the background radiation detected by the counter. This background radiation may arise in several ways: source radiation scattered from the sample (Compton scattering and coherent scattering), natural radioactivity in the sample, galactic cosmic rays, solar flare radiation, and penetrating radiation from the Viking RTG's*. The scattered radiation from the sample due to source excitation is generally unavoidable, although it can be reduced somewhat by careful design of the counter response. Other factors producing high background counting rates in the detector are negligible compared to that produced by the RTG's (exception: giant solar flare radiation events, which can be avoided by delaying the experiment a day or two if necessary).

Thus the principal item of interest is the radiation produced by the SNAP generators in the RTG's. To obtain information on this problem, we have performed experiments at Mound Laboratory, Miamisburg, Ohio by exposing several thin-window proportional counters to a SNAP-19 generator. The results of these measurements are shown in Fig. 2 where it can be seen that the interference becomes worse at the lower energies of interest. The interference was experimentally determined to be due to a highly penetrating component from the SNAP generator, presumably the 2.5 MeV gamma ray from the ^{208}Tl isotope produced in the device. Shielding the counter to reduce this background is out of the question because the effective half-thickness for such shielding is approximately 0.25" of tungsten, although rise-time discrimination with a special electronic circuit (Cu-66) could possibly be included to reduce this background. At present, the intent is to conduct the experiment with no additional countermeasures since the interference is not severe, except for the very light elements.

---

*The Viking Lander contains two Radioisotope Thermoelectric Generators (RTG's) fueled with SNAP heat units to provide electrical power during the landed phase of the mission.

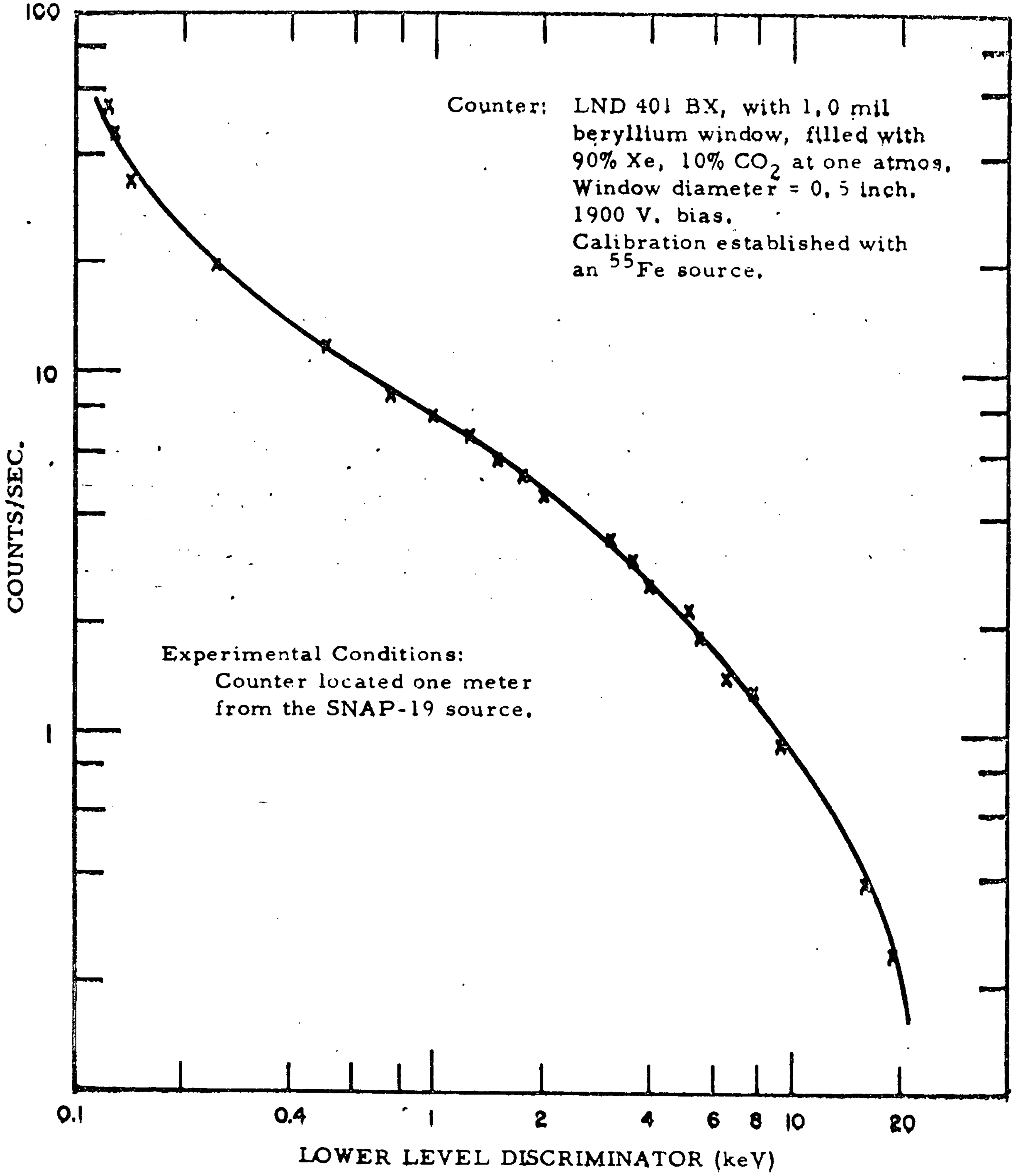

Figure 2. Measurement of RTG radiation background in a thin-window proportional counter. Experiment was performed at Mound Laboratory with a SNAP-19 source. Single channel analyzer was set with a 0.25 keV channel width.

APPENDIX K

GEOCHEMISTRY EXPERIMENT OBJECTIVES ON MARS

Information being made available today on the results of Mariner 6 and 7 fly-bys of Mars (Le-69)*, coupled with the preliminary analytical information from Apollo 11 lunar samples (LSPET-69), suggests that Mars may be in part structurally, compositionally, and historically different from both the moon and earth. An important parameter in these differences could be the major elemental composition of the planet -- long considered to be "terrestrial" in its character.

Similarities (visual) between Mars and the moon include extensive cratering of the surface, but the sharpness of relief along crater walls appears much subdued; in addition, extensive areas (e. g., Hellas) have been discovered which appear devoid of cratering. These facts suggest that surface processes on Mars of down-slope movements, weathering, and erosion might be more earth-like than moon-like.

Predictions of lunar elemental composition have been borne out in general, with some notable exceptions, i. e., unusually high concentrations of Ti, Cr, Y, and Zr, coupled with depletion of alkali elements (Na, K, Rb). We have no basis at present to expect Martian bedrock composition to be grossly different from that of earth or the moon; positively, the similar Martian density suggests a similar composition. However, if surface processes include weathering and erosion, then surface samples presented to the Lander could be highly variable in composition, depending upon where the device was landed. We must, therefore, consider three types of materials (whereas on either earth or the moon by analogy only two of the three would be important):

(1) Martian bedrock of an igneous-like character typical of the earth, or moon-like (Table I);

(2) Martian weathering products, perhaps oxides of Fe and perhaps hydrated, and possibly containing organic matter (Tables IIA and IIB); and

(3) Meteoritic materials and impact products (tektites) (Table III).

In view of the three groups of possible surface materials, the following elements should be measured quantitatively in samples presented to the Lander: Na, Mg, Al, Si, P, S, K, Ca, Ti, Cr, Mn, Fe, Ni, Y, and Zr. Combined with H_2O and CO_2 determinations from other on-board experiments, results from these analyses will permit close evaluation of the estimated compositions of possible Martian materials which are listed in Tables I, IIA, IIB, and III:

(1) H_2O and CO_2 detection will be critical to distinguish weathering products from meteoritic or bedrock materials.

(2) Total Fe, S, and Ni will be critical to the identification of meteoritic materials.

Table I. Estimated Elemental Composition of Martian Igneous or Igneous-like Bedrock (weight percent oxide)

Major Oxide	Most Mafic[1]	Most Felsic[2]	Average Igneous[3]	Lunar[4] Sample 72
SiO_2	44	71	60	45
TiO_2	2	<1	1	10
Al_2O_3	6	15	16	9
Fe_2O_3	4	2	3	--
FeO	9	2	4	17
MgO	23	1	4	8
CaO	10	2	5	9.5
Na_2O	<1	3	4	0.6
K_2O	<1	4	3	0.2
P_2O_5	<1	<1	<1	--
H_2O	<1	<2	<2	0.0

---

[1] Average, 182 ultramafic rocks, as given by Nockolds (No-54)

[2] Average, 546 granites, as given by Daly (Da-33)

[3] Average, igneous rock, as given by Clarke (Cl-24)

[4] LSPET - 69

Table IIA. Estimated Elemental Composition of Possible Martian Weathering Products (Soils, etc.)

Major Constituent	Average Sediment[1]	Oxide Coatings[2]	Average Clay (shale)[1]
SiO_2	45	--	62
TiO_2	<1	--	1
Al_2O_3	11	--	17
Fe_2O_3	4	85	4
FeO	<1	--	3
MgO	3	--	3
CaO	20	--	3
Na_2O	1	--	1
K_2O	2	--	4
P_2O_5	<1	--	1
CO_2	14	--	3
H_2O	Variable, but significant	15	Variable, but significant

Table IIB. Compositions of Organic Matter - Possible in Martian Soils (weight percent element)

Element	Carbohydrates[1]	Fats[1]	Proteins[1]	Nucleic Acids[3]
O	50	18	22	31
C	44	69	51	38
H	6	10	7	4
P	--	2	0.7	10
N	--	0.6	18	17
S	--	0.3	0.8	--
Fe	--	--	0.1	--

---

[1] Taken from Poldervart (Po-55)

[2] As given by Dollfus (Do-51)

[3] Given by Clark (Cl-69)

Table III. Compositions of Meteoritic Materials[1] (weight percent)

Constituent	Chondrites	Achondrites	Irons
SiO_2	38	40	--
TiO_2	0.1	--	--
Al_2O_3	2	4	--
Total Fe	25	31	91
MgO	24	20	--
CaO	2	4	--
Na_2O	1	0.2	--
K_2O	0.2	--	--
P_2O_5	0.2	--	--
FeS	6	--	--
Ni	1	--	9

---

[1] Given by Mason (Ma-62)

Table IV. Normative Mineralogy for Possible Martian Minerals

Katanorm (non-hydrous minerals)	Mesonorm (hydrous and non-hydrous minerals)
Anorthite-albite	Anorthite-albite
Orthoclase	Orthoclase
Quartz	Quartz
Diopside	Biotite
Enstatite	Hornblende
Hypersthene	Apatite
Corundum	Magnetite
Leucite	
Nepheline	
Olivine	
Magnetite	

(3) P and S will be of value in determination of possible organic matter similar to that of terrestrial life forms.

(4) Ti, Cr, Sr, Zr, Ca, and K will be important in differentiating between an earth-igneous or lunar-mare mineralogy.

(5) For silicates, the measurement of major elements, Mg, Si, Al, K, Ca, Ti, and Fe will permit the calculation of normative mineralogies. Normative calculations provide a close approximation to the actual minerals present. These calculations recap the chemical results in sets of standard mineral phases. Based upon lunar results, the standard normative calculation will provide a good estimate of the mineral composition at the Lander site. These may be either katanorms (for non-hydrous minerals) or mesonorms (for hydrous phases). Table IV lists the options.

APPENDIX L

SCIENTIFIC BENEFITS OF A GEOCHEMICAL ANALYSIS EXPERIMENT ON THE VIKING LANDER

Life on Mars

The Viking '75 mission to Mars will search for the presence of life and organic compounds in surface soil. Any information, such as elemental analysis, on the nature of this soil will greatly complement these investigations. Indeed, the selection of landing sites for the Viking spacecraft may correlate strongly with certain apparent geological features. Green and Larmore (Gr-70) state,

> "To determine the possibility of life on the planets we must find out if the planet has been differentiated. If it has been differentiated, it had to defluidize. If it defluidized, it would release warmth and moisture to the surface at discrete places determined by planetary tectonics. Warmth and moisture would favor the generation of life forms......Such centers may be the fountainhead of possible life forms on an arid planet such as Mars."

Geological History of Mars

Although the primary mission of Viking '75 remains the search for extraterrestrial life, the results of the Mariner 6 and 7 Mars fly-bys and the finding of no appreciable organic carbon in the Apollo 11 and 12 samples have led many to suggest a reappraisal of goals. Wetherill (We-70) has argued for inclusion of soil elemental analysis on the Viking payload. Murray, Soderblom, Sharp, and Cutts (Mu-71) conclude their important analysis of the television pictures of Mars with the following comments:

> "The basis for emphasis on Mars as the prime target in the search for extra-terrestrial life seems to be weakened by the strong resemblance of its surface to the uplands of the moon. Rather, Mars should be accorded priority geologically

> as exhibiting important aspects of planetary evolution unknown elsewhere in this Solar System, such as the replacement of cratered terrains by younger uncratered terrains....... Only on Mars can there be found a carbon dioxide frost cap with all its associated phenomena. There are erosional processes and modification episodes recorded on the martian surface unlike those yet known on any other body. The unravelling of these characteristically martian processes and the associated surface history provides a compelling and rewarding intellectual focus for exploration of that planet."

Analysis of the abundant elements in the Martian surface, especially if accomplished at different sites, will be of inestimable value in unravelling the geological story of Mars. Indeed, the geochemical analyses of lunar samples have already disproved certain models of the moon, and have laid the framework for more sophisticated and complete models (e.g., Wo-70, An-70, Ri-70, etc.).

Origin and History of the Solar System

A very thorough and objective analysis of current models of the evolution of the solar system has been made by Adams, Conel, Dunne, Fanale, Holstrom, and Loomis (Ad-69). In considering several possible evolutionary models, they concluded that the master strategy for scientific exploration of the planets should be to obtain as much data as possible to answer five key questions:

(1) Were there elemental and isotopic nonuniformities in the primordial nebula?

(2) What was the state of the sun-cloud system when it first appeared as a recognizable unit?

(3) Was the sun-cloud chemically homogenous?

(4) Did accretion into planets result in the present array of planets, or was the array subsequently altered?

(5) Are the individual planets chemically uniform or nonuniform?

The authors go further to define the experiments which should be performed to gather the data required to answer these questions and recommend the following "essential investigations" for planetary surfaces:

(a) Elemental abundances
(b) Mineral phases and assemblages
(c) Heat flow
(d) Isotopic abundances of certain elements

Experiment (a), the quantitative measurement of the key chemical elements, would provide data which could make a large contribution toward answering questions (3) through (5) above.

APPENDIX M

MAJOR AND MINOR ELEMENTS IN ROCKS

In the following pages are tabulated compositions of the elements Na, Mg, Al, Si, P, S, K, Ca, Ti, and Fe in a variety of rocks and minerals. Samples include earth (igneous, sedimentary, metamorphic), lunar (Apollo 11 and 12), tektites, meteorites, and numerous geochemical standards and minerals. All data is in terms of per cent by weight of each element. This information is punched onto computer cards and is used as input to continuing studies of the effects of possible design changes in the X-ray fluorescence spectrometer.

```
                  NA     MG     AL     SI     P      S      K      CA     TI     FE

RATIO(1),NUMER    1.     0.     0.     0.     0.     0.     0.     0.     0.     0.
RATIO(1),DENOM    0.     0.     0.     0.     1.     0.     0.     0.     0.     0.

RATIO(2),NUMER    0.     1.     0.     0.     0.     0.     0.     0.     0.     0.
RATIO(2),DENOM    0.     0.     0.     0.     1.     0.     0.     0.     0.     0.

RATIO(3),NUMER    0.     0.     1.     0.     0.     0.     0.     0.     0.     0.
RATIO(3),DENOM    0.     0.     0.     0.     1.     0.     0.     0.     0.     0.

RATIO(4),NUMER    0.     0.     0.     1.     0.     0.     0.     0.     0.     0.
RATIO(4),DENOM    0.     0.     0.     0.     1.     0.     0.     0.     0.     0.

RATIO(5),NUMER    0.     0.     0.     0.     1.     0.     0.     0.     0.     0.
RATIO(5),DENOM    0.     0.     0.     0.     1.     0.     0.     0.     0.     0.
```

		(1)	(2)	(3)	(4)	(5)
		Na	Mg	Al	Si	P
	***** GENERAL *****					
100	PERIDOTITE(ULTRA-BASIC ROC	.30	22.31	1.06	20.36	.00
107	CRUST	2.40	1.95	8.20	28.20	.11
104	CRUST	2.30	2.95	7.93	27.47	.00
127	HCP AVE IGNEOUS	2.85	2.10	8.09	27.66	.13
211	CONTINENTAL CRUST	2.89	2.17	8.25	28.13	.13
212	OCEANIC CRUST	2.08	4.40	9.15	23.35	.09
108	BASALTIC ACHONDRITE	.37	4.75	6.88	22.70	.08
109	OCEANIC THOLEIITE BASALT	2.07	4.65	8.57	23.40	.06
110	ALKALI OLIVINE BASALT	2.77	3.17	8.46	22.46	.18
111	AVERAGE CHONDRITE	.70	14.50	1.10	17.90	.10
112	AVERAGE ACHONDRITE	.15	12.10	2.10	18.90	.10
101	BASALTIC ROCK (BASIC ROCK)	1.71	5.19	8.20	22.70	.00
102	INTERMEDIATE ROCK	3.12	2.29	8.68	25.51	.00
103	GRANITIC ROCK	2.89	.66	7.67	32.34	.00
105	SHALE	.96	1.45	8.15	27.19	.00
128	HCP AVE SHALE	.96	1.47	8.15	27.19	.07
129	HCP AVE SANDSTONE	.33	.70	2.52	36.64	.03
131	HCP AVE SEDIMENT	.84	1.60	7.09	27.10	.06
106	CHONDRITES	.68	14.40	1.30	17.80	.11
135	COSMIC ABUNDANCE	.90	20.00	2.31	25.40	.27
	***** EARTH IGNEOUS *****					
1	CALC ALKALI RHYOLITES	2.23	.18	7.19	34.73	.04
2	RHYOLITES	2.52	.24	7.14	34.59	.04
3	CALC ALKALI GRANITES	2.30	.30	7.35	33.93	.09
4	GRANITES	2.60	.54	7.72	33.13	.09
5	SILICIS IGNEOUS ROCKS	2.89	.66	7.78	32.39	.09
6	GRANDIORITES(1)	2.89	.96	8.36	31.45	.09
7	GRANDIORITES(2)	2.75	1.15	8.52	30.75	.09
8	PLUTONIC IGNEOUS	2.60	1.51	8.25	30.47	.09
9	CORD APP IGNEOUS	2.52	1.81	8.41	29.20	.13
10	ANDESITES(1)	2.67	1.69	9.26	28.22	.13
11	AVE IGNEOUS	2.89	2.11	8.25	28.13	.13
12	DIORITES	2.52	2.53	8.94	26.96	.13
13	INTERMEDIATE IGNEOUS	3.12	2.29	8.83	25.69	.17
14	ANDESITES(2)	2.75	2.65	9.20	25.55	.13
15	PARENTAL CALC ALK MAGMAS	2.52	3.32	9.57	25.32	.09

		Na	Mg	Al	Si	P
16	DIORITES(2)	2.52	3.68	8.73	24.52	.17
17	NORMAL THOLEITES	1.71	3.86	7.51	24.01	.09
18	AVE THOLEITE	1.63	4.22	8.25	23.87	.09
19	BASALTS	2.37	3.80	8.46	23.35	.17
20	PLATEAU BASALTS	1.93	4.10	7.51	23.26	.13
21	MAFIC IGNEOUS	1.71	5.25	8.31	22.74	.13
22	AVE OLIVINE BASALT PACIFIC	2.00	4.76	7.99	22.00	.13
23	NORMAL ALK BASALTS	2.00	5.67	7.83	21.57	.17
24	PERIDOTITE NODULES IN BASA	.07	24.96	1.53	20.87	.00
25	ULTRAMAFIC IGNEOUS	.59	13.69	3.23	20.59	.13
26	PERIDOTITES	.45	20.68	2.12	20.55	.04
27	DUNITES(DALY)	.07	28.76	.48	19.52	.04
28	DUNITES (NOCKOLDS)	.22	26.17	.42	18.91	.00
	***** EARTH SEDIMENTARY *****					
29	AVE ORTHOQUARTZITE	.07	.06	.74	43.29	.00
30	AVE QUARTZITE FINLAND	.59	.42	3.39	39.08	.26
31	AVE SANDSTONE	.37	.72	2.54	37.30	.04
32	AVE SUBGRAYWACKE	1.56	.96	5.08	36.93	.09
33	AVE DIATOM OOZE	.07	1.09	2.70	36.32	.04
34	AVE ARKOSE	1.48	.06	6.08	35.61	.00
35	AVE MISSISSIPPI SILT	1.19	.90	5.98	34.96	.09
36	AVE GRAYWACKE	2.60	1.81	7.62	30.79	.04
37	AVE RADIOLARIAN OOZE	.74	1.99	7.25	29.86	.13
38	PALEZOIC SHALES	.82	1.51	9.26	29.81	.09
39	AVE BLUE MUD	1.78	1.33	8.57	29.62	.09
40	AVE SHALE	1.04	1.57	8.73	29.11	.09
41	GLACIAL CLAYS	1.63	2.11	8.78	29.06	.09
42	AVE TERRIGENOUS MUD	1.78	1.39	9.84	28.78	.09
43	CLAYS AND SOILS	.96	1.99	8.41	27.89	.04
44	MESO AND CENOZOIC SHALES	1.41	1.75	7.83	27.75	.09
45	AVE RED CLAY	1.04	1.21	8.94	25.04	.09
	***** EARTH METAMORPHIC *****					
48	METAQUARTZITES	1.41	.60	5.08	37.53	.00
49	LEPTITES AND HAELLEFLINTAS	2.37	.60	7.04	34.54	.04
50	QUARTZOFELDSPATHIC GNEISSE	2.37	.72	7.67	33.09	.09
51	PLUTONIC GNEISSES	2.60	.72	7.83	32.90	.00
52	AVE MICA SCHIST FINLAND	2.00	1.09	8.73	32.10	.04
53	AVE PRECAMBRIAN FINLAND	2.30	1.03	7.83	32.01	.04
54	MICA SCHISTS NORWAY	.96	2.05	8.09	31.87	.00
55	TWO-MICA GNEISSES	2.30	1.09	8.78	31.68	.00
56	MICA SCHISTS (1)	1.34	1.21	9.47	31.59	.04
57	KINZIGITES FINLAND	1.85	1.75	8.41	31.08	.04
58	SLATES (1)	2.00	1.87	9.15	30.37	.00
59	ROOFING SLATES	.96	.96	10.21	30.33	.00
60	MICA SCHISTS (2)	1.19	1.63	10.16	30.23	.00
61	MICA SCHISTS (3)	1.41	1.63	9.26	30.09	.09
62	PHYLLITES NORWAY	1.11	1.33	10.69	29.95	.00
63	AVE PRECAMBRIAN CANADA	2.75	1.09	8.99	29.91	.00
64	SLATES AND PHYLLITES	.96	1.75	10.84	28.97	.00
65	SLATES (2)	1.26	1.75	10.10	28.92	.04
66	PRECAMBRIAN SLATES	.96	1.63	9.79	28.27	.09
67	PHYLLITES	1.48	1.75	10.95	28.08	.09
68	AMPHIBOLITES (1)	2.15	4.22	8.31	23.54	.13
69	AMPHIBOLITES (2)	2.15	4.16	8.78	23.54	.00
70	ECLOGITES	1.85	5.37	7.67	22.93	.00
	***** METEORITES *****					
712	AUBRITES	.98	21.65	.35	25.27	.01

		Na	Mg	Al	Si	P
713	DIOGENITES	.00	15.62	.62	24.38	.01
710	SHERGOTTITE	.94	6.00	3.11	23.40	.01
711	HOWARDITES	.79	7.12	5.26	23.07	.01
716	NAKHLITES	.30	7.24	.92	22.84	.01
709	EUCRITES	.32	5.10	6.88	22.28	.01
715	ANGRITES	.19	6.03	4.61	20.55	.01
708	AMPHOTERITES	.77	15.98	.96	19.09	.01
703	HYPERSTHENE CHONDRITES	.70	14.83	1.49	18.58	.01
714	UREILITES	.32	21.53	.20	18.21	.01
707	ENSTATITE CHONDRITES	.74	12.66	.99	18.06	.01
701	ORDINARY CHRONDITES	.67	14.41	1.44	17.92	.01
721	MANTLE CAVE STONY METEORIT	.74	14.47	1.32	17.92	.01
702	BRONZITE CHRONDITES	.69	13.93	1.38	17.04	.01
718	SIDEROPHYRES	.01	6.09	.01	16.19	.01
706	CARBONAC. CHRONDITES, TYPE	.41	14.41	1.40	15.82	.01
719	LODRANITES	.01	14.05	.10	13.53	.01
705	CARBONAC. CHONDRITES, TYPE	.40	11.46	1.22	12.78	.01
704	CARBONAC. CHONDRITES, TYPE	.56	9.41	.94	10.81	.01
720	MESOSIDERITES	.13	3.84	2.17	9.13	.01
717	PALLASITES	.05	11.94	.20	8.00	.01
	***** APOLLO 11 *****					
601	LSPET A 72	.44	4.80	4.80	21.00	.01
600	LSPET A 22	.30	3.90	4.10	20.00	.01
605	LSPET B 58	.41	3.90	6.90	20.00	.01
608	LSPET C 21	.15	4.50	5.80	20.00	.01
610	LSPET D 37	.40	4.80	6.90	20.00	.01
606	LSPET B 45	.38	4.20	6.90	19.60	.01
611	LSPET 54 (BULK SAMPLE)	.38	4.60	6.90	19.60	.01
612	10044 GABBRO	.36	3.77	6.19	19.66	.03
614	10084=28 REGOLITH (DUST)	.36	4.79	7.56	19.42	.04
615	10017 29	.38	4.61	4.30	19.09	.06
637	10047	.48	3.68	5.18	19.33	.00
638	10049	.53	4.24	5.03	19.19	.00
639	10050	.49	4.84	4.71	19.14	.00
640	10058 (WHOLE ROCK)	.59	3.77	5.66	19.38	.00
642	10019	.69	4.74	7.25	19.23	.00
643	10048	.39	4.55	6.82	19.75	.00
644	10060	.58	4.53	6.24	19.42	.00
645	311079	.40	4.79	7.46	19.75	.00
641	10062	.51	4.35	6.40	18.16	.00
604	LSPET B 17	.48	5.10	5.30	18.70	.01
609	LSPET C 61	.37	5.40	5.80	18.70	.01
613	10057 VESICULAR DIABASE	.40	4.61	5.71	18.63	.07
616	10020 30	.27	4.71	5.29	18.67	.03
617	10072	.39	4.86	4.12	18.81	.08
635	10022	.68	4.67	4.55	18.77	.00
636	10024	.59	4.89	5.03	18.25	.00
634	10003	.63	4.34	5.82	17.69	.00
603	LSPET A 20	.44	4.80	5.80	17.80	.01
607	LSPET B 50	.38	6.00	5.80	17.80	.01
602	LSPET A 57	.40	5.70	5.80	16.80	.01
	***** APOLLO 12 *****					
633	LSPET 12013	.51	3.62	6.35	28.55	.00
627	LSPET 12038,CRYS	.45	3.92	6.35	22.93	.00
631	LSPET 12010 BRECCIA	.39	6.63	6.08	20.12	.00
625	LSPET 12052,CRYS	.33	6.03	5.82	19.66	.00
623	LSPET 12009,CRYS	.38	7.54	5.82	19.19	.00

		Na	Mg	Al	Si	P
629	LSPET 12070 FINES	.30	7.24	7.41	19.66	.00
630	LSPET 12073 BRECCIA	.37	6.63	7.93	19.19	.00
632	LSPET 12033 LIGHT FINES	.40	6.63	8.46	19.19	.00
624	LSPET 12065,CRYS	.29	5.43	6.35	18.25	.00
626	LSPET 12064,CRYS	.31	4.82	6.35	18.72	.00
628	LSPET CRYS ROCKS,AVE	.33	7.06	5.92	18.72	.00
620	LSPET 12004,CRYS	.36	9.04	5.55	17.32	.00
621	LSPET 12015,CRYS	.27	8.44	5.82	17.78	.00
619	LSPET 12012,CRYS	.39	10.55	5.82	16.38	.00
622	LSPET 12022,CRYS	.27	7.84	5.82	16.85	.00
	***** TEKTITES *****					
301	J-86 JAVANITE TEKTITE	.59	4.82	6.45	30.00	.00
300	J-87 JAVANITE TEKTITE	.52	4.10	6.67	29.72	.00
	***** SAMPLES AND STANDARDS *****					
124	P-23 GRANDIORITE	2.35	.27	7.19	34.59	.02
113	USGS STAND G-1	2.55	.22	7.46	33.93	.04
121	P-17 BIOTITE QUARTZ MONZON	2.90	.30	7.72	33.70	.03
115	USGS STAND G-2	3.08	.46	8.09	32.43	.07
122	P-4 BIOTITE QUARTZ MONZON	3.20	.62	8.20	31.59	.07
116	USGS STAND GSP-1	2.12	.57	7.88	31.50	.13
123	P-19 BIOTITE GRANDIORITE	3.15	.75	9.05	30.79	.06
126	P-26 TONALITE (2)	3.40	1.20	10.05	28.08	.08
117	USGS STAND AGV-1	3.21	.92	8.94	27.66	.21
125	P-25 TONALITE (1)	2.34	2.17	9.31	27.24	.06
118	USGS STAND BCR-1	2.46	2.09	7.09	25.37	.17
114	USGS STAND W-1	1.67	3.99	7.88	24.62	.06
119	USGS STAND PCC-1	.00	26.11	.38	19.56	.00
120	USGS STAND DTS-1	.00	30.03	.16	18.95	.00
281	AVE OLIVINE	.00	14.10	.00	16.30	.00
285	AVE PYROXENE	3.40	5.30	2.00	24.70	.00
286	AVE AMPHIBOLE (W/O HORNBLE	1.70	6.90	1.00	25.50	.00
287	AVE HORNBLENDE	2.40	5.00	7.00	23.20	.00
288	AVE BIOTITE	.00	8.30	.00	19.30	.00
274	MUSCOVITE (MICA)	.00	.00	20.30	21.20	.00
278	ORTHOCLASE (FELDSPAR)	.00	.00	9.70	30.30	.00
280	ANORTHITE (FELDSPAR)	.00	.00	19.40	20.20	.00
279	ALBITE (FELDSPAR)	8.80	.00	10.30	32.10	.00
		1.20	5.12	6.07	23.50	.04

```
                     NA     MG     AL     SI     P      S      K      CA     TI     FE

RATIO(1),NUMER       0.     0.     0.     0.     0.     1.     0.     0.     0.     0.
RATIO(1),DENOM       0.     0.     0.     0.     1.     0.     0.     0.     0.     0.

RATIO(2),NUMER       0.     0.     0.     0.     0.     0.     1.     0.     0.     0.
RATIO(2),DENOM       0.     0.     0.     0.     1.     0.     0.     0.     0.     0.

RATIO(3),NUMER       0.     0.     0.     0.     0.     0.     0.     1.     0.     0.
RATIO(3),DENOM       0.     0.     0.     0.     1.     0.     0.     0.     0.     0.

RATIO(4),NUMER       0.     0.     0.     0.     0.     0.     0.     0.     1.     0.
RATIO(4),DENOM       0.     0.     0.     0.     1.     0.     0.     0.     0.     0.

RATIO(5),NUMER       0.     0.     0.     0.     0.     0.     0.     0.     0.     1.
RATIO(5),DENOM       0.     0.     0.     0.     1.     0.     0.     0.     0.     0.
```

		(1) S	(2) K	(3) Ca	(4) Ti	(5) Fe
	***** GENERAL *****					
100	PERIDOTITE(ULTRA-BASIC ROC	.01	.08	2.15	.48	9.44
107	CRUST	.03	2.10	4.20	.57	5.60
104	CRUST	.01	1.91	4.79	.72	5.65
127	HCP AVE IGNEOUS	.01	2.60	3.63	.63	5.11
211	CONTINENTAL CRUST	.01	2.66	3.72	.66	5.20
212	OCEANIC CRUST	.01	.17	8.51	.90	6.76
108	BASALTIC ACHONDRITE	.01	.07	7.86	.29	13.13
109	OCEANIC THOLEIITE BASALT	.01	.18	8.08	.82	7.12
110	ALKALI OLIVINE BASALT	.01	1.57	6.46	1.75	8.58
111	AVERAGE CHONDRITE	1.80	.20	1.40	.10	25.00
112	AVERAGE ACHONDRITE	2.10	.01	2.90	.01	31.00
101	BASALTIC ROCK (BASIC ROCK)	.01	.58	7.65	1.08	8.25
102	INTERMEDIATE ROCK	.01	2.66	4.65	.90	6.35
103	GRANITIC ROCK	.01	3.15	1.86	.30	2.90
105	SHALE	.01	2.66	2.22	.42	4.74
128	HCP AVE SHALE	.01	2.69	2.22	.39	4.72
129	HCP AVE SANDSTONE	.01	1.09	3.93	.15	.98
131	HCP AVE SEDIMENT	.01	2.37	4.21	.34	4.05
106	CHONDRITES	2.30	.09	1.40	.08	25.10
135	COSMIC ABUNDANCE	10.90	.11	1.77	.10	30.30
	***** EARTH IGNEOUS *****					
1	CALC ALKALI RHYOLITES	.01	4.48	.79	.12	1.53
2	RHYOLITES	.01	3.90	.86	.18	1.76
3	CALC ALKALI GRANITES	.01	4.48	.93	.24	1.95
4	GRANITES	.01	3.40	1.43	.24	2.52
5	SILICIS IGNEOUS ROCKS	.01	3.15	1.86	.30	2.90
6	GRANDIORITES(1)	.01	2.57	2.57	.36	2.93
7	GRANDIORITES(2)	.01	2.32	3.22	.36	3.29
8	PLUTONIC IGNEOUS	.01	3.07	3.07	.30	3.41
9	CORD APP IGNEOUS	.01	2.24	3.65	.42	4.66
10	ANDESITES(1)	.01	1.74	4.22	.48	4.79
11	AVE IGNEOUS	.01	2.66	3.72	.66	5.20
12	DIORITES	.01	1.83	4.86	.48	5.74
13	INTERMEDIATE IGNEOUS	.01	2.66	4.72	.90	6.35
14	ANDESITES(2)	.01	.91	5.72	.78	6.72
15	PARENTAL CALC ALK MAGMAS	.01	.83	6.01	.54	6.26

		S	K	Ca	Ti	Fe
16	DIORITES(2)	.01	1.08	6.08	.90	7.33
17	NORMAL THOLEITES	.01	.75	7.51	1.20	9.10
18	AVE THOLEITE	.01	.83	7.51	.84	8.38
19	BASALTS	.01	1.24	6.51	.84	8.83
20	PLATEAU BASALTS	.01	.58	6.86	1.32	10.36
21	MAFIC IGNEOUS	.01	.58	7.72	1.08	8.25
22	AVE OLIVINE BASALT PACIFIC	.01	.83	7.79	1.80	8.88
23	NORMAL ALK BASALTS	.01	.83	7.72	1.56	9.08
24	PERIDOTITE NODULES IN BASA	.01	.01	1.79	.12	6.31
25	ULTRAMAFIC IGNEOUS	.01	.58	7.29	1.02	9.99
26	PERIDOTITES	.01	.17	2.50	.48	9.44
27	DUNITES(DALY)	.01	.01	.50	.01	6.46
28	DUNITES (NOCKOLDS)	.01	.08	.57	.12	10.58
	***** EARTH SEDIMENTARY *****					
29	AVE ORTHOQUARTZITE	.01	.08	2.15	.01	.37
30	AVE QUARTZITE FINLAND	.01	1.49	1.22	.01	2.46
31	AVE SANDSTONE	.01	1.08	4.00	.18	1.00
32	AVE SUBGRAYWACKE	.01	1.24	.86	.36	2.73
33	AVE DIATOM OOZE	.01	.08	5.15	.18	1.62
34	AVE ARKOSE	.01	4.73	1.14	.01	1.69
35	AVE MISSISSIPPI SILT	.01	2.08	1.64	.36	2.60
36	AVE GRAYWACKE	.01	1.74	2.57	.30	4.04
37	AVE RADIOLARIAN OOZE	.01	1.41	2.22	.36	6.66
38	PALEZOIC SHALES	.01	3.15	1.07	.48	5.42
39	AVE BLUE MUD	.01	1.41	1.86	.48	5.82
40	AVE SHALE	.01	2.91	2.36	.42	5.03
41	GLACIAL CLAYS	.01	3.40	2.29	.48	5.12
42	AVE TERRIGENOUS MUD	.01	.91	1.57	.84	5.79
43	CLAYS AND SOILS	.01	1.91	3.86	.30	5.38
44	MESO AND CENOZOIC SHALES	.01	2.41	4.58	.30	4.49
45	AVE RED CLAY	.01	1.66	4.29	.48	9.11
	***** EARTH METAMORPHIC *****					
48	METAQUARTZITES	.01	2.16	.79	.01	2.62
49	LEPTITES AND HAELLEFLINTAS	.01	3.07	1.14	.12	2.22
50	QUARTZOFELDSPATHIC GNEISSE	.01	3.15	1.57	.30	2.67
51	PLUTONIC GNEISSES	.01	3.57	1.36	.01	2.95
52	AVE MICA SCHIST FINLAND	.01	3.15	1.79	.18	2.80
53	AVE PRECAMBRIAN FINLAND	.01	2.99	2.43	.24	3.40
54	MICA SCHISTS NORWAY	.01	3.15	.93	.01	5.29
55	TWO-MICA GNEISSES	.01	2.91	1.43	.01	3.97
56	MICA SCHISTS (1)	.01	2.82	.93	.36	4.04
57	KINZIGITES FINLAND	.01	2.66	1.00	.36	5.18
58	SLATES (1)	.01	2.74	.79	.54	4.98
59	ROOFING SLATES	.01	3.24	2.00	.01	4.59
60	MICA SCHISTS (2)	.01	3.49	1.14	.01	4.53
61	MICA SCHISTS (3)	.01	3.07	1.36	.60	5.04
62	PHYLLITES NORWAY	.01	3.90	.29	.01	5.45
63	AVE PRECAMBRIAN CANADA	.01	2.57	2.93	.48	4.01
64	SLATES AND PHYLLITES	.01	2.99	1.00	.01	6.22
65	SLATES (2)	.01	3.15	.71	.42	6.51
66	PRECAMBRIAN SLATES	.01	3.40	.79	.48	8.08
67	PHYLLITES	.01	3.32	.86	.66	5.83
68	AMPHIBOLITES (1)	.01	.91	6.79	.96	8.58
69	AMPHIBOLITES (2)	.01	.58	7.15	.01	9.51
70	ECLOGITES	.01	.58	8.22	.01	9.73
	***** METEORITES *****					
712	AUBRITES	.46	.08	.65	.04	3.84

		S	K	Ca	Ti	Fe
713	DIOGENITES	.41	.00	1.01	.11	14.01
710	SHERGOTTITE	.00	.15	7.44	.01	17.19
711	HOWARDITES	.22	.30	5.51	.06	14.10
716	NAKHLITES	.06	.12	10.80	.23	16.20
709	EUCRITES	.20	.05	7.29	.26	14.43
715	ANGRITES	.46	.16	17.52	1.43	7.48
708	AMPHOTERITES	1.46	.20	1.20	.01	20.21
703	HYPERSTHENE CHONDRITES	2.21	.09	1.37	.07	22.09
714	UREILITES	.00	.01	.56	.05	18.00
707	ENSTATITE CHONDRITES	3.91	.09	.69	.04	27.91
701	ORDINARY CHRONDITES	2.15	.08	1.36	.07	24.76
721	MANTLE (AVE STONY METEORIT	2.12	.17	1.43	.06	25.30
702	BRONZITE CHRONDITES	2.07	.08	1.34	.07	27.99
718	SIDEROPHYRES	.00	.01	.01	.01	49.43
706	CARBONAC. CHRONDITES, TYPE	2.22	.04	1.66	.07	25.08
719	LODRANITES	2.70	.01	.13	.01	38.49
705	CARBONAC. CHONDRITES, TYPE	3.13	.04	1.45	.06	21.08
704	CARBONAC. CHONDRITES, TYPE	6.17	.06	1.08	.05	18.84
720	MESOSIDERITES	1.03	.01	2.07	.01	53.80
717	PALLASITES	.19	.02	.20	.01	54.50
	***** APOLLO 11 *****					
601	LSPET A 72	.01	.17	6.80	6.00	13.00
600	LSPET A 22	.01	.17	6.40	6.60	16.00
605	LSPET B 58	.01	.09	7.50	5.40	13.00
608	LSPET C 21	.01	.12	7.90	5.20	14.80
610	LSPET D 37	.01	.10	8.60	4.20	12.40
606	LSPET B 45	.01	.08	7.10	4.80	14.00
611	LSPET 54 (BULK SAMPLE)	.01	.11	8.30	4.20	12.10
612	10044 GABBRO	.01	.09	8.72	5.28	13.99
614	10084=28 REGOLITH (DUST)	.01	.13	8.44	4.49	12.13
615	10017 29	.01	.25	7.58	7.01	15.39
637	10047	.01	.09	8.72	6.11	14.76
638	10049	.01	.30	7.86	6.77	14.53
639	10050	.01	.04	8.08	7.55	13.44
640	10058 (WHOLE ROCK)	.01	.06	8.65	6.65	13.44
642	10019	.01	.12	8.51	4.94	12.20
643	10048	.01	.14	8.15	5.36	12.20
644	10060	.01	.15	8.29	5.48	13.21
645	311079	.01	.12	8.65	4.55	11.89
641	10062	.01	.06	8.58	6.17	14.22
604	LSPET B 17	.01	.18	7.10	6.60	14.70
609	LSPET C 61	.01	.15	7.90	5.40	12.40
613	10057 VESICULAR DIABASE	.01	.27	7.22	6.83	15.08
616	10020 30	.01	.04	8.01	6.41	15.08
617	10072	.01	.24	7.36	7.37	15.39
635	10022	.01	.25	7.65	7.31	14.69
636	10024	.01	.23	7.15	7.91	14.37
634	10003	.01	.04	7.86	7.19	15.38
603	LSPET A 20	.01	.05	7.10	7.20	14.00
607	LSPET B 50	.01	.05	7.10	5.40	15.50
602	LSPET A 57	.01	.15	7.10	7.50	15.50
	***** APOLLO 12 *****					
633	LSPET 12013	.01	1.66	4.50	.72	7.78
627	LSPET 12038,CRYS	.01	.05	7.86	1.92	13.22
631	LSPET 12010 BRECCIA	.01	.13	7.15	2.22	15.16
625	LSPET 12052,CRYS	.01	.06	7.86	2.16	16.32
623	LSPET 12039,CRYS	.01	.05	7.15	1.98	15.55

		S	K	Ca	Ti	Fe
629	LSPET 12070 FINES	.01	.15	7.15	1.86	13.22
630	LSPET 12073 BRECCIA	.01	.21	8.22	1.86	13.22
632	LSPET 12033 LIGHT FINES	.01	.32	8.22	1.56	12.44
624	LSPET 12065,CRYS	.01	.06	9.01	2.28	17.10
626	LSPET 12064,CRYS	.01	.07	8.58	2.94	17.10
628	LSPET CRYS ROCKS,AVE	.01	.05	7.65	2.22	16.56
620	LSPET 12004,CRYS	.01	.05	7.15	2.04	17.88
621	LSPET 12015,CRYS	.01	.05	7.01	1.92	17.10
619	LSPET 12012,CRYS	.01	.05	6.65	1.86	17.88
622	LSPET 12022,CRYS	.01	.06	7.86	3.05	17.10
	***** TEKTITES *****					
301	J-86 JAVANITE TEKTITE	.01	1.24	2.29	.48	7.00
300	J-87 JAVANITE TEKTITE	.01	1.24	2.72	.48	6.61
	***** SAMPLES AND STANDARDS *****					
124	P-23 GRANDIORITE	.01	3.84	1.35	.12	1.26
113	USGS STAND G-1	.01	4.63	.98	.16	1.32
121	P-17 BIOTITE QUARTZ MONZON	.01	3.45	1.35	.21	1.34
115	USGS STAND G-2	.01	3.74	1.43	.29	1.84
122	P-4 BIOTITE QUARTZ MONZON	.01	3.34	1.68	.35	2.73
116	USGS STAND GSP-1	.01	4.58	1.47	.40	2.97
123	P-19 BIOTITE GRANDIORITE	.01	1.63	3.22	.35	2.52
126	P-26 TONALITE (2)	.01	1.14	4.25	.43	4.06
117	USGS STAND AGV-1	.01	2.42	3.56	.63	4.70
125	P-25 TONALITE (1)	.01	1.36	5.06	.47	5.16
118	USGS STAND BCR-1	.01	1.41	5.00	1.33	9.38
114	USGS STAND W-1	.01	.53	7.79	.65	7.73
119	USGS STAND PCC-1	.01	.00	.39	.01	5.70
120	USGS STAND DTS-1	.01	.00	.02	.01	6.05
281	AVE OLIVINE	.00	.00	.00	.00	32.40
285	AVE PYROXENE	.00	.00	5.90	.00	16.40
286	AVE AMPHIBOLE (W/O HORNBLE	.00	.00	3.00	.00	18.00
287	AVE HORNBLENDE	.00	.00	8.30	.00	14.40
288	AVE BIOTITE	.00	8.90	.00	.00	19.20
274	MUSCOVITE (MICA)	.00	9.80	.00	.00	.00
278	ORTHOCLASE (FELDSPAR)	.00	14.00	.00	.00	.00
280	ANORTHITE (FELDSPAR)	.00	.00	14.40	.00	.00
279	ALBITE (FELDSPAR)	.00	.00	.00	.00	.00
		.26	1.30	4.21	1.38	10.09

APPENDIX N

RESULTS OF TESTS ON UNKNOWNS

INTRODUCTION

Unknowns were delivered by J. Allingham and F. Cuttitta* on Dec. 8, 1971 for quantitative chemical analysis by the ultraminiature X-ray fluorescence spectrometer. The purpose was to test the capability of this new instrument to obtain meaningful geochemical data on each of four diverse rock specimens. Data were taken over a five-hour period and the samples returned to Allingham and Cuttitta. Analysis of the data was accomplished during the two week period of Dec. 9-23. Results were formally presented on Jan. 4 to the Chief of Planetology, S. J. Dwornik, and members of a special panel convened by him. What follows is a comparison of results obtained by our ultraminiature spectrometer with laboratory analyses of the unknowns. The latter were provided to us during the formal presentation.

EXPERIMENTAL PROCEDURE

The X-ray fluorescence spectrometer (Ref. 1) consists of four proportional counter detectors and two radiation sources: ^{55}Fe ($T_{\frac{1}{2}}$ = 2.60 yrs.) and ^{109}Cd ($T_{\frac{1}{2}}$ = 1.24 yrs.). Fixed filters are used to provide enhanced sensitivity to Mg, Al, and K. Pulse-height analysis of detector outputs was made with a Northern-Scientific NS-630 multichannel analyzer.

Unknowns were supplied in the form of finely ground powder. For our measurements, each unknown was spread in the bottom of a two-inch diameter petri dish to an average depth of one-eighth inch. No special preparation techniques were required, e.g., no weighing, no smoothing with a knife edge, no dehydration of the sample. The loaded petri dishes were placed in an eight-position carousel mounted inside the chamber containing the X-ray spectrometer. While taking data, this chamber was kept at 50 μm Hg pressure with a roughing pump.** Fine adjustments of sample position were not required as the instrument performs satisfactorily over a considerable range of sample-to-detector distances. The energy scale of the multichannel analyzer was calibrated using the fluorescent radiation from a CaO target as an energy reference point. In contrast to conventional laboratory X-ray fluorescence analysis, our instrument utilizes the source radiation backscatter peak as the reference point from which all element percentages are determined. This completely obviates the necessity for a set of standards and at the same time allows a quantitative determination of the total amount of light elements (atomic numbers 1 through 11) in the sample.

SUMMARY OF RESULTS

Real time inspection of the spectra during data acquisition allowed us to draw the following conclusions:

---

*Address: U.S. Dept. of Interior, Geological Survey, Washington, D.C. 20242

**Previous experiments as well as theoretical analysis shows the 5 to 10 mbar Martian atmosphere would have negligible effect on the results obtained.

1. None of the unknowns appeared to be meteoritic in origin (Si, Ti, Sr, and Zr were so high as to exclude the great majority of known meteorites).

2. None of the unknowns is an extreme sedimentary differentiate (Si/Ca too high for a carbonate; Fe too low for limonite; Si too low and and most other elements too high for high-quartz sand or sandstone).

3. Unknown D is lunar-like (low K, high Ca, Ti, Fe), but unknowns A, B, and E are not.

Detailed analysis of the data by computer reduction and laboratory simulations verified these conclusions and provided weight percentages for eleven elements in each sample: Al, Ca, Fe, K, Mg, Si, Ti, Rb, Sr, Zr, and "oxygen"*. All 44 values so obtained by the ultraminiature X-ray spectrometer agree satisfactorily (criteria stated below) with the wet chemistry values for these samples. This comparison is shown in Table I and Figures 1, 2, and 3. We consider this agreement quite satisfactory for the following reasons:

(a) The enrichment and depletion factors one calculates relative to the presumed primordial abundances of the elements (Ref. 2) show the same important trends regardless of whether one uses the "measured" X-ray values or the wet chemistry "actuals" (See Fig. 4).

(b) The differentiated nature of all four unknowns is correctly established and the possibility of extensive geochemical alteration of these rocks by sedimentary processes is correctly rejected.

(c) The results are sufficiently accurate for determination of rock type, assuming an igneous origin (See Appendix B).

(d) The calculated normative mineralogies are in good agreement with norms derived from "actuals" and the inference of rock densities are always within 0.1 g/cm^3 of those calculated from the "actuals" (See Figures 5 and 6).

(e) The radioactive element potassium is detected even at low concentrations (See unknown D).

(f) Perhaps the most important geochemical ratio is K/Ca (Ref. 3). This ratio varies by as much as x500 in igneous rocks and is determined here to an accuracy within a factor of 2 or less for all unknowns, except D (within x3).

(g) Accuracy is unaffected by the physical and mineralogical state of the sample. Included in the unknowns are a glass (unknown A, a tektite), a mechanical mixture (unknown B), and normal ground rock samples (D and E).

---

*Elements in this group include all those with atomic numbers between 1 and 11. Typically, for silicate rocks, this group is approximately 95% oxygen, 4% sodium, and 1% or less for all other elements.

(h) Upper limits placed on elements not detected, such as S, CO_2, P, Cl, etc., are never exceeded by "actuals".

(i) Unknown D is correctly adjudged lunar-like (Apollo 14 samples) in major element abundances but distinctly anomalous, by a factor of 10, in Zr/Sr and therefore presumably of terrestrial origin (it is, in fact, a Hawaiian basalt). See Table II.

(j) Errors are in many cases less than, and in all cases not more than a few times the interlaboratory errors for wet chemical analyses of similar rocks. See Table III.

(k) Errors are usually less than the natural variability among individual rock samples from a single geologic setting.

A CRITICAL SELF-APPRAISAL

Analytical accuracy of the X-ray fluorescence spectrometer varies with the element, but in general, it is better for higher atomic number elements than lower. Thus, Mg and Al accuracies are poor, as may be seen from the error limits given in Exhibit I of Appendix A. Indeed, the value of (Mg + Al) is more accurately determined by this technique than the value of either element alone, and one can verify by inspection of Table I that this is true for each unknown. On the other hand, the measurements obtained for higher atomic number elements are, in most cases, very close to the actuals, and this excellent accuracy is typical for the X-ray technique.

Of the 44 measurements given, 12 are in error by amounts greater than predicted by Exhibit I of Appendix A. Since it was intended that the error estimates be for the 90% confidence level, only 4 to 6 such results were expected. One has only to notice, however, that 7 of the 8 K and Ca results are outside their predicted limits. From Figure 2, it is seen that our K measurements are systematically low, while our Ca results are systematically high.

This general result is quite inconsistent with analyses made of a suite of "knowns" just following the analyses of the unknowns. For these knowns, the K and Ca values obtained were closer to and randomly distributed about the "actuals". Three days after the unknowns were analyzed, our pulse-height analyzer suffered a sudden, large change in gain and linearity. Before the malfunction could be isolated, it reverted to its normal state. It is possible that during analysis of the unknowns a similar, but less noticeable malfunction occured to produce the systematic errors observed. This point is perhaps belabored since the K and Ca results we obtained are still adequate for most geochemical purposes. Nevertheless, we believe the ultraminiature X-ray fluorescence technique is inherently capable of better accuracies for K and Ca than is evidenced by the results presented herein.

Unknowns A, B, D, and E are distinctly different rocks, as seen from their chemistry. On the other hand, these rocks do not represent any of the possible extremes such as ultrabasic rocks, very acidic rocks, or sedimentary differentiates. They, therefore, provide an excellent test of the discrimination capability of the instrument. It is of interest, then, that the X-ray results correctly identified the compositional trends among the four samples (e.g., which unknown has highest silica, which 2nd, 3rd, 4th) for 9 of the 11 elements detected, with only minor irregularities for Mg and "O". The capability for establishing the comparative chemistry of samples is potentially quite important for a Mars mission since separate samples of surface, near surface (4-10 cm), and windblown material may be made available for analysis by the devices on the Viking Lander.

REFERENCES

1. B. C. Clark and A. K. Baird, "An X-Ray Fluorescence Spectrometer for Geochemical Analysis of the Martian Surface", Nov., 1971.

2. A. G. W. Cameron, "A New Table of Abundances of the Elements in the Solar System", in Origin and Distribution of the Elements, Ed. by L. H. Ahrens, Pergamon Press, New York (1968).

3. At the 1967 Summer Study of Lunar Science and Exploration, it was the opinion of the Geochemistry Working Group that "the K/Ca ratio is a much better index by which to classify chemical variation than an analysis for Al, Mg, Si, and Fe. The K/Ca ratio varies by a factor of 500 in common rock types, where Mg/Si or Mg/Fe ratios vary by less than a factor of 10". p. 239, NASA SP-157.

4. Lunar Sample Preliminary Examination Team, "Preliminary Examination of Lunar Samples from Apollo 14", Science 173 (1971) 681.

5. U.S.G.S. Bulletin 980, Table 14.

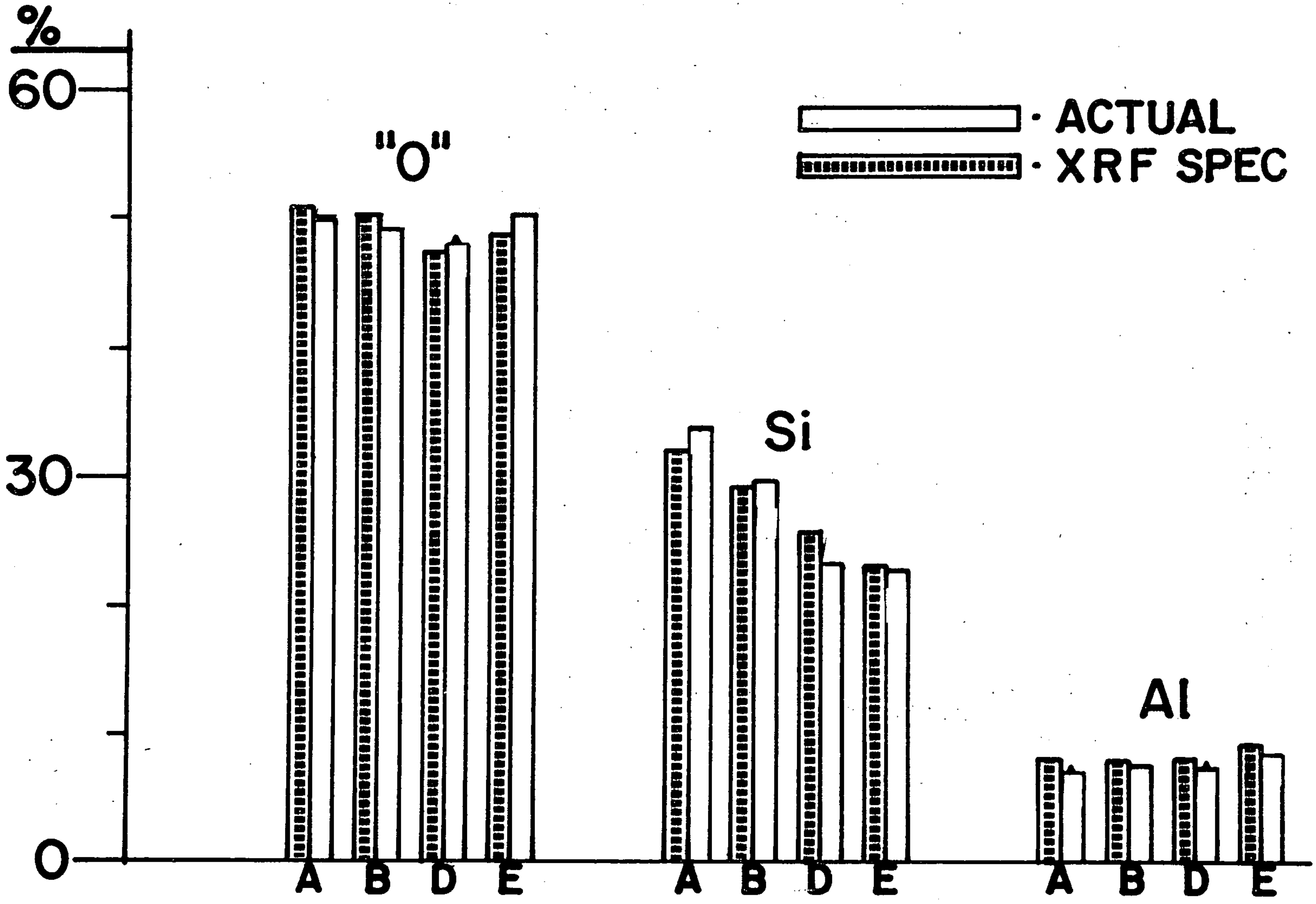

Fig. 1. Comparison of Results for Specimens A, B, D, and E.
"O" includes C, O, and Na.

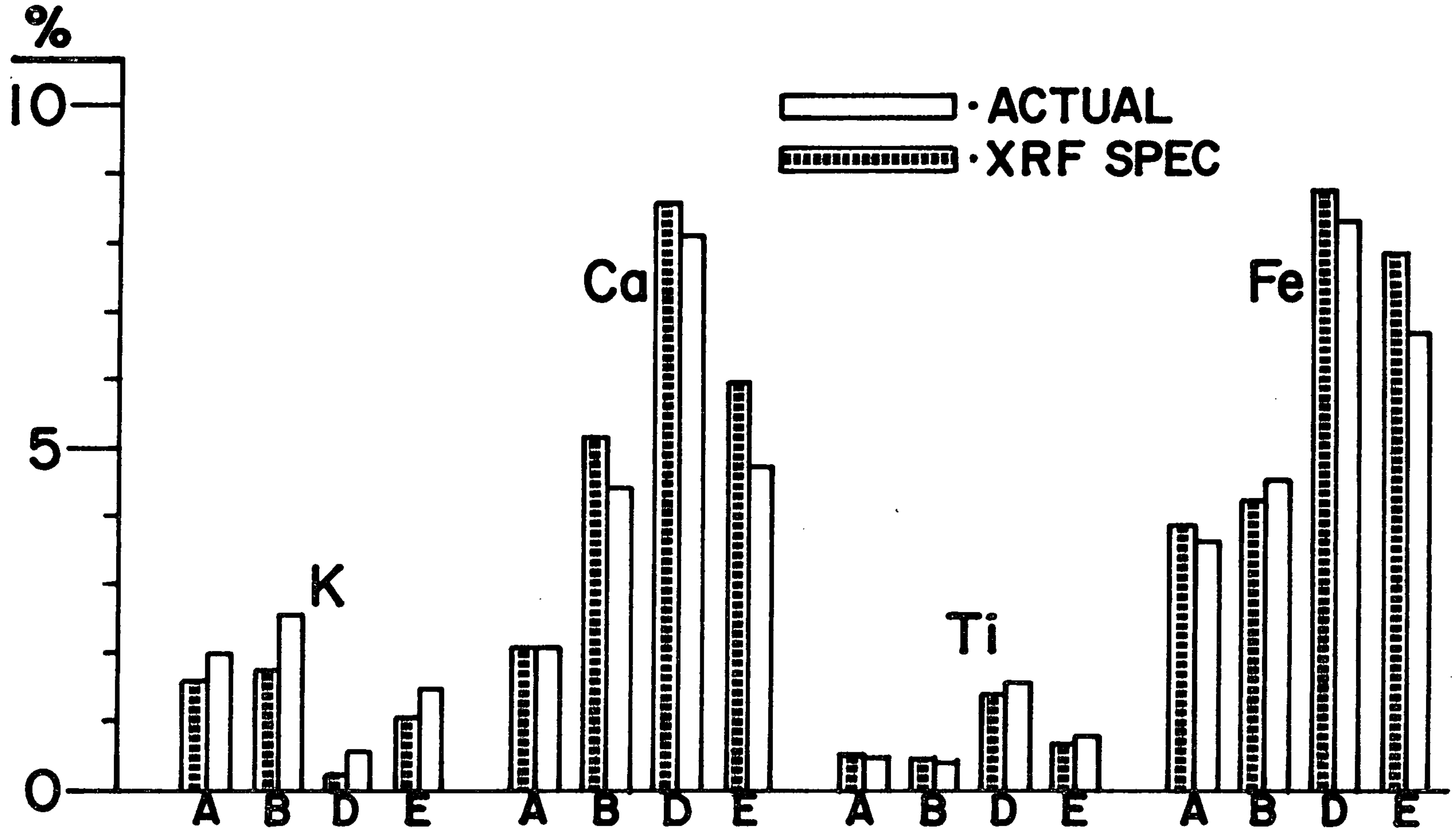

Fig. 2. Comparison of results. Note that the X-ray fluorescence spectrometer results are consistently low for K and high for Ca, but that accuracies are quite adequate for distinguishing one sample from another.

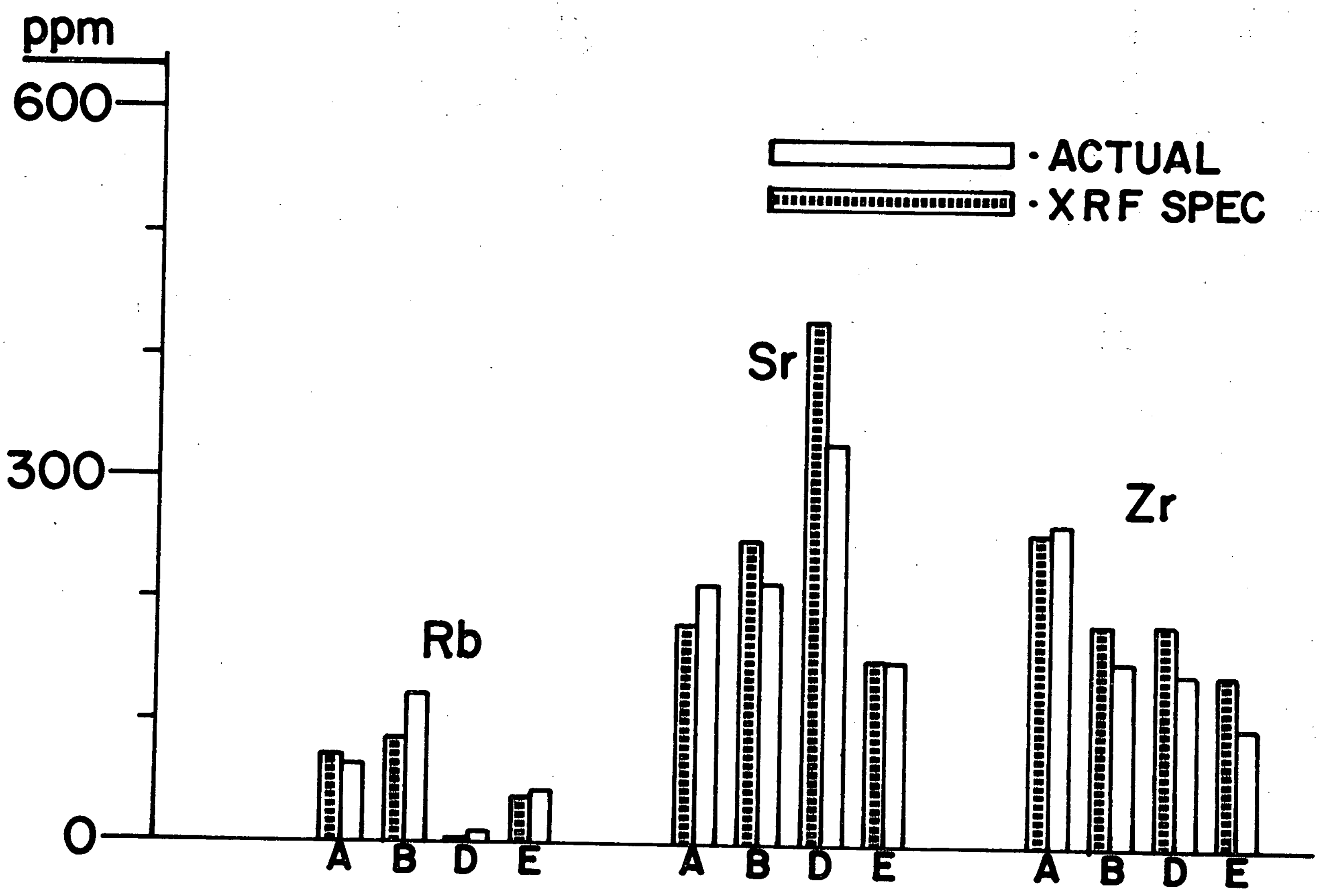

Fig. 3. Comparison of results. These three trace elements are often diagnostic of the differentiation processes a rock has undergone.

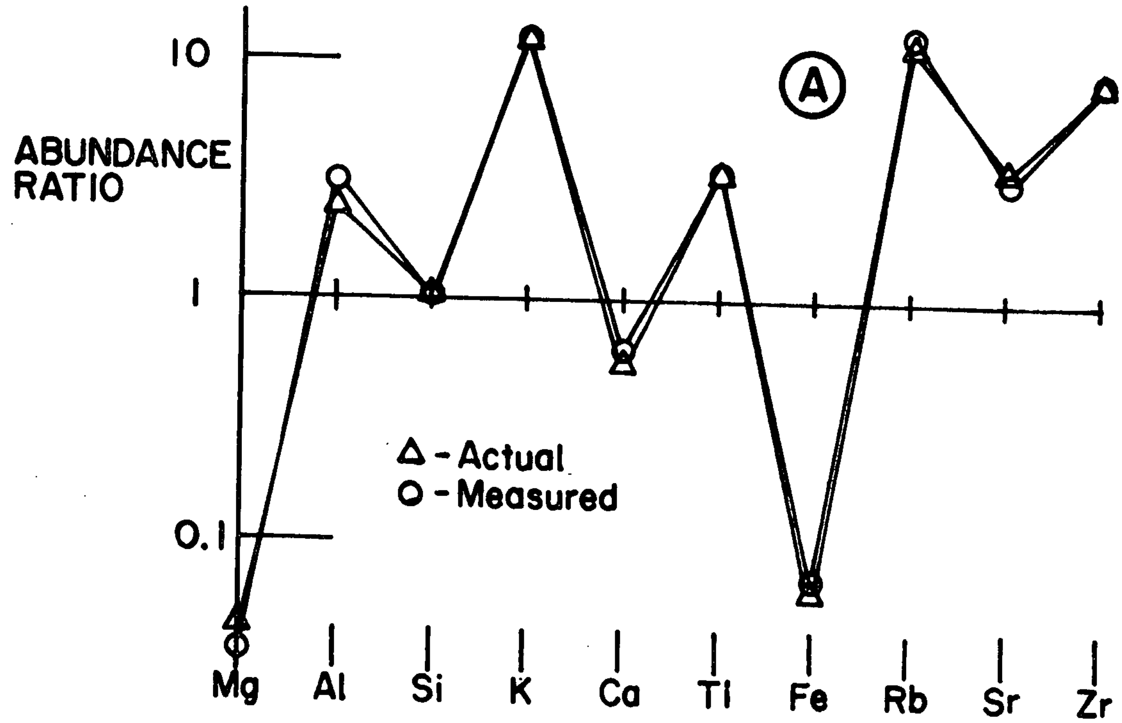

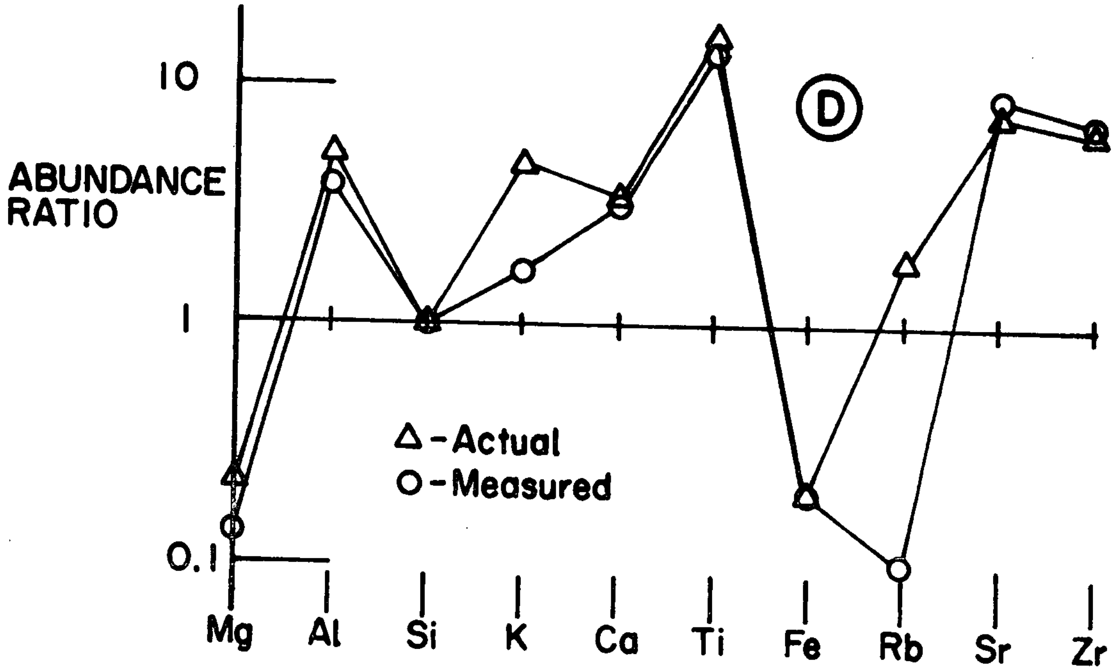

Fig. 4. Ratios of elemental abundances to the presumed primordial abundances of the elements (Ref. 2), normalized to silicon content. Only the results for unknowns A and D are shown above but curves for unknowns B and E show the same quality of agreement as for unknown A.

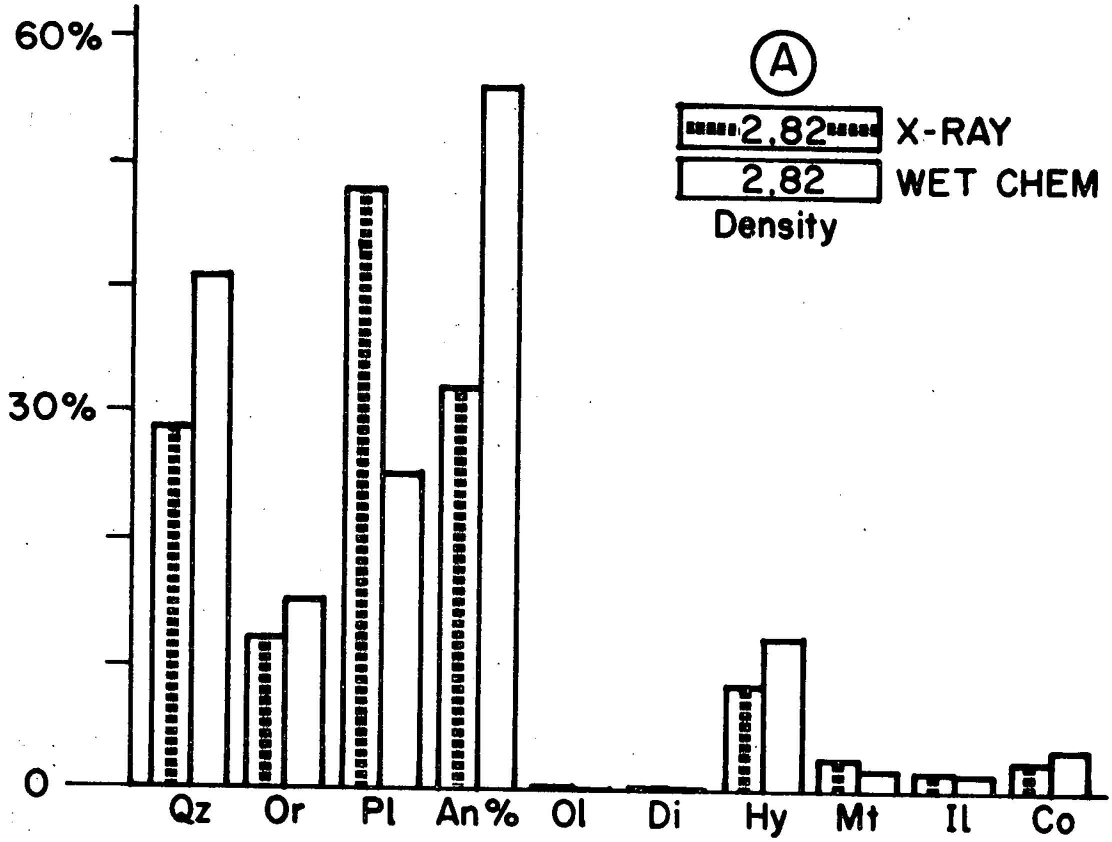

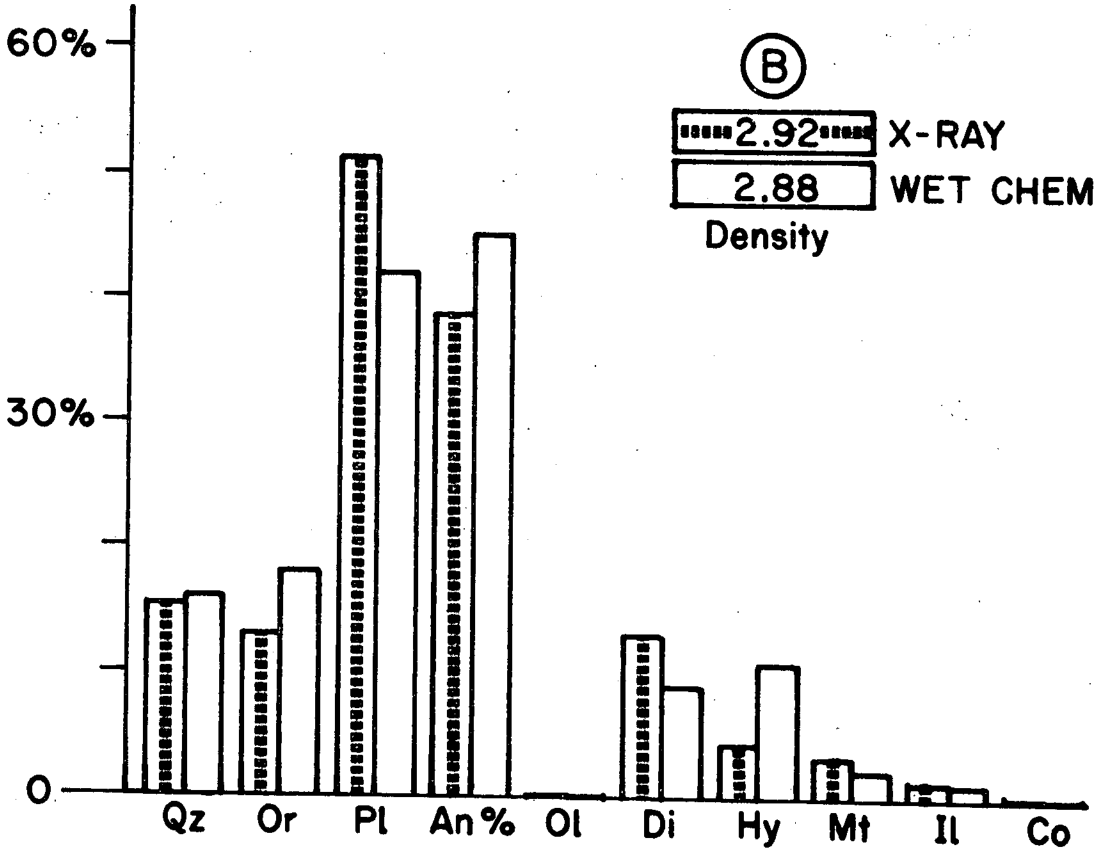

Fig. 5. Calculated normative mineralogies and densities for unknowns A and B using first the X-ray "measured" values and then the wet chemistry "actuals". For further discussion, see Appendix B.

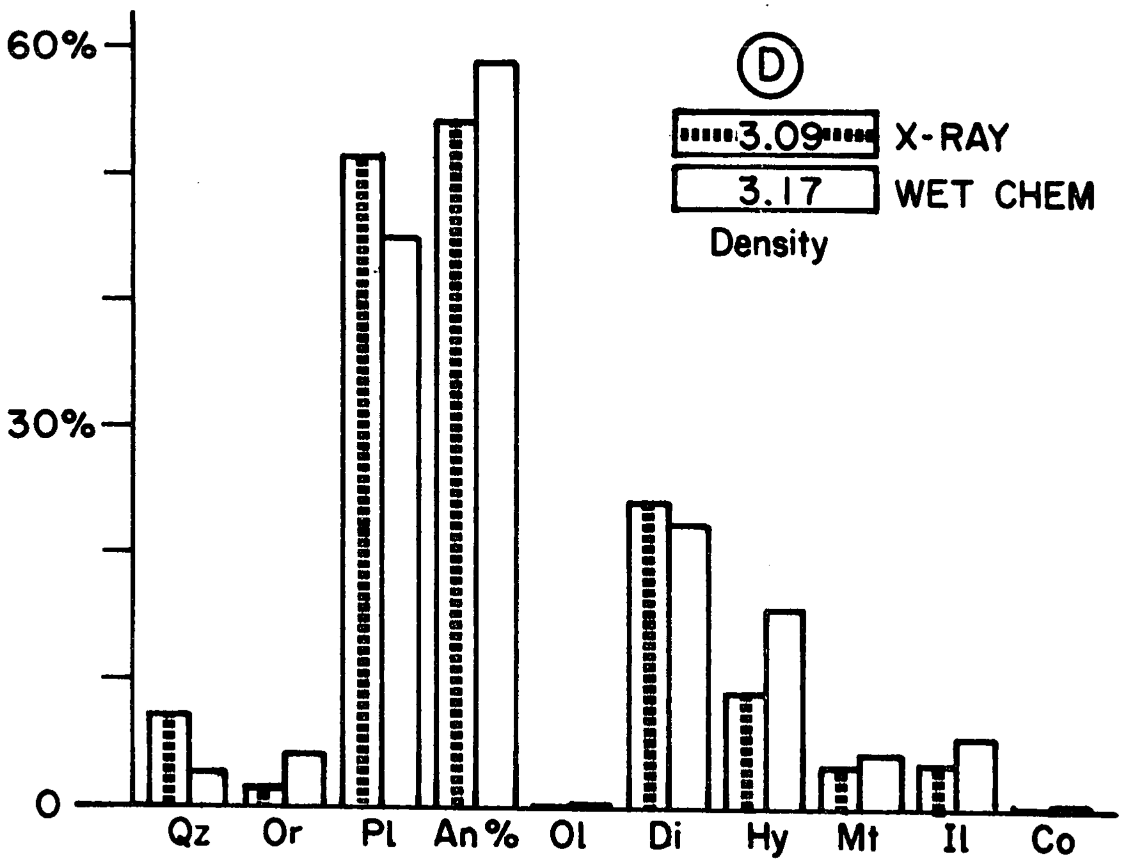

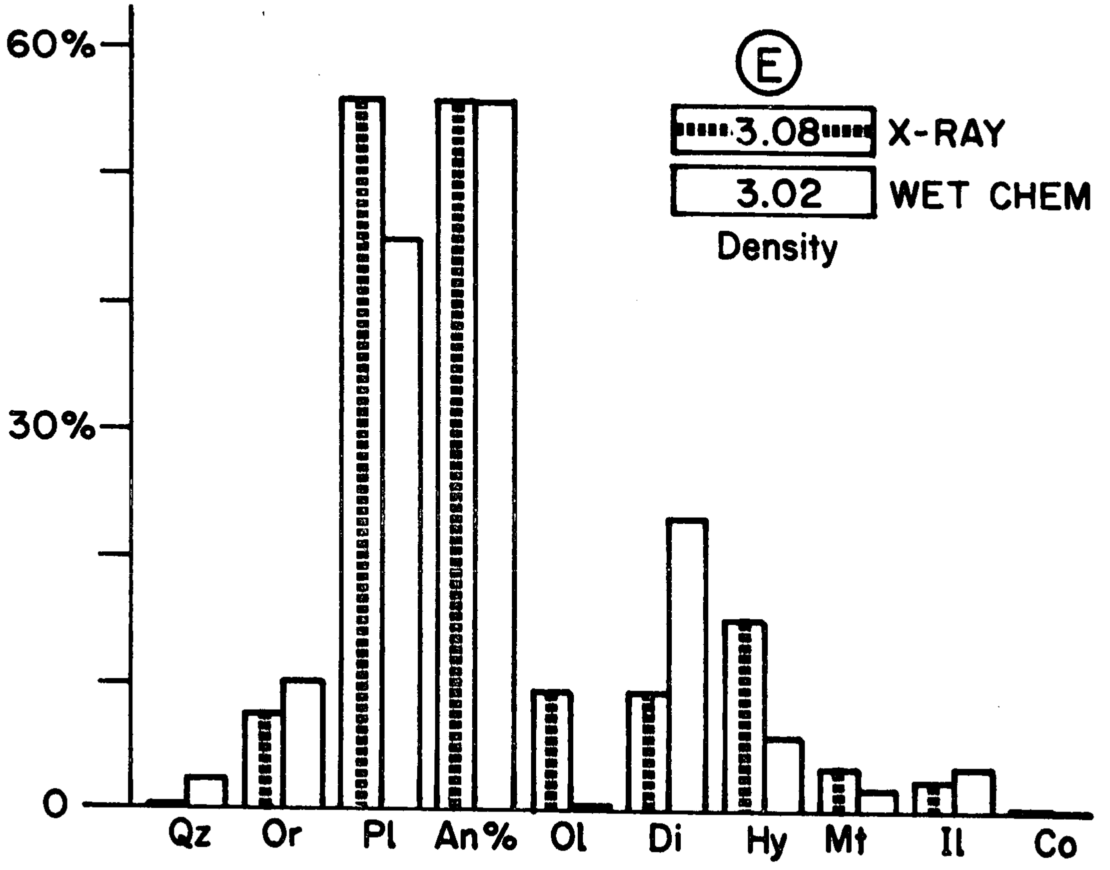

Fig. 6. Same as Fig. 5, but for unknowns D and E. For discussion of these results, see Appendix B.

TABLE I. COMPARISON OF RESULTS

"Actual" are the values determined by laboratory analysis.
"Meas." are the results obtained with the ultraminiature X-Ray fluorescence spectrometer (see Appendix A). Units are per cent by weight.

	UNK A		UNK B		UNK D		UNK E	
Elements	Actual	Meas.	Actual	Meas.	Actual	Meas.	Actual	Meas.
"Oxygen" *	49.6	51.2	48.8	50.0	45.7	44.2	51.0	47.4
Al	7.1	8	7.8	8	7.4	8	8.0	9
Ca	2.10	2.10	4.41	5.15	8.08	8.60	4.76	6.00
Fe	3.66	3.90	4.58	4.30	8.36	8.80	6.70	7.90
K	2.00	1.60	2.54	1.75	0.52	0.20	1.40	1.00
Mg	1.4	1	2.1	2	4.3	3	3.4	5
Si	33.6	31.8	29.2	28.5	23.3	25.7	22.7	23.0
Ti	0.46	0.41	0.41	0.37	1.60	1.45	0.85	0.70
Rb (ppm)	65	70	121	85	8	0	40	35
Sr (ppm)	215	180	215	250	326	430	150	150
Zr (ppm)	265	260	155	185	145	185	100	140
Upper Limits:								
S	--	<1.0	--	<1.0	--	<0.8	0.03	<0.8
CO_2	--	<5.0	0.07	<5.0	--	<3.0	4.9	<5.0
P	0.03	<2.0	0.05	<2.0	0.14	<1.5	0.07	<1.5
Cl	--	<0.3	--	<0.3	--	<0.2	0.01	<0.3
Ratios:								
K/Ca	0.95	0.75	0.57	0.34	0.062	0.023	0.29	0.17
Ca/Si	0.063	0.066	0.15	0.18	0.35	0.33	0.21	0.26
Ti/Fe	0.123	0.103	0.089	0.085	0.190	0.165	0.127	0.088
Sr/Ca	102	86	49	50	40	50	32	25
K/Rb	308	229	210	206	650	∞	350	286
Rb/Sr	0.30	0.39	0.56	0.34	0.02	0.00	0.27	0.23

*"Oxygen" includes elements 1 through 11 (e.g., C, O, Na)

Table II. Comparison of unknown D (a Hawaiian basalt) with Apollo 14 samples (Ref. 4). Rock 14042 is the best match to D, but they are readily distinguished by their Zr/Sr ratio. Note the large range of values for certain elements in the Apollo 14 samples analyzed by LSPET.

	UNK D		APOLLO 14	
ELEMENT	MEAS.	ACTUAL	ROCK 14042	RANGE
"Oxygen"*	44.2	45.7	45.6	--
Al	8	7.4	8.5	7-11
Ca	8.60	8.08	7.4	5-9
Fe	8.80	8.36	7.4	5-13
K	0.20	0.52	0.52	0.1-1.0
Mg	3	4.3	5.2	5-8
Na	--	1.6	0.4	0.3-0.7
Si	25.7	23.3	24.0	22-24
Ti	1.45	1.60	1.10	0.6-1.4
Rb (ppm)	0	8	14	2-33
Sr (ppm)	430	326	210	140-250
Zr (ppm)	185	145	1030	310-1030
Zr/Sr	0.43	0.44	4.9	3.9-4.9

*"Oxygen" is the combined O and Na

TABLE III. Comparison of X-ray Errors with Interlab Wet Chemistry Errors for Similar Rocks. All Errors are Expressed in Percent.

ELEMENT	UNKNOWN A		UNKNOWN B		UNKNOWN D		UNKNOWN E	
	X-RAY ERROR	INTERLAB ERRORS*	X-RAY ERROR	INTERLAB ERRORS*	X-RAY ERROR	INTERLAB ERRORS*	X-RAY ERROR	INTERLAB ERRORS*
Si	5.4	1.2	2.4	1.4	10.3	1.6	1.3	1.6
Ti	10.9	51.6	9.8	43.0	9.4	32.9	17.7	32.9
Al	25	7.5	37	9.9	37	12.3	30	12.3
Fe	6.6	32.1	6.1	18.4	5.3	4.6	17.9	4.6
Mg	100	69.3	100	42.6	67	16.0	60	16.0
Ca	0	21.4	17.0	12.5	6.4	3.6	26.1	3.6
K	20.0	19.7	31.1	37.5	61.6	55.2	28.6	55.2

*Two relative standard deviations from mean, using data of 24 laboratories (Ref 5).

A is for G-1, B for combination of G-1 and W-1, and D and E are for W-1

"X-ray error" is [100 x (meas.-actual)/actual] except for Mg and Al, where it is (100 x ϵ/actual) with ϵ being the error limits estimated for these two elements in Exhibit I of Appendix A.

APPENDIX A

EXHIBIT I. This table was distributed to the panel members at the Jan. 4 formal presentation.

X-RAY FLUORESCENCE SPECTROMETER RESULTS

(Per cent by Weight)

Element	UNK A	UNK B	UNK D	UNK E
"Oxygen"*	51.2 ± 3.0	50.0 ± 3.0	44.2 ± 3.0	47.4 ± 3.0
Al	8 ± 3	8 ± 3	8 ± 3	9 ± 3
Ca	2.10 ± 0.30	5.15 ± 0.30	8.60 ± 0.40	6.00 ± 0.30
Fe	3.90 ± 0.30	4.30 ± 0.40	8.80 ± 0.25	7.90 ± 0.80
K	1.60 ± 0.30	1.75 ± 0.30	0.20 ± 0.15	1.00 ± 0.30
Mg	1 ± 2	2 ± 2	3 ± 2	5 ± 3
Si	31.8 ± 0.8	28.5 ± 0.8	25.7 ± 0.7	23.0 ± 0.7
Ti	0.41 ± 0.20	0.37 ± 0.20	1.45 ± 0.25	0.70 ± 0.20
Rb (ppm)	70 (40-100)	85 (50-120)	0 (0-80)	35 (20-60)
Sr (ppm)	180 (90-250)	250 (150-350)	430 (350-550)	150 (100-250)
Zr (ppm)	260 (150-350)	185 (95-300)	185 (95-300)	140 (80-250)
Ratios:				
K/Ca	0.75	0.34	0.023	0.17
Ti/Fe	0.103	0.086	0.165	0.088
Sr/Ca	81	50	50	25

SELECTED UPPER LIMITS

S	1.0	1.0	0.8	0.8
Ni	1.0	1.0	1.5	1.5
Ni/Fe	0.25	0.23	0.17	0.19
CO_2	5.0	5.0	3.0	5.0
P	2.0	2.0	1.5	1.5
Cl	0.3	0.3	0.2	0.3
Pb	0.01	0.01	0.01	0.01?
Zn	0.1	0.1	0.2	0.2

* "Oxygen" includes elements 1 through 11 (e.g., C, O, Na, and water)

TEST SAMPLE "A"

Philippinite Po-300

From Mandaluyung, Luzon, Philippines

(Weight Percent)

	Constituent as Oxide			Constituent as Element	
	"as is"	H_2O^- Free basis		"as is"	H_2O^- Free Basis
SiO_2	71.78	71.81	Si	33.56	33.57
Al_2O_3	13.36	13.37	Al	7.07	7.08
Fe_2O_3	0.36	0.36	Fe^{3+}	0.25	0.25
FeO	4.39	4.39	Fe^{2+}	3.41	3.41
MgO	2.35	2.35	Mg	1.42	1.42
CaO	2.94	2.94	Ca	2.10	2.10
Na_2O	1.33	1.33	Na	0.99	0.99
K_2O	2.41	2.41	K	2.00	2.00
H_2O+	0.05	0.05	H+	0.006	0.006
H_2O-	0.04	——	H^-	0.004	——
TiO_2	0.76	0.76	Ti	0.46	0.46
P_2O_5	0.07	0.07	P	0.03	0.03
MnO	0.10	0.10	Mn	0.077	0.077
TOTAL	99.94	99.94		51.38	51.39
Total Iron as Fe	3.66	3.66		3.66	3.66
Oxygen by difference	——	——		48.56	48.56

EXHIBIT II. Results of Laboratory Analysis of Unknown A (Supplied by F. Cuttitta).

TEST SAMPLE "B"

1:1 Mixture of Granite G-1 and Diabase W-1

(Weight Percent)

	Constituent as Oxide			Constituent as Element	
	"as is"	H_2O^- Free Basis		"as is"	H_2O^- Free Basis
SiO_2	62.44	62.50	Si	29.19	29.22
Al_2O_3	14.68	14.70	Al	7.77	7.78
Fe_2O_3	1.13	1.13	Fe^{3+}	0.79	0.79
FeO	4.87	4.88	Fe^{2+}	3.79	3.79
MgO	3.51	3.51	Mg	2.12	2.12
CaO	6.17	6.18	Ca	4.41	4.42
Na_2O	2.69	2.69	Na	2.00	2.00
K_2O	3.06	3.06	K	2.54	2.54
H_2O^+	0.43	0.43	H+	0.048	0.048
H_2O^-	0.10	——	H^-	0.01	——
TiO_2	0.68	0.68	Ti	0.41	0.41
P_2O_5	0.12	0.12	P	0.052	0.052
MnO	0.10	0.10	Mn	0.078	0.078
CO_2	0.07	0.07	C	0.019	0.019
TOTAL	100.05	100.05		53.23	53.27
Total Iron as Fe	4.57	4.58		4.58	4.58
Oxygen by Difference	——	——		46.82	46.82

EXHIBIT III. Results of Laboratory Analysis of Unknown B (Supplied by F. Cuttitta).

TEST SAMPLE "D"

Hawaiian Basalt, BHVO-1 (Weight Percent)

	Constituents as Oxides			Constituents as Elements	
	"as is"	H_2O^- Free Basis		"as is"	H_2O^- Free Basis
SiO_2	49.9	49.93	Si	23.33	23.34
Al_2O_3	14.0	14.01	Al	7.41	7.41
Fe_2O_3	2.5	2.50	Fe^{3+}	1.75	1.75
FeO	8.5	8.51	Fe^{2+}	6.61	6.61
MgO	7.2	7.20	Mg	4.34	4.34
CaO	11.3	11.31	Ca	8.08	8.09
Na_2O	2.2	2.20	Na	1.63	1.63
K_2O	0.62	0.62	K	0.52	0.52
H_2O^+	0.25	0.25	H+	0.03	0.03
H_2O^-	0.06	——	H^-	0.007	——
TiO_2	2.66	2.66	Ti	1.60	1.60
P_2O_5	0.32	0.32	P	0.14	0.14
MnO	0.18	0.18	Mn	0.14	0.14
TOTAL	99.69	99.69		55.59	55.60
Total iron as Fe	8.36	8.36		8.36	8.36
Oxygen by difference	——	——		44.10	44.09

EXHIBIT IV. Results of Laboratory Analysis of Unknow D (Supplied by F. Cuttitta).

EXHIBIT V. **Results of Laboratory Analysis of Unknown E (Supplied by F. Cuttitta).**

TEST SAMPLE "E"

SPILITE E-4-95, Washington County, Maine (Weight Percent)

	Constituents as Oxides			Constituents as Elements	
	"as is"	H_2O^- Free Basis		"as is"	H_2O^- Free Basis
SiO_2	48.46	48.57	Si	22.66	22.71
Al_2O_3	15.04	15.08	Al	7.96	7.98
Fe_2O_3	0.80	0.80	Fe^{3+}	0.56	0.56
FeO	7.88	7.90	Fe^{2+}	6.13	6.14
MgO	5.64	5.65	Mg	3.40	3.41
CaO	6.64	6.66	Ca	4.76	4.77
Na_2O	2.37	2.38	Na	1.76	1.76
K_2O	1.68	1.68	K	1.40	1.40
H_2O^+	4.07	4.08	H^+	0.46	0.46
H_2O^-	0.23	——	H^-	0.03	——
TiO_2	1.41	1.41	Ti	0.85	0.85
P_2O_5	0.15	0.15	P	0.066	0.066
MnO	0.24	0.24	Mn	0.19	0.19
CO_2	4.89	4.90	C	1.34	1.34
Cl	0.01	0.01	Cl	0.01	0.01
F	0.05	0.05	F	0.05	0.05
S	0.03	0.03	S	0.03	0.03
Subtotal	99.59	99.59		51.66	51.73
Less O	0.04	0.04		——	——
TOTAL	99.55	99.55		51.66	51.73
Total Iron as Fe	6.69	6.71		6.69	6.71
Oxygen by difference	——	——		47.89	47.82

Appendix B. Petrological Interpretation of Results

Because geologists and petrologists are more accustomed to viewing and comparing chemical analyses of rocks in the classical oxide form, the major and minor element data from Table I are recast in Table B-I. For purposes of later discussion, these are considered "best values". (Analyses for rock C are presented, but not discussed further because this sample was not included in the comparison of analytical methods.)

From Table B-I (and trace element values presented above) it is immediately apparent that a number of significant chemical differences exist between these samples. A few of the more important differences are:

a) From A to E a regular decrease in SiO_2

b) A general two-fold grouping with A and B tending toward an "acidic" nature, and D and E tending toward a "basic" nature

c) Gross differences in the K/Ca ratio from sample to sample

d) Rock D clearly delineated by high iron, calcium and strontium, and by very low potassium and a Rb/Sr approaching zero.

An important interpretive goal of Martian surface chemical analysis is determination of the rock type(s). Of the three main rock families, igneous, sedimentary and metamorphic, sufficient chemical differences exist between and within the first two families to permit designations of rock name -- and thus provide indications of crustal origin and evolution. In contrast, most metamorphic rocks are simply isochemical transformations of pre-existing igneous or sedimentary rocks.

Igneous rocks are named on the basis of mineralogy and texture (Table B-II) with the former exhibiting strong chemical control. Textural differences (largely grain size relationships) determine volcanic or plutonic mode of formation and are independent of chemistry.

Sedimentary rocks are formed from the weathering products of pre-existing rocks. Some types, produced by mechanical action, are chemically indistinguishable from their parent materials (e.g., some graywacke sandstones). Others form from products of extensive chemical alteration of the parent and may have diagnostic chemical features: pure quartz sandstones ($\sim$100% SiO_2); lateritic material (high in oxides of Fe and Al); carbonate rocks (high in Ca and/or Mg and CO_2).

Examination of Table B-I shows that all unknowns are relatively high in silica, but cannot be high in total CO_2 or H_2O. We therefore eliminate carbonate rocks, high quartz sandstones, and water saturated sediments.

A convenient method for comparing analyses of silicate rocks is to calculate a set of standard minerals which can then be used to classify rock types. Table B-III lists the normative mineralogy and density, calculated* by the C.I.P.W. method; the critical parameters for determing rock name are compiled in Table B-IV. Deduced rock names, assuming magmatic origin, are indicated in Table B-II by circled letters, and on the bottom line of Table B-IV.

The rock names derived from normative mineralogy delineate the unknowns as:

A = siliceous (quartzose) igneous

B = intermediate igneous (minor quartz)

D = basaltic igneous

E = olivine basaltic igneous, perhaps somewhat alkaline

Because textural information is lacking, plutonic, volcanic, glassy or clastic nature cannot be determined.

Figures 5 and 6 of the text compare normative mineralogy derived from the ultraminiature X-ray spectrometer results with norms from accepted wet chemical values, and shows rock densities calculated from each norm. Except for rock A, the agreement between norms is good, and for A it should be noted that the X-ray norm contains corundum--the usual case in tektite normative mineralogy because of the depletion of alkalies relative to silica-alumina. In terms of derived rock names, assuming magmatic origin, no major differences would exist between X-ray and wet-chemical data. Rock A is, normatively, a siliceous igneous rock, perhaps more closely related to quartz monzonite than granodiorite; however, the high An%, with high quartz, is atypical of such a rock and is characteristic of Philippinite tektites. Designations of B and D as intermediate igneous and basaltic, respectively, are confirmed. For E, basaltic rather than olivine basaltic is the correct normative designation, but this difference hinges only on the small amount of quartz generated in the wet chemical norm versus the 9% olivine in the X-ray norm.

Calculated normative rock densities are in good agreement. For A, both densities are in gross error compared with actual values for tektites (about 2.4), because the norm assumes a crystalline character for what is a glass. Values for B, D, and E are reasonable for those rock types, but actual densities are not available for comparison.

---

*Calculation of the CIPW norm requires ferrous-ferric iron ratios. These, and values for Na_2O, were estimated by statistical correlations with remaining oxides in each analysis.

TABLE B-I. OXIDE SUMMARY FOR UNKNOWNS

Oxide	Weight Percent				
	A	B	C	D	E
SiO_2	68.2	61.1	62.8	55.1	49.4
TiO_2	0.7	0.6	0.6	2.4	1.2
Al_2O_3	15.1	15.1	16.1	15.1	17.0
Fe_2O_3*	5.0	5.6	4.8	11.3	10.2
MgO	1.7	3.3	1.7	5.0	8.3
CaO	2.9	7.2	3.1	12.0	8.4
K_2O	1.9	2.1	2.3	0.2	1.2
TOTAL**	95.4	95.0	91.4	101.1	95.7

---

*Total Fe calculated as Fe_2O_3

**Does not include $H_2O^{\pm}$, CO_2, Na_2O, traces

TABLE B-II. Simplified Classification of Igneous Rocks
Deduced rock types for unknowns A, B, D, and E are indicated by circled letters.

	ORTHOCLASE DOMINANT ↔						PLAGIOCLASE DOMINANT		NO FELDSPAR
	PLAGIOCLASE An% < 50						An% > 50		ULTRAMAFIC ROCKS
	NO QUARTZ	QUARTZ	NO QUARTZ	QUARTZ	QUARTZ	NO QUARTZ	NO QUARTZ	OLIVINE	
PLUTONIC: (Coarse-grained)	SYENITE	GRANITE	MONZONITE	QUARTZ MONZONITE	GRANO-DIORITE Ⓐ	DIORITE Ⓑ	GABBRO Ⓓ	OLIVINE GABBRO Ⓔ	
VOLCANIC: (Fine-grained to glassy)	TRACHYTE	RHYOLITE	LATITE	QUARTZ LATITE	DACITE	ANDESITE	BASALT	OLIVINE BASALT	

increasing Fe, Mg, Ca and density →

← increasing Si, K and Na

TABLE B-III. Normative Mineralogy (C.I.P.W.)

MINERAL NAME	A	B	D	E
	MOLECULAR PERCENT			
Essential Minerals				
Quartz	29	15	7	0
Orthoclase	12	13	1	7
Plagioclase	48	51	51	56
An %	32	39	54	56
Olivine	0	0	0	9
Varietal Minerals				
Diopside	0	13	24	9
Hypersthene	8	4	9	15
En %	84	87	65	74
Accessary Minerals				
Magnetite	2	3	3	3
Ilmenite	1	1	3	2
Corundum	2	0	0	0
Calculated Density (from weight norm.)	2.82	2.92	3.09	3.08

TABLE B-IV. Parameters for Rock Name, from the Normative Mineralogy, Assuming Magmatic Origin.

PARAMETER	A	B	D	E
Total Feldspar	>50%	>50%	>50%	>50%
Percentage of Feldspar as Plagioclase	79	80	97	88
Type of Plagioclase	Olig/And An < 50%	And An <50%	Lab An >50%	Lab An >50%
Quartz Content	Abund.	Low-Mod	Low	Absent
Olivine Content	Absent	Absent	Absent	Moderate
Rock Name				
(Intrusive)	Granodiorite	Quartz bearing Diorite	Gabbro	Olivine Gabbro
(Extrusive)	Dacite	Andesite	Basalt	Olivine Basalt